MEASURING THE VISCOUS FLOW BEHAVIOUR OF MOLTEN METALS UNDER SHEAR

A thesis submitted for the degree of Doctor of Philosophy

by

Ritwik

Brunel Centre for Advanced Solidification Technology

Brunel University

United Kingdom

UB8 3PH

May 2012

“Truth is ever to be found in simplicity, and not in the multiplicity and confusion of things.”

Isaac Newton.

Contents

Abstract

The flow behaviour of liquid metals (Sn, Pb and Sn-Pb eutectic) under different shearing conditions is investigated. Experiments were performed with two designs of concentric cylinder viscometers: rotating the inner cylinder (Searle) and rotating the outer cylinder (Couette). The latter technique is uncommon and the equipment was optimised with standard oils. The flow behaviour for the metals differs in the two systems. The curves of "apparent" viscosity versus shear rate may be divided into two regimes:

I. At lower shear rates ($<200s^{-1}$): a reduction of "apparent" viscosity with shear was observed with both viscometers. It is suggested that the high density and high surface tension of the metals and eccentricity between the cylinders at low shear rates, leads to instabilities. Results at low shear rates were therefore discarded and further detailed analysis would be required for a fuller understanding of this behaviour.

II. At higher shear rates: a steady, shear-independent behaviour of "apparent" viscosity with shear rate is observed in the Couette system (upto $600s^{-1}$) whereas in the Searle system the "apparent" viscosity increases with shear rate (upto $2600s^{-1}$). From hydrodynamic theory about Newtonian fluids, it is suggested that in the Searle type viscometer, the fluid is unstable and Taylor vortices are expected at low shear rates (~80 s^{-1}). This gives rise to an increase in the "apparent" viscosity with shear rate. Whereas, in the Couette type, the flow is more stable, resulting in a steady "apparent" viscosity. This interpretation is consistent with liquid metals behaving as Newtonian fluids, but further research is required to confirm this. The author suggests further experiments, with the prime one being the investigation of the fluid with counter and co-rotation of the cylinders in order to observe more complex flows.
The results are expected to have implications in the modelling of flow for liquid metal processes, especially the initiation of Taylor vortices under the unstable flow conditions produced by rotating the inner cylinder.

Acknowledgement

I would like to express my gratitude to my supervisor, Dr. Peter Quested, for his guidance, wisdom and support during the course of this project.

I thank Dr. Martin Rides (National Physical Laboratory, London) and Dr. Christopher Gourlay (Imperial College, London) for helpful guidance in conducting the research work and for the many stimulating discussions.

I would also like to thank Prof. Zhongyun Fan (Brunel Centre for Advanced Solidification Technology, Brunel University) for giving me the opportunity to work on such an exciting project. I thank Prof. B. K. Dhindaw, Indian Institute of Technology, Ropar, India for giving me the chance to pursue my interest in research at Brunel University, UK. I am grateful to my parents who have always supported my dream of doing research and have been a source of my strength.

I am extremely thankful to Ms. Xun Wang for being the source of my inspiration, throughout the difficult times of this study. I thank my friends, Abdus, Magda and Liang for always encouraging me in my work.

I also thank Mr. Steve Cook, for helping me over the years and Mr. Peter Lloyd, for always being patient with my requests for manufacturing new components. I also thank my colleagues Dr. Jayesh Patel, Dr. Prasad Rao and Dr. Mingxu Xia for being my mentors in various aspects of my PhD experience in the research group.

List of Tables

List of Figures

List of Symbols

Special characters:

$\overline{\Delta R}$	Mean gap thickness between the concentric cylinders
$\bar{a}$	Displacement of the axes of the concentric cylinders from each other
$\bar{h}$	Effective height of the column of liquid
$\bar{n}$	Constant in Hagen–Poiseuille equation
T_{R_b}	Torque measured at radius of bob

Latin alphabets:

A	Shear area
a	Polynomial constant describing slope of discharge coefficient curve
A_m	Atomic weight
b	Polynomial constant describing y-intercept of discharge coefficient curve
c	Constant in Power law for fluids
c_d	Discharge coefficient
De	Deborah number
dv	Change of velocity
dz	Change in distance
F	Shear force
f	Force constant of the torsion wire
g	Acceleration due to gravity = 9.81 m/s^2
$g(r_m)$	Pair distribution function value at first peak
h	Distance of separation
h_{exp}	Experimental liquid height above a reference point
h_o	Height of liquid in gap
I_o	Moment of inertia of an empty cup and suspension
k	Thermal conductivity
l	Length of capillary
L	Function of density and viscosity of the fluid being measured
l_b	Length of inner cylinder (bob)
m	Constant in Hagen–Poiseuille equation

M	Actual torque reading
m^a	Mass of the atom
M_o	Observed torque reading
n	Constant in Power law for fluids
no	Average number density
$P(T)$	Probability that the atom will stay in a state of oscillation around a fixed coordinate position
Q_{exp}	Experimental volumetric flow rate
r	Radial distance
r_1	Radius of inner ring
r_2	Radius of outer ring
R_b	Outer radius of inner cylinder (bob)
R_c	Inner radius of outer cylinder (cup)
r_{cap}	Radius of capillary
r_{drop}	Radius of the drop of sample being tested
Re	Reynolds number
r_{or}	Radius of orifice
r_m	Position of the first peak in the pair distribution function
r_o	Position of the left-hand edge in the pair distribution function
t	Time
Ta	Taylor number
T_r	Torque at radial distance r
T_m	Melting temperature
v	Velocity
V	Volume of mixture
V_A	Volume of a gram-atom at temperature T_m
V_{dis}	Volume of liquid discharged

Greek characters:

α	Angle of taper
δ_{cc}	$= R_c/R_b$
Δ	Thickness of annulus between concentric cylinder $= R_c - R_b$
η	Dynamic Viscosity

η_o	Viscosity of fluid medium
$\dot{\gamma}$	Shear rate
λ	Relaxation time
μ	Shear viscosity
ν	Kinematic Viscosity
ν_o	A constant corresponding to the frequency of oscillation when no net displacement, i.e., diffusion, of the oscillating atom takes place
ω	Speed of rotation of cylinder in revolutions per minute
Ω	Angular velocity of rotating cylinder = $(2\pi/60) * \omega$
Ω_1	Speed of rotation of inner ring
Ω_2	Speed of rotation of outer ring
π	Pi
ρ	Density of fluid
σ	Surface tension of fluid
θ	Angle of displacement of any small segment of fluid from equilibrium
τ_y	Yield stress
τ	Shearing stress
$\boldsymbol{v}$	Volume of solid particles
ζ	Decay constant of the oscillating drop

Chapter 1

Introduction

"*All liquid metals are believed to be Newtonian*."

This line from the book, "The Physical Properties of Liquid Metals" by T. Iida and R. I. L. Guthrie (Iida & Guthrie, 1988), summarizes the generally accepted belief that molten metals behave as Newtonian liquids. But there is little experimental evidence to support this view. Theoretical explanations for this assumption base the behaviour on the metals being monoatomic. Yet, rheological studies with the variation of shear rate in molten metal, are sparse. A paper on plutonium that suggests non-Newtonian behaviour, (Wittenberg, Ofte and Curtiss, 1968) , measured the rheological properties with an oscillating cup viscometer.

Recently, works using concentric cylinder inner cylinder rotating viscometers varying the shear rate in metals (Malik *et al.*, 2010; Varsani, 2006), suggest more complex behaviour in metals than first envisaged, with a rapid decrease of apparent viscosity with increasing shear rate and then (Varsani, 2006) illustrate an increase in apparent viscosity at higher shear rates.

In light of the efforts made, this study aims at gaining more experimental understanding of the flow behaviour of liquid metals under shear. Employing viscometers based on different working principles, this study has demonstrated the different flow characteristics within the molten melt when different measurement techniques are employed. Since metals are known to be chemically reactive in their molten state, care has been taken while devising and developing the techniques which are used in this study. Starting this thesis with a brief summary outlining the aim of this thesis, Chapter 2 summarises the fundamentals of Rheology, the different measurement techniques available and a brief outline of the various

factors affecting measurements in concentric cylinders technique in particular. Describing the experimental technique employed in this study, Chapter 3 describes the equipment, the materials tested and a detailed summary of the improvements undertaken in the equipment. Chapter 4 aims at discussing the necessary experiments and results with standard Newtonian oils and other liquids which enabled choosing the correct procedure and experimental geometry for testing molten state metals. Summarising the results with metals in Chapter 5, an intensive discussion on the results along with a critical overview of the results by past experimentalists in molten state metal study, is presented in Chapter 6. Summarising the findings from the experimental study, Chapter 7 enlists the important conclusions reached from this study. Finally Chapter 8 provides future experimentalists in this field with ideas for improvements along with the future work planned for this project. A bibliography summarising all the references is given at the end.

These discussions are far from just being academic in purpose. Many industrial processes are now simulated and the viscosity of the metal used in the models is an important parameter. The flow effects on the mould-filling, passage of metal through runners and gates etc. are important in industrial practices. Thus the fundamental understanding of the flow properties during these simulations, limit the application of these models. Through the chapters described above, the author aims to extend the current knowledge of the readers on the flow behaviour of molten state metals, a knowledge based primarily on assumptions made several decades earlier.

Chapter 2

Background study

The resistance which arises from the lack of slipperiness originating in a fluid – other things being equal – is proportional to the velocity by which the parts of the fluid are being separated from each other.

Isaac S. Newton, *Philosophiae Naturalis Principia Mathematica*, 1st Ed., 1687, Book 2, Section IX (Van Wazer, 1963).

2.1 Rheology – meaning & origin

Chamber's Technical Dictionary describes Rheology as "*The Science of the flow of matter. The critical study of elasticity, viscosity and plasticity*" (Chambers, 2011). Rheology is one of the few disciplines in Science whose origin can be traced to an exact date. The word was coined by leading scientists E. C. Bingham and M. Reiner, who wanted to address common problems in Colloid Chemistry faced by engineers and chemists (Reiner, 1964). Taking Heraclitus's "*παυτα ρεί*" or "*everything flows*" as the motto of the subject, they phrased the term "Rheology" at the Third Plasticity Symposium, April 29, 1929. The high level of interest in this new discipline led to the formation of The Society of Rheology.

2.2 Rheology – contents

Rheology describes the deformation and flow behaviour in all types of matter: from Euclidean "rigid bodies of solid mechanics" to the ideal fluids as defined by Pascalian fluids, which exhibit no resistance to flow. Deformation is the process of changing the relative position of the various parts in a body. Upon deformation, spontaneous return to the undeformed shape is called elasticity, whereas an irreversible change leading to dissipation of the mechanical energy as heat is termed 'flow'.

To create flow, a stress must be applied. Under an applied stress one type of deformation is shear. Simple shear can be visualised as a set of infinitely thin parallel plates sliding over one another as in a deck of cards (Fig. 2.1). Since each plane is reluctant to move with respect to the other, there is a "resistance" to flow. Newton in his *Principia* described "resistance" observed in ideal fluids. This "resistance" is what we now refer as viscosity. Due to the similarity between the frictional forces in solids, which resists the motion of one solid over another, and the resistance to flow in fluids, the "resistance" is sometimes also referred to as "internal friction". Thus viscosity gives an idea of the "internal friction" inside the fluid.

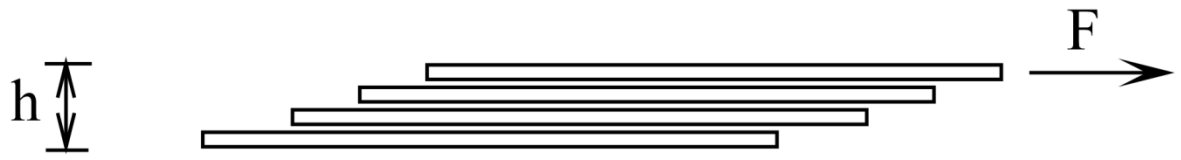

Fig. 2.1. A deck of cards sliding with respect to one another due to the effect of a force F applied at one end.

The main aim of studying Rheology is to define the fundamental relations between forces and deformations which are the constitutive relations of a system. Since most of the existing theories in Rheology are based on ideal situations involving first order differential equations, these theories are unable to describe the characteristics of the system accurately. In fact most of the real materials studied have both elastic and viscous contributions in their behaviour, which are the two ideal scenarios. Thus a study of Rheology first involves understanding the common terms which describe the deformation in a system. For simplicity, let us consider the simple system of fluid held between two parallel plates, under the influence of a force applied at one end of the arrangement (Fig. 2.2).

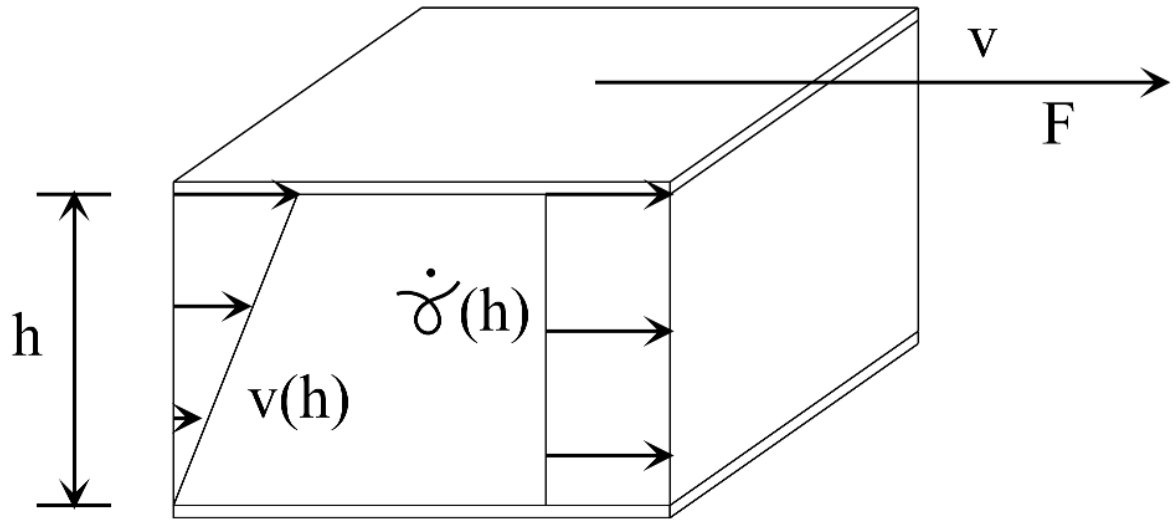

Fig. 2.2. Fluid held between two parallel plates. Force (F) applied at one end to observe effect of velocity variation {v(h)} and shear rate variation {$\dot{\gamma}$(h)} with distance from the reference plane. Distance of separation between the plates is h.

2.2.1 Shear stress

Shear stress is the force acting on the system per unit area which leads to deformation of the system. Depicted usually as "τ", it is given by the following formula:

$$\tau = \frac{F}{A} \tag{2.1}$$

where, F is in Newton, A is in m^2 and τ is in Pascal (Fig. 2.2).

2.2.2 Shear rate

The shear rate in a system under a force is defined as the rate of change of velocity with distance. Generally denoted by the symbol "$\dot{\gamma}$", from Fig. 2.2, the shear rate is given by the formula:

$$\dot{\gamma} = \frac{v}{h} \tag{2.2}$$

where, v is in m/s, h in m and $\dot{\gamma}$ is in s^{-1}.

2.2.3 Viscosity

Sometimes referred to as "shear viscosity", it is the physical property of a fluid which is observed only when there is a relative motion between the different layers of the fluid (represented by Fig. 2.1) under a uniform shear stress (Iida and Guthrie, 1988). The viscous forces in the fluid tend to cause slow-moving regions in the fluid to move faster and the faster-moving regions to move slowly. Thus on a microscopic scale, the viscosity of a fluid determines a measure of the frictional forces acting on an atom in the moving fluid. Newton, in his *Principia*, described the coefficient of viscosity in the equation:

$$\tau = \mu \frac{dv}{dz} \tag{2.3}$$

where, dv/dz is the shear rate (rate of change of velocity with distance). Thus from Newton's formula (equation 2.3), the shear stress is proportional to shear rate, the constant of proportionality being μ, the coefficient of viscosity or simply 'viscosity'. The viscosity defined by equation 2.3 is also termed 'dynamic viscosity' of the fluid. This equation is the classic "Newton's Law of Viscosity". It was later proven to be applicable to only a certain group of fluids which are now referred to as Newtonian fluids. From the equation 2.3 one can derive the units of viscosity.

The S.I. unit of viscosity is Pa.s.

For low viscosity fluids, the unit mPa.s is commonly used. The old metric unit of viscosity was Poise (P) and for low viscosity fluids centi-Poise (cP). Although less popular, the unit centi-Poise (cP) is still used commercially since $1\ \mathrm{mPa.s} = 1\ \mathrm{cP}$.

Some formulations also use 'kinematic viscosity', which is defined as the ratio of the dynamic viscosity and the density of the fluid, otherwise given by the formula:

$$\nu = \frac{\eta}{\rho} \tag{2.4}$$

where, ν is in m^2/s, η in Pa.s and ρ in kg/m^3. Thus viscosity is crucial for a fluid system since it helps to categorize the fluids based on the change of viscosity with external parameters such as temperature, pressure and shear rate. Since all fluids exhibit a decrease of viscosity with increase in temperature and pressure (Macosko, 1994), to categorize fluids, a study of the variation of shear stress with shear rate must be conducted. Based on this variation, fluid behaviour may be categorized as below.

2.3 Types of fluids

A wide range of information regarding a fluid's rheological properties can be obtained from a graph of the shearing stress vs. shear rate in the fluid, commonly known as a "flow curve". This curve can be obtained by either varying the shear rate and measuring the shear stress generated in the fluid or introducing a known shearing stress within the fluid and then recording the shear rate flow behaviour of the fluid. Either way, a "flow curve" acts like a '*zodiac sign*' of the fluids being tested and discloses vital information regarding the fluid's flow behaviour. Different classifications of the fluids have different flow curves and similar curves can be grouped together, thereby enabling researchers to classify various fluids. There are four major groups of fluids (Macosko, 1994; Collyer, 1974; Collyer, 1973):

1) Time independent or purely viscous fluids
    (a) Newtonian fluids
    (b) Non – Newtonian fluids
2) Time dependent fluids
    (a) Thixotropic fluids
    (b) Negative thixotropic fluids
3) Viscoelastic fluids
4) Complex Rheological fluids.

Let us analyse each type of fluid in further detail.

2.3.1 Time independent fluids

For this group of fluids, provided the temperature of the fluid remains constant, the shear rate depends only on the shear stress and is a single valued function of it. Within this class are two sub-groups: (a) Newtonian fluids (b) Non-Newtonian fluids.

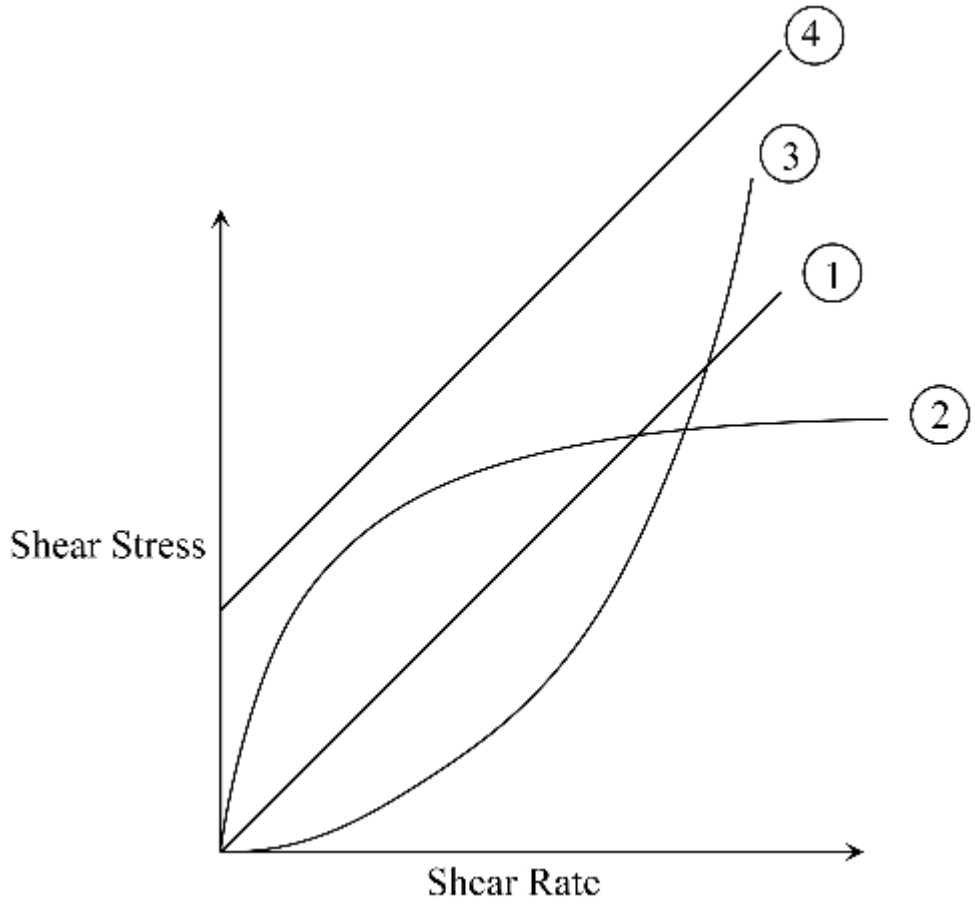

Fig. 2.3. Flow curves of different time independent fluids 1-Newtonian, 2-Shear thinning, 3- Shear thickening and 4-Bingham plastic fluid.

(a) Newtonian fluids

As mentioned earlier, Newtonian fluids are those which follow Newton's Law of Viscosity (shear rate proportional shear stress) and can be described by equation 2.3. At a particular given temperature, the viscosity of such a fluid is constant (Fig. 2.3, line 1). This behaviour is exhibited by gases and in general by liquids and solutions of low molecular weights. Due to their small atomic size, molten metals may be Newtonian as well. Since viscosity is perceived as a measure of the friction between atoms, in Newtonian fluids, collisions between the small molecules or atoms lead to the viscous dissipation of energy. Collyer postulates that such Newtonian fluids may become Non-Newtonian at high shear stresses (Collyer, 1973).

(b) Non-Newtonian fluids

Fluids whose viscosity is a single valued function of the rate of shear are termed Non-Newtonian fluids (Collyer, 1973). In such fluids the ratio of the shearing stress to the rate of shear is not constant. Thus the term 'apparent viscosity' is usually preferable in such cases. Based on the fluid's reaction on being subjected to a shearing stress, this subgroup can be classified into three classes:

(i) Bingham plastic and plastic behaviour.

(ii) Shear thinning behaviour.

(iii) Shear thickening behaviour.

(i) Bingham plastic and plastic behaviour

On plotting the rate of shear against the shearing stress, Bingham observed that the relation between the two quantities was linear over a wide range of shearing stresses (Fig. 2.3, line 4); the line when extrapolated cuts the stress axis at a point above the origin (Macosko, 1994). This point, he referred to as the 'yield point' of the fluid and expressed the equation as:

$$\tau - \tau_y = \eta \frac{dv}{dz} \qquad (2.5)$$

Thus an ideal Bingham plastic is characterized by the fact that the shear rate is proportional to the shear stress after a finite value of shear stress (yield stress) is achieved. Also, the viscosity of the ideal Bingham plastic is strongly temperature dependent. This makes the fluid almost Newtonian above the yield stress. Below the yield stress value the fluid behaves as a plastic solid. Microscopic analysis of a Bingham plastic reveals that such fluids possess a three-dimensional network structure which at first resists the shearing stresses

until the yield stress (hence the plastic solid behaviour at low shear stresses). Beyond yield stress the structure breaks down leading to the flow behaviour observed. Upon reducing the shear stress below the yield stress value, the dimensional structure is formed once again.

(ii) Shear thinning fluids

As the name self suggests these fluids 'thin' upon shearing. In more elaborate terms, the apparent viscosity of such fluids reduces upon increasing the rate of shear on the fluid. Fig. 2.3, line 2 illustrates a shear thinning fluid. Another representation of such fluids is a logarithmic plot (Fig. 2.4) between shear stress and shear rate, which is generally linear with a slope less than 1.

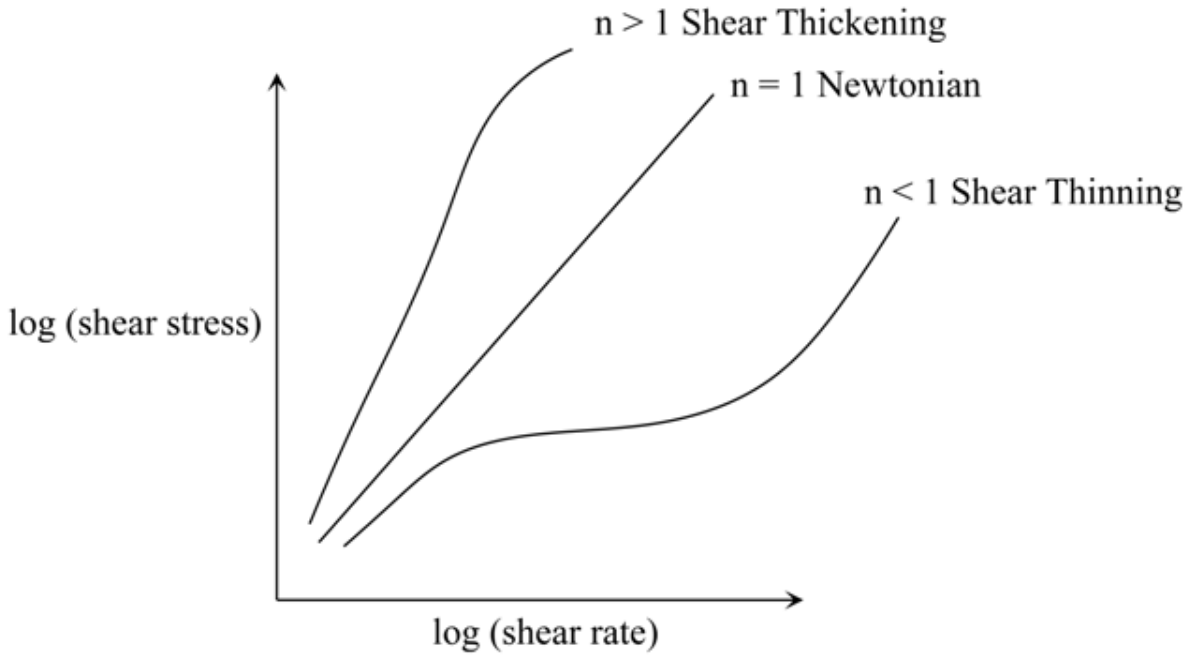

Fig. 2.4. Logarithmic plot representing flow curves in Newtonian, Shear Thickening and Shear Thinning systems.

From Fig. 2.4, the slope for shear thinning fluids is almost unity at the two extremities, i.e. at high and low shear rates these fluids behave as Newtonian fluids. Due to the linear segment in the logarithmic plot of shear stress to shear rate, both shear thinning fluids and shear thickening fluids (described later)

can be represented by a power law, which means the fluids can be defined by the following equation:

$$\tau = c\,(\frac{dv}{dz})^{n} \qquad (2.6)$$

with n < 1 for shear thinning fluids, n>1 for shear thickening fluids and n = 1 for Newtonian fluids.

From equation 2.6 the apparent viscosity for such fluids would be defined as,

$$\eta = \frac{\tau}{dv/dz} = c\,(\frac{dv}{dz})^{n-1} \qquad (2.7)$$

Some examples of shear thinning fluids include dilute polymer solutions, printing inks with lower solute content, paints, napalm etc.

(iii) Shear thickening fluids

These fluids behave in the converse manner to shear thinning fluids and as their name indicates, these fluids 'thicken' on shearing – their apparent viscosity increases with shear rate (Fig. 2.3, line 3).

Such fluids are less common in comparison to the shear thinning fluids and also satisfy the power law (equation 2.6) with n > 1. Thus the slope of logarithmic plot of shear stress vs. shear rate is greater than unity (Fig. 2.4).

Some researchers have observed this phenomenon of shear thickening at the beach and have classified sand-water combination type materials, generally called 'granular materials', as shear thickening systems.

Recent studies indicate that the phenomenon of shear thickening occurs during the solidification of molten metals, especially when the molten metal or alloy system transit from a purely molten state to a semi-solid (Gourlay and Dahle,

2007). These semi-solid materials have exhibited characteristics similar to granular materials including an increase in apparent viscosity.

2.3.2 Time dependent fluids

These fluids are a class of fluids in which the shearing stress is a function of the shear rate as well as the duration of shear. Thus such fluids are greatly influenced by the previous history of the fluid sample under study (Collyer, 1974).

Thus time dependent fluids can even have varying viscosities at a specific shear rate but different history of usage; thus the term 'apparent viscosity' is used. Based on the change in apparent viscosity in these fluids under shear, the time dependent fluids have been classified as below:

(a) Thixotropic fluids.

(b) Inverse thixotropic fluids or sometimes negative thixotropic fluids.

(a) Thixotropic fluids

The word 'thixotropy' named by Freundlich from θίξις, *the touch* and τρέπω, *to change*, describes the behaviour of these fluids which exhibit an isothermal reversible decrease of viscosity with increase in shear rate (McLelland *et al.*, 1997).

On stirring, the fluid becomes runny (forming a sol) and resets on standing (forming a gel). Thus thixotropic fluids could be described as a reversible isothermal gel-sol-gel transformation. Strictly speaking, thixotropy in a fluid can be said to have occurred only when there is complete recovery of the fluid's original structure (Atkinson, 2008). Within a thixotropic fluid, reduction of apparent viscosity is a result of a two-stage breakdown of structure. One is a decrease in apparent viscosity due to motion, in other words, breakdown of structure with time, at a particular shear rate. The second is a decrease in apparent viscosity due to shear rate, i.e., a breakdown of structure due

to increased shear rate at a fixed time. Thus a hysteresis loop shaped flow curve (Fig. 2.5) can describe a thixotropic fluid conveniently.

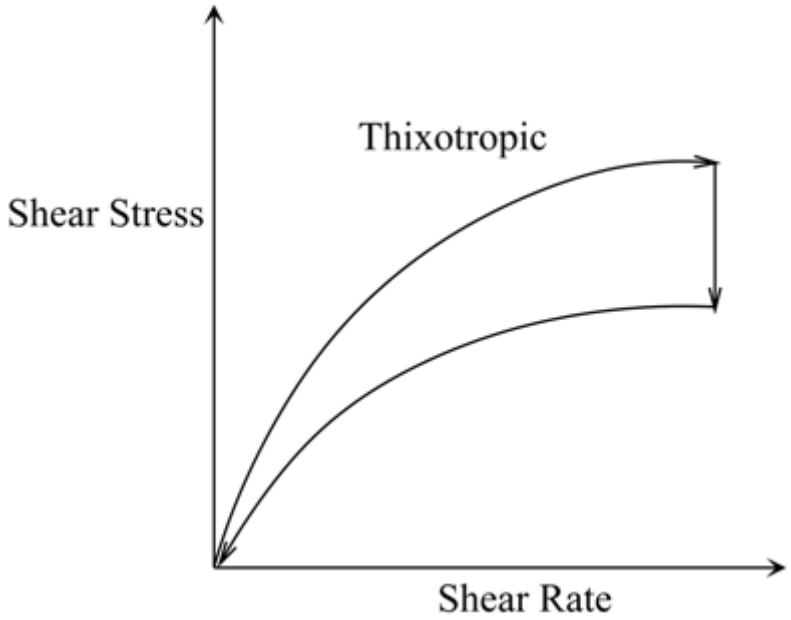

Fig. 2.5. Flow curve of a thixotropic material.

The area within the loop is a measure of the liquid's degree of thixotropy. Thus based on the type of hysteresis loop obtained, thixotropic fluids can be further divided into two subgroups:

(i) **True thixotropic fluids**: The structure of these fluids undergoes a complete breakdown on shearing and is fully regained on standing.

(ii) **False bodied fluids**: These fluids do not lose their structure completely on shearing although their yield stress does reduce by shear. They regain their original yield stress after being kept standing for long durations.

(b) Negative thixotropic fluids or inverse thixotropic fluids

Generally uncommon, these fluids are accompanied by a reversible increase of apparent viscosity with increasing shear stress and the time duration of the shear. Researchers postulate that the shear enables formation of more bonds within the fluid than present in the fluid at rest (Collyer, 1974). Due to the moderate shear, a number of

bonds are also broken but the rate of formation of new bonds overshadows this phenomenon. Thus a network develops within the fluid which leads to the formation of a 'gel' which is displayed as an increase in apparent viscosity. Some examples of such fluids are solutions of polymethacrylic acid.

2.3.3 Viscoelastic fluids

Fluids which display both viscous and elastic properties are termed 'viscoelastic'. This phenomenon is mostly observed in polymeric fluids like amorphous polymers and biopolymers. One key term usually employed in viscoelastic measurements is the Deborah number, which is defined as the ratio of the material's characteristic relaxation time and the characteristic flow time under the influence of a shearing stress.

$$\mathrm{De} = \frac{\text{relaxation time } (\lambda)}{\text{flow time } (t)} \tag{2.8}$$

2.3.4 Complex rheological fluids

These are a group of fluids which exhibit any combination of the aforementioned types of fluids. Such fluids are more complicated and their flow curves are any combination of the types of fluids described earlier. A detailed analysis of such complex rheological fluids – multi-component systems, like emulsions and food products, is beyond the scope of this study.

2.4 Measuring rheological properties - Rheometry

'Rheometry' is a measuring technology used to quantitatively determine the rheological parameters (Atkinson, 2008). It involves measuring systems, instruments, analysis and various tests, all aimed to understand better the behaviour of the solid or fluid under a deformation. Rheometry includes viscous behaviour characterization in fluids by rotational and oscillatory tests as well as studying the viscoelastic behaviour through creep tests and relaxation tests in solids. One of the key outputs in Rheometry is the viscosity of the fluids. Based on the specific properties of the fluid, a diverse range of measurement apparatus exist, each with their own principle of working, advantages and disadvantages as well as the diversity of the results obtained from them. In general, the key output necessary from such apparatus is the fluid flow curve, i.e., the functional dependence of shear stress in the fluid on the shear rate.

In this study the rheological behaviour of molten metals and molten metallic alloys has been studied. Before discussing the procedure of measurement it is important to describe the available options for conducting viscosity measurements for molten metals. High temperature experiments, prone to oxidation and high chemical reactivity are some of the issues facing rheological measurements of molten metals and molten metallic alloys (Iida and Guthrie, 1988). Thus out of numerous available measurement techniques, the following techniques are considered to be suitable for conducting the experiments with molten metal:

(1) Capillary method.

(2) Oscillating type method.

(3) Draining vessel method.

(4) Levitation method.

(5) Concentric cylinders method.

The following section discusses the principle of operation, advantages and disadvantages of each of the techniques.

2.4.1 Capillary method

(i) Principle of operation:

In the capillary method (Fig. 2.6) the time required for a definite volume of liquid to be discharged through a capillary tube, under gravity or under the influence of an externally applied pressure, is related to the viscosity of the liquid.

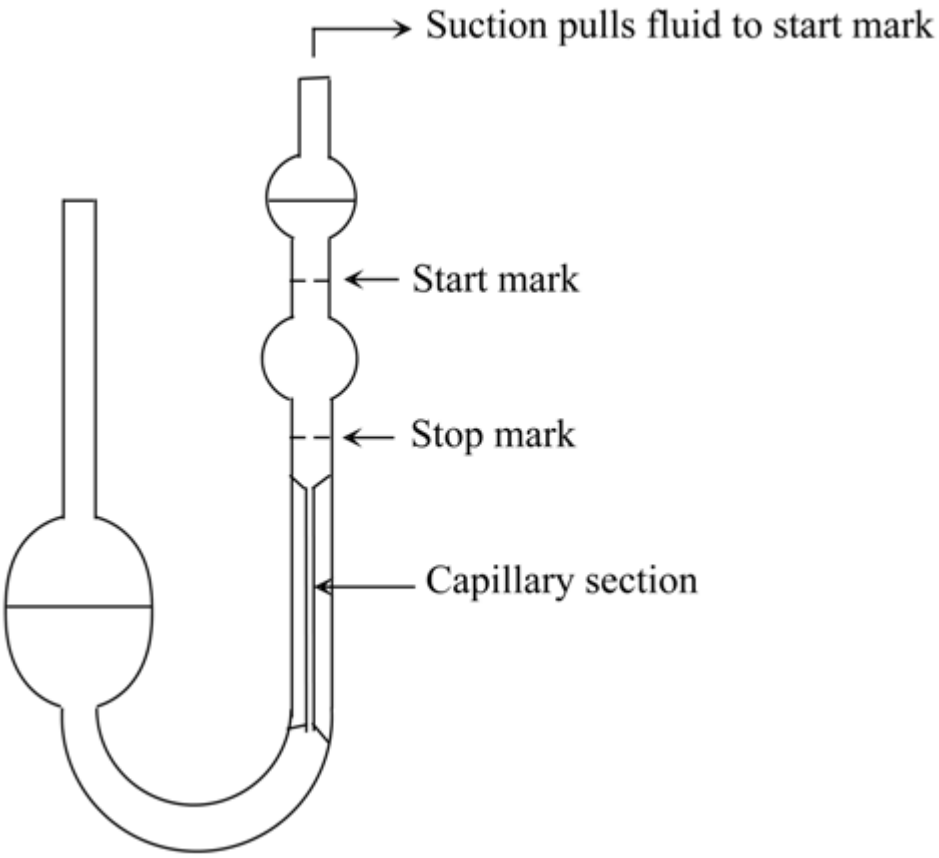

Fig. 2.6. Schematic representation of a common capillary viscometer.

During an experiment the parameters are chosen to ensure a steady, isothermal and laminar flow since the flow of fluid in the capillary is "non-homogeneous" i.e. shear stress is non-uniform throughout the liquid (Fig. 2.7).

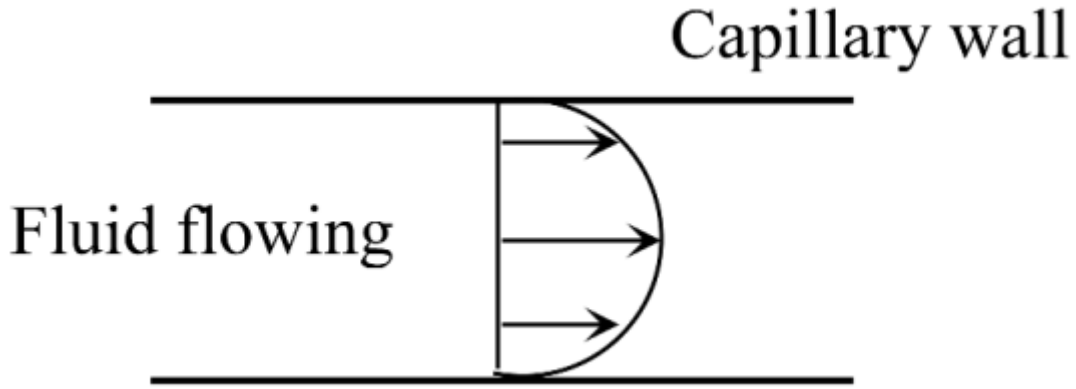

Fig. 2.7. Flow of fluid inside the capillary tube. Maximum velocity at the centre of the tube, zero velocity at the walls.

(ii) Equation:

The Hagen–Poiseuille equation is generally employed for correlating the different parameters (Iida and Guthrie, 1988).

$$\eta = \frac{\pi r^4 \rho g \bar{h} t}{8V_{dis}(l + nr_{cap})} - \frac{m\rho V}{8\pi(l + nr_{cap})t} \qquad (2.9)$$

The term 'nr_{cap}' is the end correction and correction for surface tension effects at the exit.

(iii) Major errors in Capillary method:

Table 2.1. Major errors and causes in Capillary method (Ferguson and Kemblowski, 1991)

FACTOR	CAUSE
Kinetic energy losses	Loss of effective pressure because of the kinetic energy in issuing stream
Viscous end effect	Energy losses due to viscous or elastic behaviour when a fluid converges or diverges at the ends of a capillary
Elastic energy	Energy loss by elastic deformation of the fluid not recovered during flow in the capillary
Turbulence	Departure from the laminar flow
Pressure losses prior to the capillary	Sticking of the piston or energy dissipated in flow of the material within the cylinder before entering the

	capillary
Surface tension effects	Variations of surface tension from one fluid to another
Heat effects	Conversion of pressure energy into heat energy during flow in capillary
Wall effects	Surface phenomena at the liquid and wall interface
Effect of time-dependent properties	Variations of residence time in the capillary

(iv) Advantages:

(1) Applicable to a wide range of materials at low temperatures.

(2) Well developed theory and technique.

(v) Disadvantages:

(1) The capillaries need to be fine and long bore ones with accurate dimensions.

(2) Very long capillaries are needed to measure the low viscosity molten metals at low Reynolds Number condition (laminar condition) (Thresh and Crawley, 1970). This renders measurements quite difficult owing to the dimensional size of the capillaries.

(3) Uniform temperature throughout the bore is required which means furnaces of equivalent length as the capillary would also be required.

(4) Since metals in molten state oxidise, even in very clean and inert atmosphere, agglomeration of the oxides may lead to blockage of the capillaries.

(5) Due to the high melting point of metals and their alloys, only a limited number of materials can be used as the body of the capillaries.

Despite the disadvantages mentioned above, (Lewis, 1936) has successfully measured the absolute viscosity of molten tin with capillary method and also obtained the variation of viscosity values with temperature. Results with Ga, In, Sn, Bi, Pb, Cd, Zn, Sb, Ag and Cu have also been presented to 1100^{o}C with an accuracy of ±0.5% (Iida, Morita and Takeuchi,

1975). But the non-homogeneous flow of liquid within the bore of the capillary render the data generated difficult to apply, since for viscosity measurements, the liquid must be homogeneous and laminar (Mezger, 2006). Thus other techniques are considered.

2.4.2 Oscillating type method

The oscillating type method (Fig. 2.8) is the most commonly used method for measuring the viscosity of molten metals and its alloys. Most of the data on molten metals and their alloys in the databases are from measurements involving some form of the oscillating type method.

(i) Principle of Operation:

A body set in oscillation about a vertical axis in a fluid medium will be damped on account of the frictional energy absorption and the dissipation of energy owing to the viscous forces within the fluid.

Based on this underlying principle, there are two types of oscillating type viscometers:

- **Oscillating vessel type**: The liquid is held in a vessel suspended with a torsion wire. The decay in angular displacement of the vessel and time period of oscillation are measured and related to the viscosity of the liquid held, by solving a second order differential equation (Kehr, Hoyer and Egry, 2007; Brooks, Dinsdale and Quested, 2005; Dinsdale and Quested, 2004; Terasaki *et al.*, 2001).
- **Oscillating body type**: A fixed vessel contains the liquid and the decay behaviour of a suspended body (usually a disc) immersed in the liquid is correlated to the viscosity of the liquid to be measured through a second order differential equation (Stott, 1933). Over time, this technique has been employed more for studying polymeric melts than molten metals or alloys.

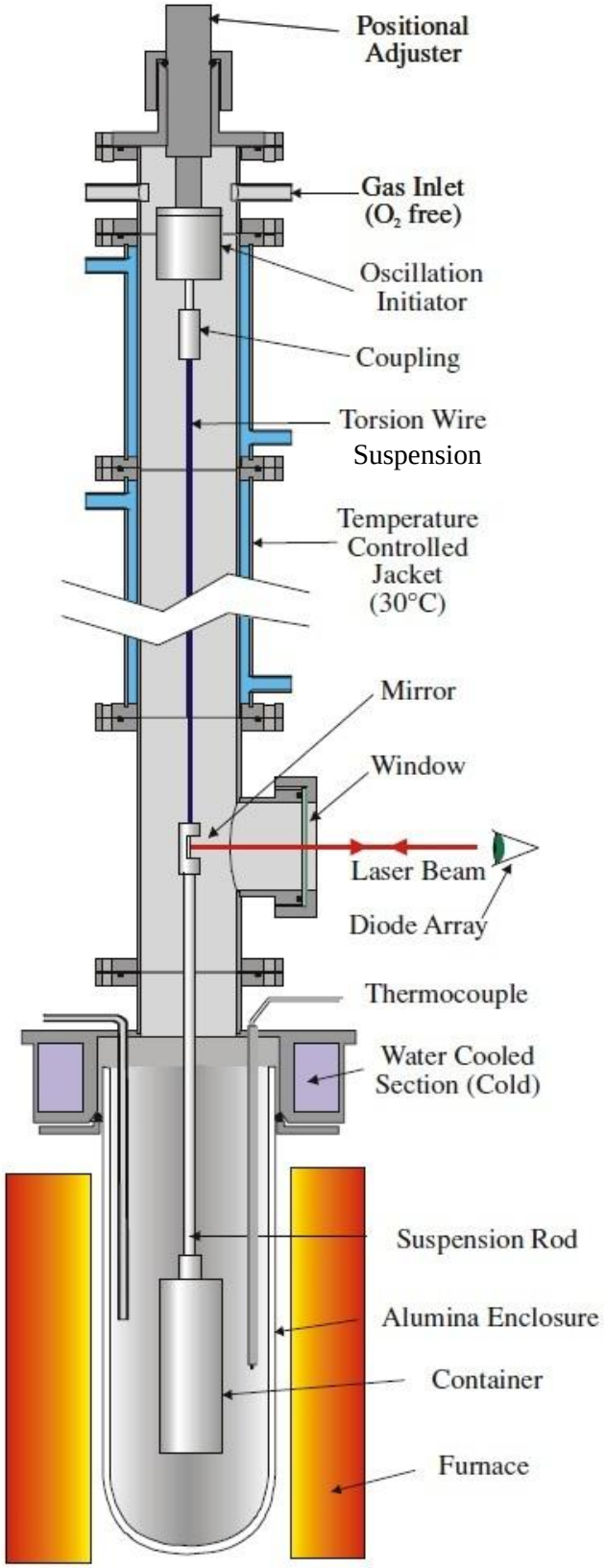

Fig. 2.8. Example of an oscillating cup viscometer employed at National Physical Laboratory, London (UK) (Brooks, Dinsdale and Quested, 2005).

(ii) Equation:

For the oscillating type technique the viscosity of the liquid is correlated to the decay behaviour through the moment of inertia of the system along with the properties of the torsion wire used in the study. From (Iida and Guthrie, 1988), the equation reads:

$$I_o\left(\frac{d^2\theta}{dt^2}\right) + L\left(\frac{d\theta}{dt}\right) + f\theta = 0 \qquad (2.10)$$

(iii) Advantages:

(1) Extensive theoretical research into solving the second order differential equation (eq. 2.10) by Knappworst (Knappworst, 1952) and Shvidkovskiy (Roscoe, 1958)(Shvidkovskiy, 1962) which was superseded by the treatment by Roscoe (Roscoe, 1958) and Beckwith (Beckwith and Newell, 1957) have been conducted. Ferriss and Quested (Ferriss and Quested, 2000), demonstrated that for a limited data set, the relevant Beckwith-Newell and the Roscoe equations for the oscillating cup viscometer give almost identical results.

(2) Apparatus is simple in design with no complicated segments.

(3) Sample size is quite small.

(4) Quick measurements as well as easy cleaning and maintenance of the apparatus.

(5) This measurement technique has been applied to numerous liquid metals.

(iv) Disadvantages:

(1) Despite its popularity, there is no commercial equipment available unlike the rotational viscometers (concentric cylinders, cone-plate viscometers).

(2) Shear rates within the fluid are very low in magnitude (~1 s^{-1}).

(3) Accurate dimensions of the vessel are required.

(4) Iida and Guthrie (Iida and Guthrie, 1988) demonstrate the importance of wetting of the cylinder wall by the liquid being tested on the results. At times, slippage

between the liquid-wall interfaces, may lead to errors due to lower damping of the viscous forces.

2.4.3 Draining vessel method

(i) Principle of operation:

This simple technique relates the volumetric flow rate of a liquid draining through an orifice under the influence of gravity with the surface tension, viscosity and density of the liquid (Roach and Henein, 2005). Only molten aluminium has been attempted with this technique.

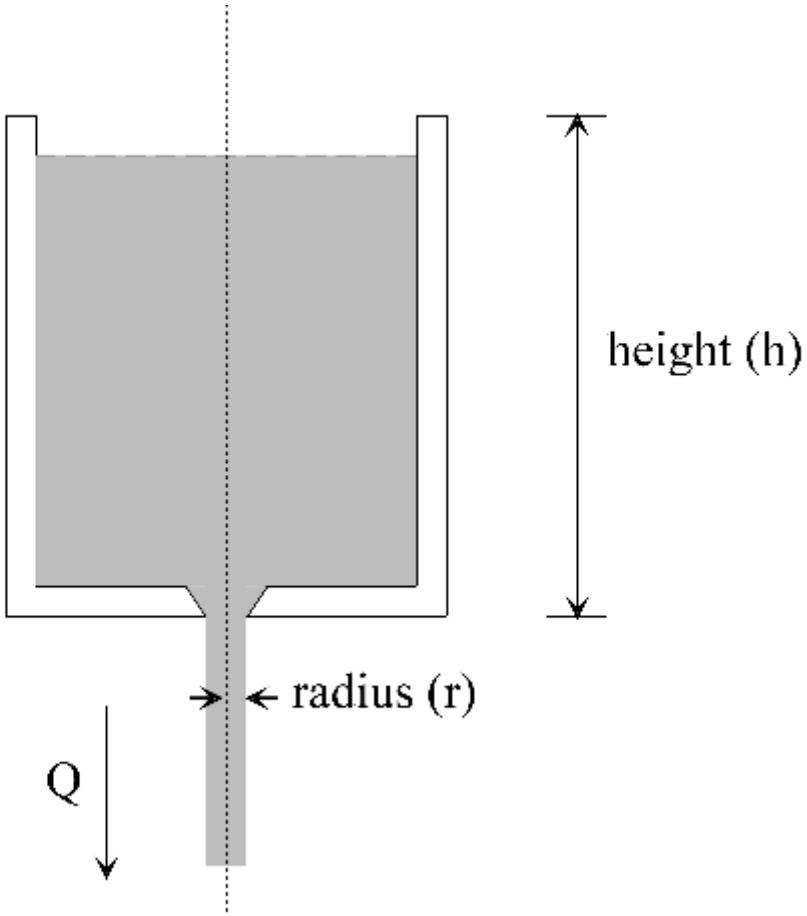

Fig. 2.9. Schematic representation of a draining vessel viscometer.

(ii) Equation:

From Fig. 2.9 the volumetric flow rate (Q) of the liquid can be correlated to its discharge coefficient (c_d), which in turn can be employed to measure the viscosity of the liquid.

$$Q = \pi r_o^2 c_d \sqrt{2 g \left(h - \frac{\sigma}{\rho g r_o}\right)} \quad (2.11)$$

This volumetric flow rate in the experiment (termed in equation 2.12 as Q_{exp}) is then employed to measure the viscosity of the liquid in question.

$$\eta = \frac{2Q_{exp} a \rho r_o}{\frac{Q_{exp}}{\sqrt{2g\left(h_{exp} - \frac{\sigma}{\rho g r_o}\right)}} - \pi r_o^2 b} \quad (2.12)$$

(iii) Advantages:

(1) Simplicity in design.

(2) No moving components.

(iv) Disadvantages:

(1) Since induction coils are employed in this technique to melt the sample, the electromagnetic forces derived from the induction coil create vortices within the melt which is usually neglected in the calculations. To avoid this effect, the induction coil is switched off after melting the sample and the experiment is conducted. This leads to a drop in temperature and subsequent change in the viscosity of the melt, since viscosity is dependent on the temperature.

(2) Reynolds number values of the order of 4000 are generally observed in this technique. This implies that the liquid is in a turbulent state rather than laminar since liquid transforms from the laminar state to turbulent state at Reynolds number of 2100 for such systems.

2.4.4 Levitation method

To overcome the problem of contamination of the sample due to reaction with the container wall, different forms of the levitation technique have been developed to enable measurement

of thermophysical properties such as viscosity and surface tension. This method is sometimes referred to as "containerless" method.

(i) Principle:

There are three variations to the levitation technique based on the process of levitating the material being tested. They are:

- **Electromagnetic** – Levitating the sample drop against gravity in a magnetic field. The sample is self-heated in this form of levitation.
- **Electrostatic** – Levitating the sample drop against gravity in a strong electric field. The sample is heated using lasers.
- **Aerodynamic** – Levitating the sample drop against gravity using a jet of gaseous medium. The sample is heated using lasers.

Subsequently the sample drop is oscillated and the damping of the oscillations within the sample is measured. This measurement enables the calculation of the viscosity of the liquid.

(ii) Equation: (Rhim *et al.*, 1999)

$$\eta = \frac{\rho r_{drop}^2}{5\zeta} \qquad (2.13)$$

(iii) Advantages:

(1) Containerless technique ensures there is no contamination of the sample from the container walls.

(2) Some of the levitation technique measurements are undertaken in microgravity to minimize the effect of gravity (Rhim *et al.*, 1999). This reduces the use of strong electromagnetic forces to levitate the sample.

(3) Quick measurements are also possible using gas levitation technique terrestrially.

(4) High temperatures are achievable in this technique since lasers are employed to heat up the raw materials. Temperatures exceeding 2000 K are achievable

enabling the measurement of refractory materials (Ishikawa *et al.*, 2012) e.g. zirconium, titanium and nickel.

(5) A wide range of materials have been measured especially at high temperatures.

(iv) Disadvantages:

(1) Possible turbulence within the droplets due to the electromagnetic forces is likely to affect the shape of the droplets (Bojarevics and Pericleous, 2009)which also affects the viscosity measurements.

(2) Temperature measurements of the sample in this technique require the use of radiation thermometers which have significant errors in measurements.

(3) Marangoni flows inside the droplets, induced by the lasers, lead to errors in measurements of the viscosity (Przyborowski *et al.*, 1995).

(4) Microgravity experiments are usually very expensive.

(5) Significant difference in viscosity values from oscillating cup technique has been observed which have not been resolved (Etay *et al.*, 2012).

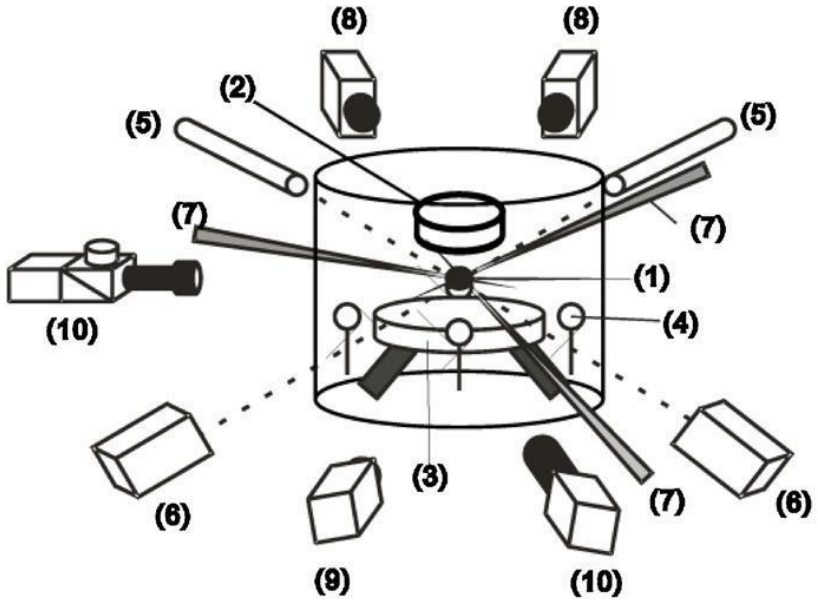

Fig. 2.10. Schematic view of the electrostatic levitation furnace and its diagnostic apparatus:(1) sample, (2) top electrode, (3) bottom electrode, (4) side electrodes, (5) He–Ne lasers, (6) position detectors, (7) CO2 laser beams, (8) pyrometers, (9) charge-coupled device (CCD) camera, (10) CCD cameras with telephoto objective lens (Ishikawa *et al.*, 2012).

2.4.5 Rotational method

The rotational method involves holding the liquid in an arrangement and rotating one of the sections. Subsequently, the shear stress generated is measured. In some cases the shear stress is introduced into a liquid system, upon which, the shear rate to be generated within the liquid to maintain the stress is recorded. Based on the geometry of the components, rotational type viscometers can be divided into:

- Concentric cylinders type.
- Cone-plate type.
- Parallel plate type viscometers.

To measure the rheological parameters in molten metals the following must be considered:

(1) Molten metals are low viscosity liquids which may run out of gaps.

(2) Uniform and steady shear must be present within the melt to measure the rheological parameters.

(3) Molten metals are not too viscous in nature. Thus buckling or tearing will not be observed during the experiments.

Based on these conditions, most of the shear measurements on molten metals are preferred with rotational type viscometers with closed shear lines, which are the concentric cylinders type viscometers (Macosko, 1994).

The concentric cylinders technique has been used previously for measuring the viscosity of fluids and is one the oldest techniques developed to understand the rheological behaviour of fluids. Based on the 'infinite plate' assumption for viscosity measurements, this technique has been studied theoretically by Newton, Coulomb and Stokes (Piau and Piau, 2005; Piau *et al.*, 1994). In the late 1800s-early 1900s, experimental realisation using concentric cylinders

contributed to pioneering research in fluid dynamics (Taylor, 1923b; Couette, 1890; Mallock, 1888; Stokes, 1880).

(ii) Principle

As the name of the technique suggests, there are two cylinders concentric with each other, with a known uniform gap around the inner cylinder, which are rotated either independent of each other or together in the same or opposite direction (Fig. 2.11). Based on the choice of the rotating cylinder, there are two classifications:

- Searle type: Inner cylinder rotating, outer cylinder fixed, no torsion wire.
- Couette type: Outer cylinder rotating, inner cylinder suspended by a torsion wire.

This rotation causes the introduction of shear forces within the liquid held in the gap between the concentric cylinders. These forces are countered by the viscous forces within the liquid which leads to a shear stress which is measured as torque on one of the concentric cylinders. Measurement of this torque, along with the knowledge of the speed of rotation, enables the user to calculate the viscosity of the liquid in the gap (more details on page 57-58).

(iii) Equation (Whorlow, 1980; Van Wazer, 1963)

$$\eta = \frac{M_o}{4\pi h\Omega}\left(\frac{1}{R_b^2} - \frac{1}{R_c^2}\right) \qquad (2.14)$$

The equation 2.14, popularly known as the Margules Equation, holds true only for Newtonian fluids. For other fluids it is the usual practice to measure the shear stress or shear rate from the equipment while varying the shear rate or shear stress respectively. Relating the flow curve generated (shear stress vs. shear rate) to the known flow curves for fluids, the flow equation is obtained and the viscosity is then calculated from equation 2.14.

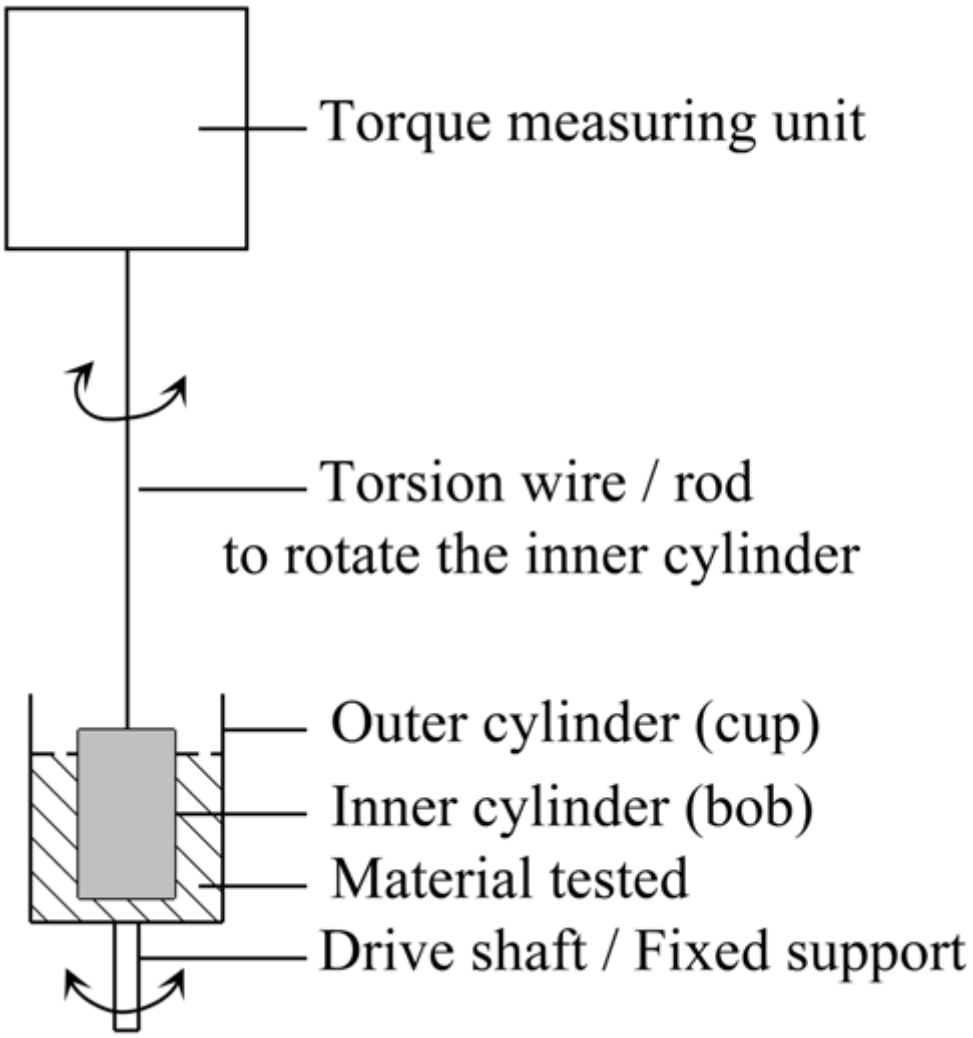

Fig. 2.11. Schematic illustration of a concentric cylinder apparatus. In the Searle type concentric cylinder viscometer, the inner cylinder is connected to the torque measuring unit by a rod which is attached with a motor. This enables rotation of the inner cylinder, keeping the outer cylinder firmly attached to the fixed support. In the Couette type concentric cylinder apparatus, the inner cylinder is suspended via a torsion wire whereas the outer cylinder is connected to the drive shaft to enable rotation.

(iii) Development of the concentric cylinders method:

Detailed history of the development in the equipment employing concentric cylinders technique is available in (Piau and Piau, 2005; Donnelly, 1991). Of these accomplishments, the following review the important developments relevant to this work.

- Newton in his *Principia*, 1687 (Van Wazer, 1963) , has described the problem involving the rotation of a cylinder in a fluid medium from which he later developed the definition of the 'resistance to flow', which we now know as viscosity.
- Coulomb in 1784 built the first known concentric cylinder apparatus to measure liquid friction (viscosity). It was made of either copper or lead with an outer cylinder 128.6 mm and an inner cylinder 42.9 mm in diameter (Piau and Piau, 2005).
- Stokes described the use of concentric cylinders to measure the liquid friction in detail (Stokes, 1880). Not only did he describe the importance of which cylinder to rotate, to ensure a stable fluid flow without eddy (vortices as they were then called), he also stressed the importance of ensuring the cylinders followed the infinite length assumption set forth by Newton. Stokes also suggested the use of 'motes' (dust particles) to observe the liquid to obtain further information about the liquid. This suggestion is now developed into the modern technique of 'Laser Doppler Velocimetry', commonly employed to visualise liquids in narrow gaps.
- Margules in 1881 was amongst the first to seriously consider building a concentric cylinder apparatus for measurements (Donnelly, 1991). His ideas were later realised independently by two research students Henry Mallock and Maurice Couette, in UK and France respectively.
- Mallock in 1888 successfully built a concentric cylinder apparatus (Fig. 2.12) capable of rotating inner and outer cylinders independently (Mallock, 1888).

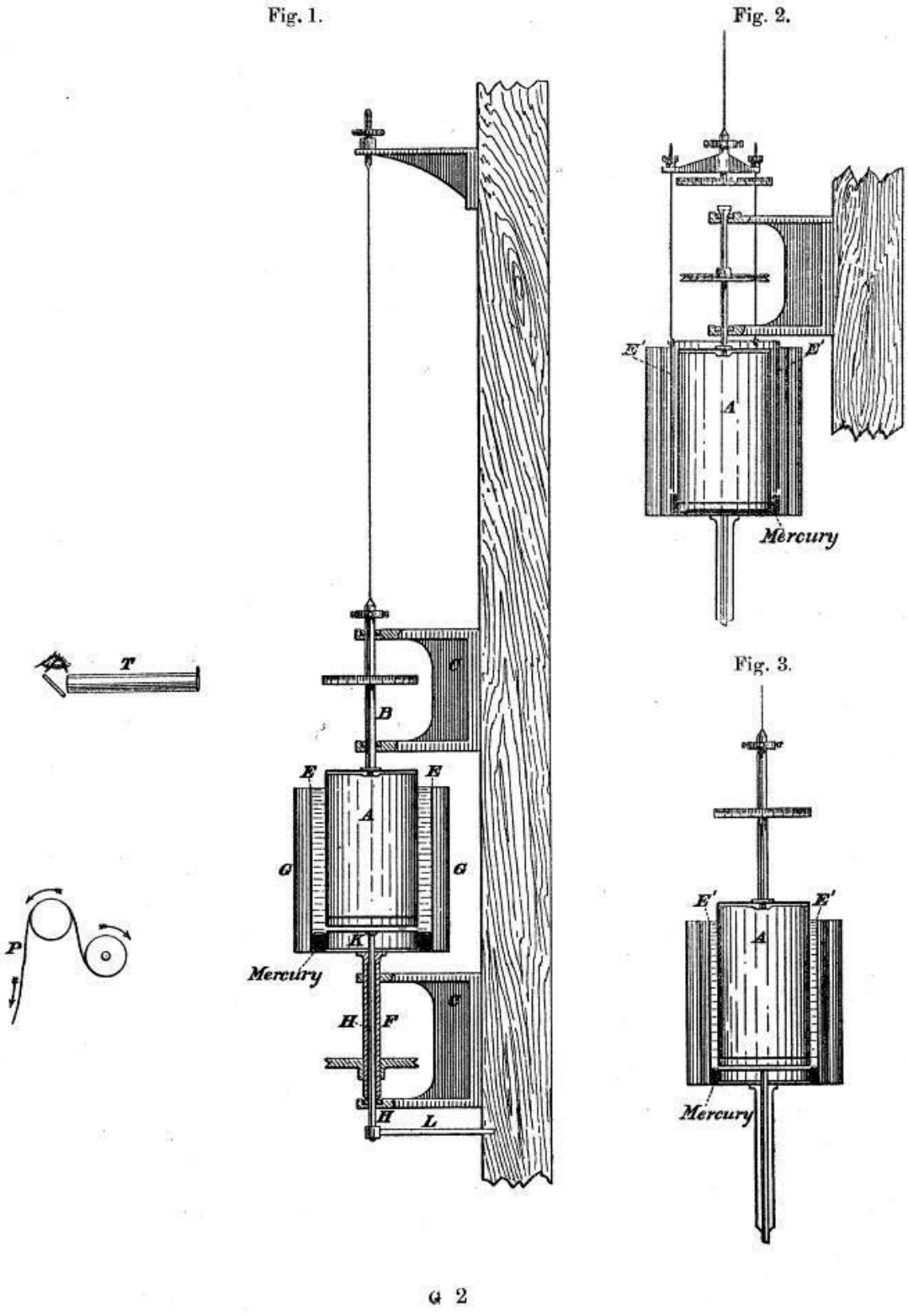

Fig. 2.12. Mallock's concentric cylinders arrangement to measure the viscosity of water (Mallock, 1895; Mallock, 1888). A-inner cylinder, B-stem, C-gunmetal castings, E-outer cylinder, F-axis of rotation, G-cylinder outside E, gap between E-G and inside A is filled with water, H-rod, K-short cylinder on H, L-arm at lower end of H, P-continuous paper to record data, T-telescope to observe.

A skilled instrument builder, Mallock measured the viscosity of water with his equipment. His results have an error of only 1% compared to the modern value followed for the viscosity of water. He ingeniously employed mercury in his apparatus under the inner cylinder to overcome end effects from the finite size of the cylinders (Mallock, 1896; Mallock, 1888).

- Couette , at the same time as Mallock, published his thesis in Paris, May of 1889, entitled "Studies on Liquid Friction" in which he described details of a concentric cylinder (Fig. 2.13) apparatus with the outer cylinder rotating and the inner cylinder suspended on a fibre to measure torque(Couette, 1890). Couette was aware of the work conducted by his forerunners Stokes and Margules prior to the development of his equipment. He took into account interferences effects from poor co-axiality and end effects. He also demonstrated the no slip condition at the wall surface which had been proposed by Stokes (Stokes, 1880). The detailed equipment became the forerunner for concentric cylinder viscometers later to come and in honour of his work and contribution, concentric cylinders apparatus with the outer cylinder rotating are referred to as Couette viscometers.

- Lord Rayleigh established the theoretical groundwork for the concentric cylinders during the time Mallock and Couette published their work. In his articles, Rayleigh established the stability criterion for maintaining laminar flow within the liquid which is rotating between the concentric cylinders. From his work (Rayleigh, 1917), it was established that the liquid in the gap is stable and free from eddies if:

$$\frac{\mathrm{d}}{\mathrm{dr}}(\mathrm{r}^2\Omega)^2 > 0. \tag{2.15}$$

From Fig. 2.14, the equation 2.15 can be written as,

$$\mathrm{r}_2^2\Omega_2 > \mathrm{r}_1^2\Omega_1 \tag{2.16}$$

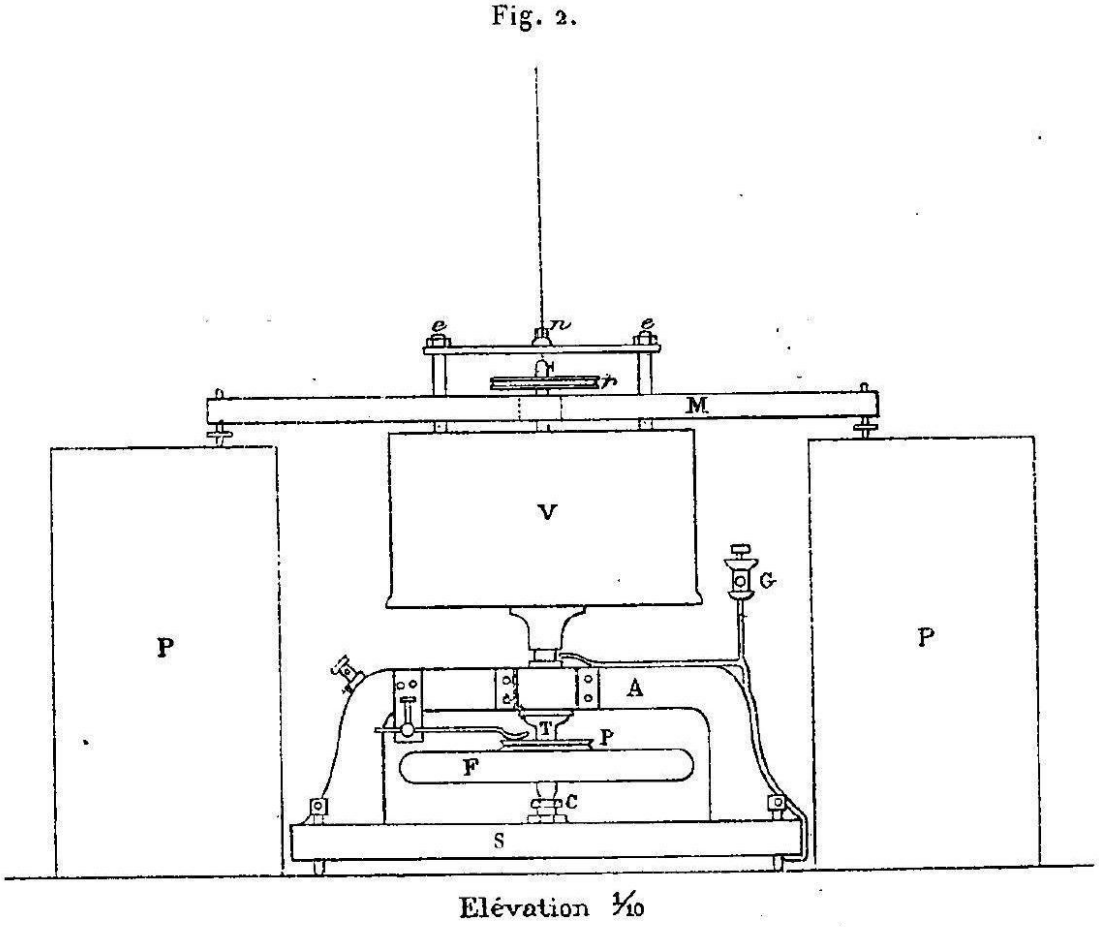

Fig. 2.13. Scan of Maurice Couette's original concentric cylinder apparatus (Couette, 1890). V-steel beaker, P-masonry pillars, A-cast iron arcade, T-vertical shaft, F-cast iron wheel, C-bronze screw to raise or lower, S-center plate, M-tripod, H-levelling screws, G-oil source for lubrication.

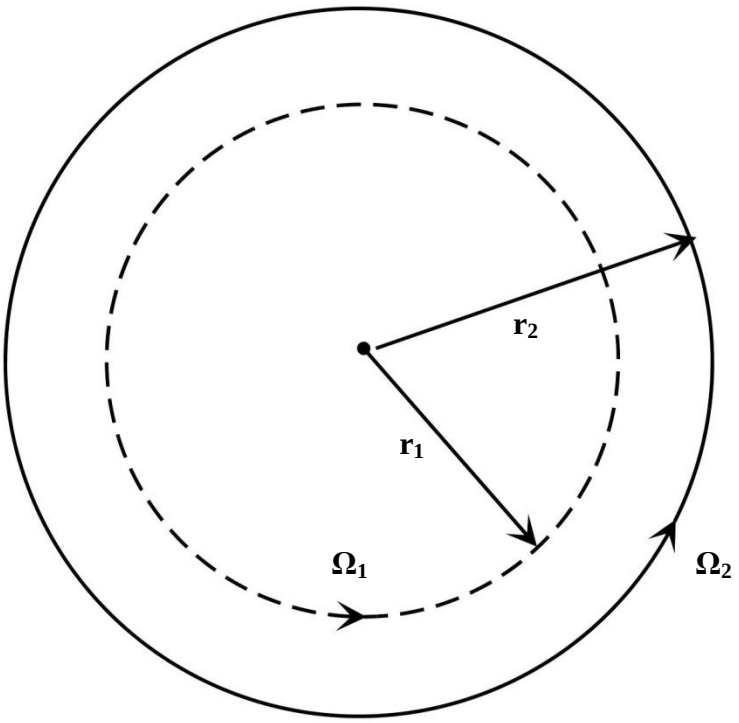

Fig. 2.14. Rayleigh's stability criteria for maintaining laminar flow in the liquid, bound within concentric cylinders, free from eddies.

Thus from Rayleigh's criterion it was established that the speed of rotation should increase outwards for a stable flow which meant that the speed of rotation of the outer cylinder should be higher than the speed of rotation of the inner. This criterion was later supported by Taylor in 1923 who demonstrated that rotating the inner cylinder, keeping the outer cylinder fixed, led to the formation of vortices.

- Taylor's papers in 1923 (Taylor, 1923a; Taylor, 1923b; Taylor, 1923c), became the basis of modern hydrodynamics. Taylor established theoretically the stability criterion for a concentric cylinder with inner cylinder rotating and proved them experimentally with an apparatus which employed water to calculate the stability criterion. The criterion (Taylor, 1936), enabled scientists to predict the introduction of instabilities, which were later termed as Taylor–Couette vortices, in a fluid system. It also enabled them to avoid the vortices by maintaining a lower speed of rotation in their equipment. In this study Taylor's criteria (Taylor, 1936) has been employed to compare

the results between two instruments with different mechanisms; one with the inner cylinder rotating and one with the outer cylinder rotating.

- Wilhelm and Wroughton (Wilhelm and Wroughton, 1939) developed a viscometer with the inner cylinder rotating for measuring the viscosity of suspensions. They demonstrated the use of baffles on the inner cylinder to prevent sedimentation of the particles and also the use of calibrating the system with standard liquids in scenarios where absolute measurement of the system was not possible.
- A significant number of studies in the middle of the last century (Davey, 1962; Chandrasekhar, 1958; Barber, Muenger and Villforth, 1955; Pai, 1943) , were conducted on developing an understanding of the Taylor–Couette vortices which were observed in numerous systems. These vortices affect the torque readings leading to a misinterpretation of the viscosity readings.
- A number of commercial equipment were developed during the 1950s for measuring viscosity. One such popular equipment is the standard ARES rheometer (TA Instruments, New Castle, DE) which is based on the principle of Mallock's concentric cylinder apparatus. Unfortunately, Mallock's contribution to this equipment has been overshadowed by other inventors (Mooney and Ewart, 1934).
- To study the rheological behaviour of polymer liquids at high rates of shear, Manrique and Porter developed an improved Couette viscometer with the inner cylinder rotating and the torque measured on the outer cylinder (Manrique and Porter, 1975). Shear rate of 3×10^6 s^{-1} in magnitude, was attained for low viscosity oils.
- Extending Taylor's work, Andereck investigated different stability states in a liquid rotated within the concentric cylinders, with co-rotating and counter-rotating cylinders. He recognised twenty four new states (Andereck, Liu and Swinney, 1986; Andereck, Dickman and Swinney, 1983), thereby extending the knowledge on flow

systems between concentric cylinders. The final graph given in his paper is illustrated in Fig. 2.15, termed in this study as the 'Andereck Diagram'. Fig. 2.15 illustrates the diverse Taylor vortex stability states generated when the inner cylinder rotates keeping the outer cylinder fixed (thereby varying the Reynolds number at the inner cylinder) as compared to the lack of Taylor vortex stability states when the outer cylinder rotates (varying the Reynolds number at the outer cylinder). This was in line with the original idea proposed by Stokes, Couette and Rayleigh.

- In recent times, Bakhtiyarov and Overfelt (Bakhtiyarov and Overfelt, 1999), also employed a concentric cylinders technique, with the inner cylinder rotating and the outer cylinder fixed, to measure the viscosity of LMA-158, an alloy of Bi, Pb, Sn and Cd. A schematic representation of the concentric cylinder apparatus employed in their study is presented in Fig. 2.16.

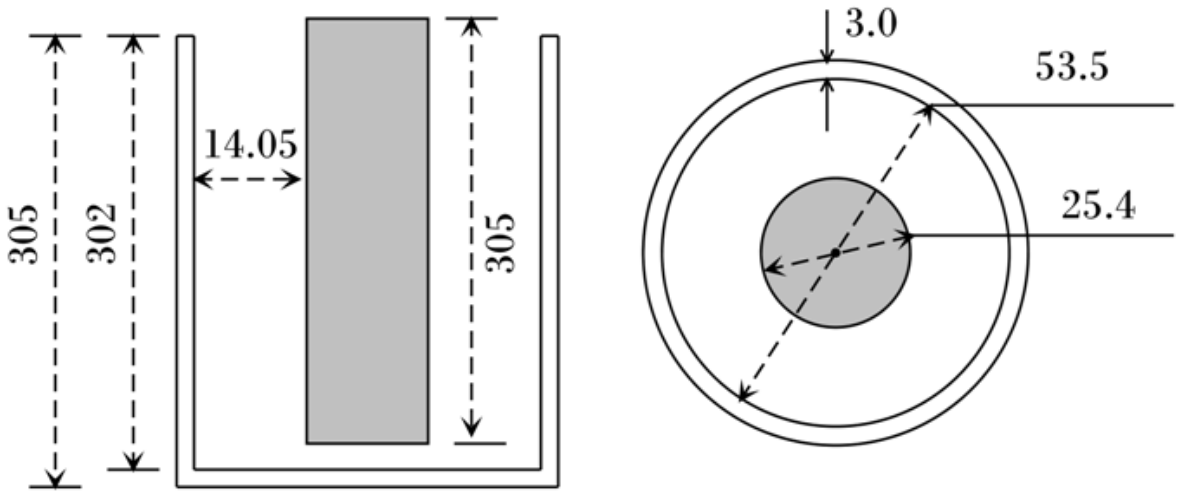

Fig. 2.16. Schematic representation of the inner cylinder rotating, large annular gap viscometer (all dimensions in mm) employed in measuring the viscosity of LMA-158 alloy by Bakhtiyarov and Overfelt (Bakhtiyarov and Overfelt, 1999).

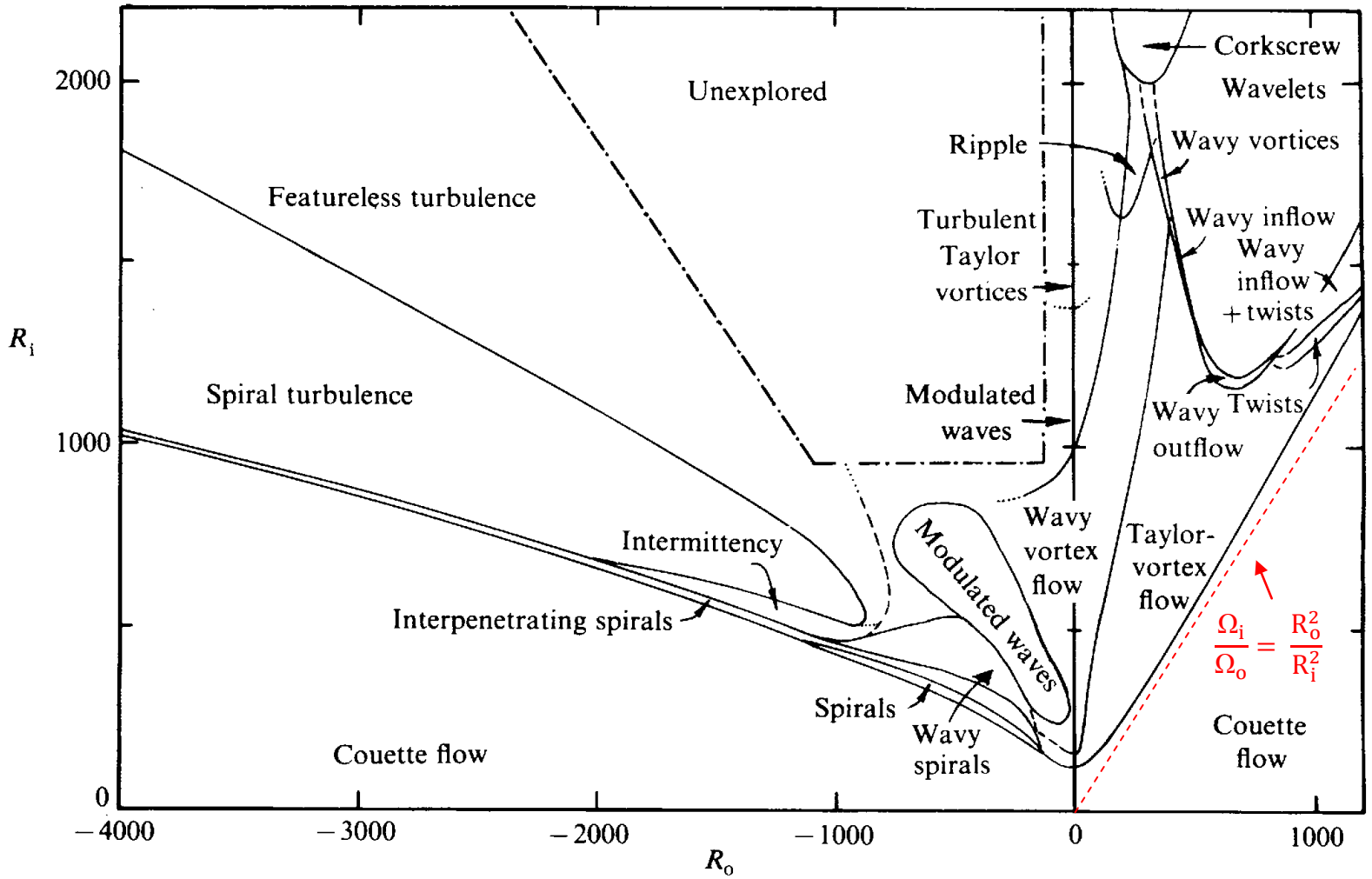

Fig. 2.15. Andereck Diagram representing the variation of Reynolds Number of the outer cylinder (R_o) with the variation of the Reynolds Number of the inner cylinder (R_i) along with the different states of the fluid within a concentric cylinder apparatus (Andereck, Liu and Swinney, 1986). Note the Rayleigh's stability criterion (marked in red) given by the dotted line from the origin.

(iv) Advantages:

(1) Low viscosity liquids can be measured conveniently with concentric cylinders since the cylinders enclose the liquid, preventing flow out, as opposed to cone-plate and parallel plate viscometers.

(2) A good control over the temperature is possible in the Searle type apparatus (inner cylinder rotating) by installing a constant temperature bath outside the outer cylinder which is fixed. Since temperature has a profound effect on viscosity (Andrade, 1952) , care must be taken to ensure uniformity of temperature throughout the sample.

(3) High shear rate can be achieved within the liquid sample by altering the gap thickness (Manrique and Porter, 1975).

(4) Uniform and laminar flow within the liquid sample, which is a necessary condition for measuring viscosity (Couette, 1890), is attainable in a concentric cylinder arrangement.

(5) The inner surface of the outer cylinder and the outer surface of the inner cylinder can be sand-blasted to prevent wall-slip.

(v) Disadvantages

(1) Cleaning up of the apparatus after each experiment requires time and considerable care owing to the delicacy of the components.

(2) Maintaining uniform temperature throughout the sample is a challenge in the Couette apparatus with the outer cylinder rotating since a constant temperature bath cannot be installed outside the outer cylinder unlike the Searle apparatus where the outer cylinder is fixed.

(3) Eccentricity between the concentric cylinders has an adverse effect on the

measurements. Thus while preparing for experiments; long durations of time are spent on ensuring that the two cylinders are concentric with each other.

(4) In low viscosity liquids, instabilities (Taylor vortices) are a possibility, leading to erroneous and misleading data. Thus a good knowledge of the stability criterion and a thorough knowledge of the vortices is a must, prior to any measurements.

(5) The concentric cylinders are based on the assumption that the cylinders are infinite in length. The finite dimension of the cylinders in practice, leads to end effects which manifests as an increase of torque measured by the equipment, necessitating the correction of the data, either by modifying the shape of the cylinders (Mooney, 1936; Mooney and Ewart, 1934) or calculating the end effect by altering the height of liquid in the gap (Highgate and Whorlow, 1969; Van Wazer, 1963).

(6) Care must be taken to calculate the necessary gap between the concentric cylinders based on the material being tested. Too narrow a gap for materials with large grains, like semi-solid processed metallic alloys, leads to erroneous measurements which vitiate the data collected.

Having described the various measurement techniques available for conducting experiments with molten metals, it is important to choose an appropriate technique to achieve the aim of the project. Since obtaining a flow curve for molten metals involves the variation of shear rate to higher orders of magnitude in a controlled uniform fashion, the concentric cylinder mechanism would make a suitable technique for conducting this study. Yet, despite the obvious choice, concentric cylinders have not been employed to measure the viscosity of molten metal and metallic alloys. Instead, oscillating type viscometers have been the most common choice. To understand the preference given to oscillating type viscometers, one must discuss the arguments placed against the concentric cylinders technique.

The arguments put forth are:

(1) Alignment of the inner cylinder coaxially to the outer cylinder requires utmost care. If the cylinders are misaligned, the inner cylinder may be held against the outer cylinder due to the high surface tension of metals (Genshaw *et al.*, 1970).

(2) High density of the metals may affect torque measurements by magnifying the end effects and introduce Taylor vortices at lower speeds of rotation compared to water, for the same Reynolds number (Taylor, 1923c).

(3) The surface of the liquid is exposed to the atmosphere, which leads to oxidation of the sample.

(4) Any slag formed on top of the liquid metal will influence torque measurements by the inner cylinder.

(5) Uniform rotation of the rotating outer cylinder is often difficult to maintain (Genshaw *et al.*, 1970).

From these arguments, it is evident that there are factors in concentric cylinders technique which will affect viscosity measurements when testing liquid metals. Thus a detailed understanding of these important factors is crucial before proceeding further. The following section describes the different factors along with relevant techniques to overcome them.

2.5 Factors affecting concentric cylinders measurement

The factors which affect measurements in concentric cylinders technique arise from the finite size of the concentric cylinders, the inherent inertia of the liquid being tested, shearing of the liquid in the gap when the cylinders rotate and the presence of foreign solid particles within the liquid. Based on these causes the factors which have profound effect on the results obtained from the equipment are described below.

2.5.1 Eccentricity

An important requirement in concentric cylinders method while measuring the rheological properties of fluids is to ensure that the fluid flows in a steady, laminar and isothermal manner (Van Wazer, 1963). This requires the cylinders to be concentric with each other. In other words, the axes of rotation of the cylinders must be the same.

But in the laboratory, making the two cylinders perfectly concentric requires great care. In most cases the axes are displaced with respect to one another by a finite distance (Fig. 2.17, a) or are inclined to each other (Fig. 2.17, b). This state is called 'eccentricity'. Eccentricity between the cylinders changes the velocity profile of the liquid leading to formation of 'saddle points' (Saatdjian and Midoux, 1992), thereby altering the torque measurements. In molten-metal experiment, eccentricity leads to the inner cylinder being pulled to one side, owing to the high surface tension of the molten metals or alloys, leading to touching of the two cylinders (Genshaw *et al.*, 1970). This can lead to severe oscillations in the torque measured leading to a failed experiment. One such example is presented in Fig. 5.4. Several correction techniques have been developed to obtain the correct torque reading from the observed values (Pinkus and Sternlicht, 1961; Inglis, 1939). These equations involve accurate measurements in the equipment. For example in the correction formula by Pinkus and Sternlicht (Pinkus and Sternlicht, 1961);

$$\frac{M}{M_o} = \frac{2\left[1 - \left(\bar{a}/\overline{\Delta R}\right)^2\right]^{1/2}}{2 + \left(\bar{a}/\overline{\Delta R}\right)^2}, \qquad (2.17)$$

measuring the term $\bar{a}$ is crucial in calculating the actual torque, but this measurement is quite difficult at times, owing to the dimensions of the equipment at hand.

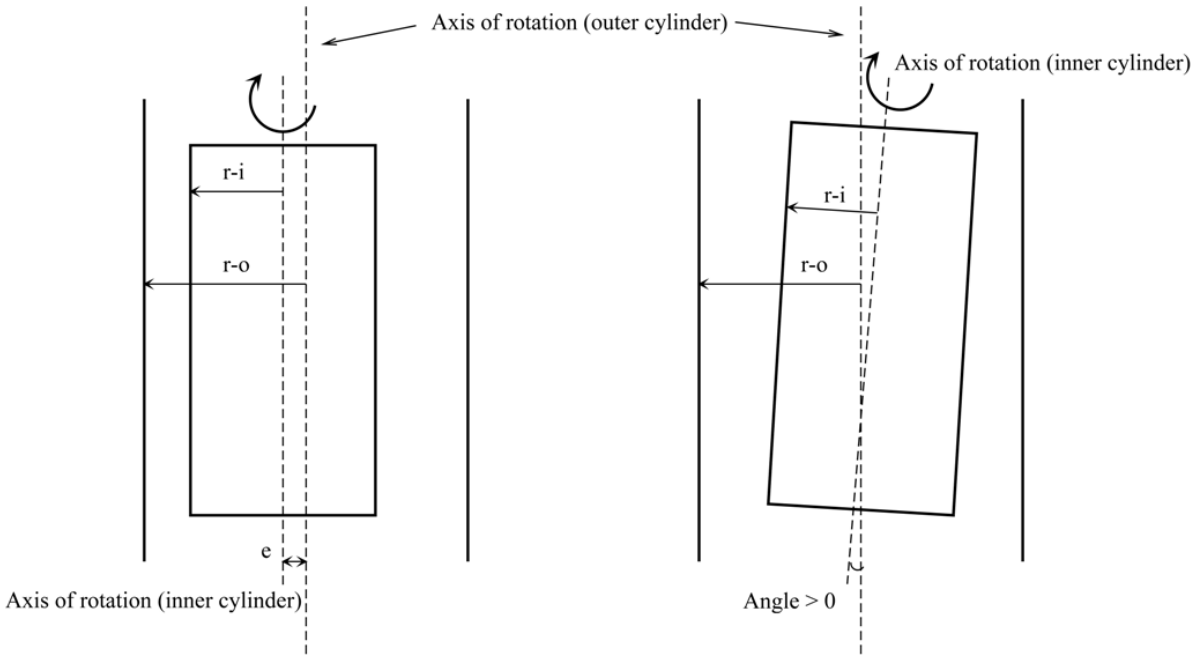

Fig. 2.17. (a) Eccentricity due to axes of the two cylinders displaced by a distance 'e'. (b) Eccentricity due to the axes of the two cylinders inclined at an angle. In this figure r-o represents the radius of the outer cylinder and r-i represents the radius of the inner cylinder.

The situations where measuring the eccentricity becomes difficult, utmost care must be taken while setting up the cylinders, to make them as concentric as possible. This would ensure that the streamlines in the liquid present in the gap are still concentric to each other (Saatdjian and Midoux, 1992).

2.5.2 End effects

The theorems frequently used in the theoretical calculations of the fluid flow within the gaps of the concentric cylinders assume that the cylinders are infinite in length. In Book II, Corollary 2 of the *Principia* (Donnelly, 1991), Newton described the flow of liquid bound by two cylinders, wherein, he called the cylinders to be infinite in length. But in practical applications, finite dimensions of concentric cylinders are employed.

The finite dimension means that the fluid below the inner cylinder in the end gap (gap between the base of the inner and outer cylinder) exerts a torque on the cylinder. Also the shear rate observed in the fluid below the inner cylinder is different from the shear rates in the annular gap between the concentric cylinders. Thus corrections are necessary to calculate the torque which would be recorded if the cylinders were infinite in length. There are two popular correction techniques:

(a) Altering the length of fluid in the gap:

This traditional technique (Bakhtiyarov and Overfelt, 1999), involves measuring the torque at a given rate of rotation of the cylinder with different lengths of fluid in the annulus (Fig. 2.18). A graph of the torque against the immersed length of the inner cylinder should be linear (Whorlow, 1980; Highgate and Whorlow, 1969; Van Wazer, 1963). The slope of the graph gives the required torque per unit length and the intercept on the x-axis (length of immersion) gives the correction height which must be added to the length in equation 2.14. This correction height obtained holds true for a specific rate of rotation and end gap.

(b) Altering the design of the cylinders:

Besides the traditional technique described above to calculate the end effect correction, different designs of the inner and outer cylinder have been employed to reduce the effect from the fluid in the end gap. Some techniques include: air bubble at the end of inner cylinder, double concentric cylinders and altering design of the cylinders. Introducing a conical slope at the end of the inner cylinder was introduced by Mooney and Ewart (Mooney and Ewart, 1934). This modification aims to ensure the shear rate is uniform throughout the body of the fluid, even in the region under the inner cylinder. It has been described as a 'conicylindrical viscometer' (Mooney, 1936). A modified equation for calculating the taper angle at the end of the inner cylinder has been employed in this study.

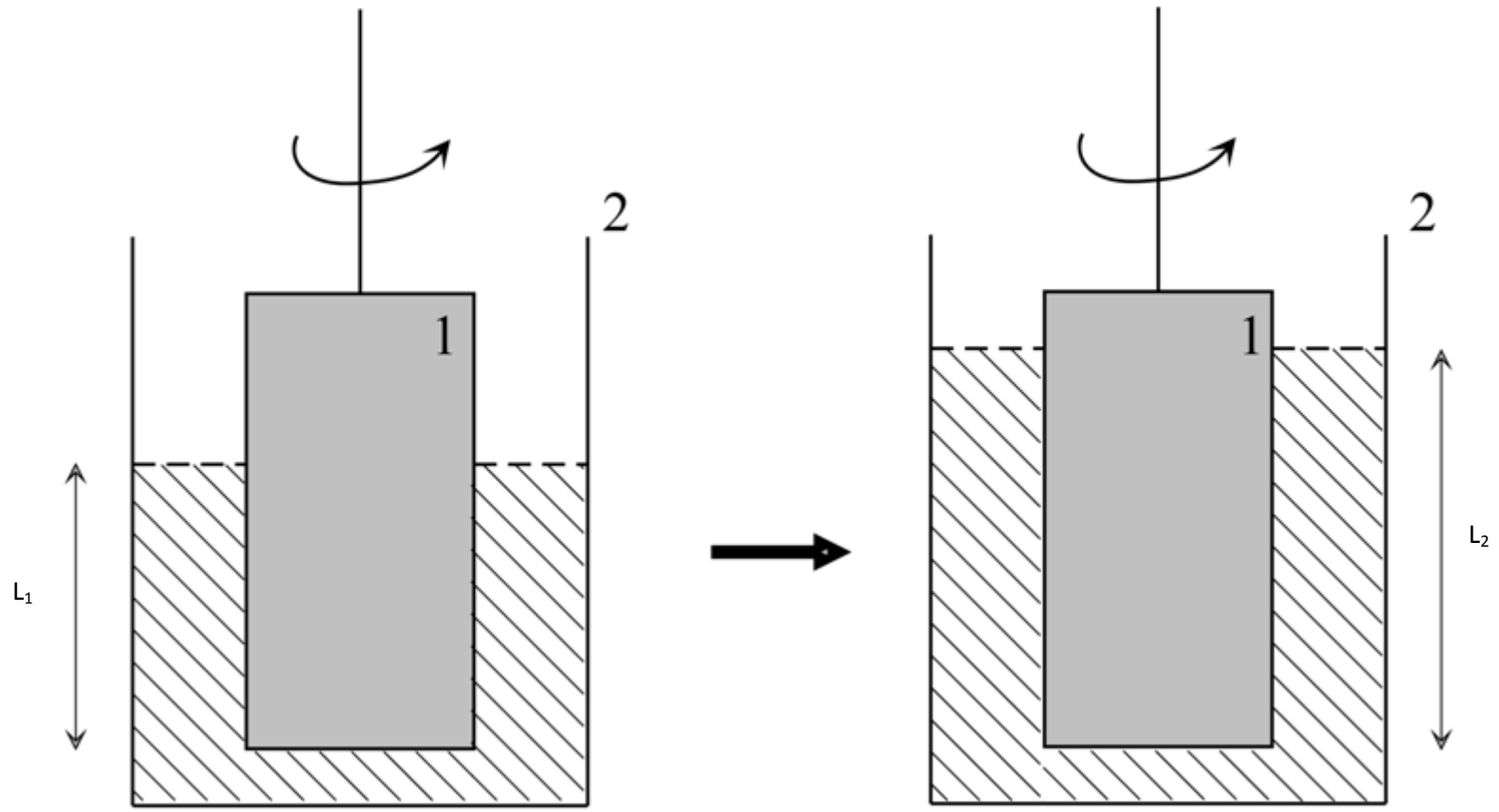

Fig. 2.18. Variation of length of liquid in the annular gap between concentric cylinders and measuring the torque on the inner cylinder (marked as 1) keeping the outer cylinder (marked as 2) fixed for obtaining end effect correction. The same procedure can be employed for the case with outer cylinder rotating. The torque generated on varying the lengths of liquid is plotted against length of inner cylinder immersed (marked L1 and L2).

The angle is calculated from (Mezger, 2006):

$$\alpha = \frac{{\delta_{cc}}^2 - 1}{{\delta_{cc}}^2 + 1} \tag{2.18}$$

where, α is in radians (Fig. 2.19) and δ_{cc} is the radius ratio, hence dimensionless.

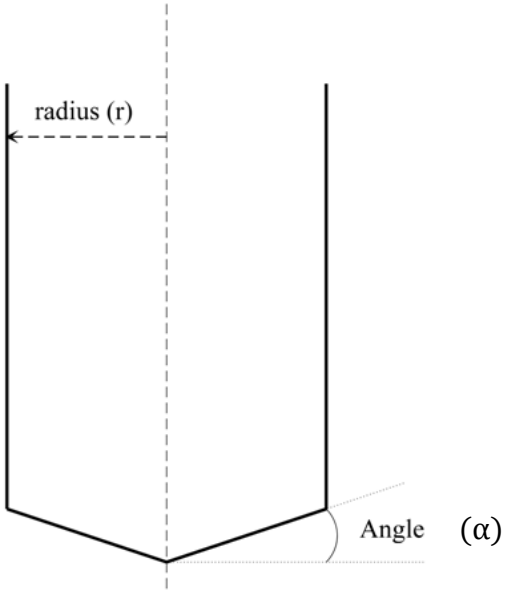

Fig. 2.19. Mooney and Ewart's (Mooney and Ewart, 1934) conicylindrical inner cylinder illustrating the conical slope at end of the inner cylinder with radius (r).

2.5.3 Inertial effects

The inertial forces within the fluid, enclosed in the annulus of the concentric cylinders, play a vital role in determining the stability of the fluid during an experiment. Based on which cylinder rotates, the inertial forces play different roles in maintaining the required laminar flow within the fluid. With the inner cylinder rotating, the fluid near the inner cylinder tends to move outwards (Whorlow, 1980)(Macosko, 1994) but the presence of the outer cylinder prohibits this movement. Thus the fluid starts circulating outwards locally in a small axisymmetric cellular secondary motion known as Taylor vortices (Macosko, 1994). These Taylor vortices (Fig. 2.20) dissipate energy and lead to the increase in the measured torque values (Drazin and Reid, 2004; Collyer and Clegg, 1998).

For formulating the equations of flow, a laminar flow is assumed. To check this assumption, the Reynolds number (Re) for the fluid is calculated; well defined for Newtonian fluids in concentric cylinders (Mezger, 2006; Van Wazer, 1963):

$$\mathrm{Re} = \frac{\Omega\rho\left(\mathrm{R_c^2} - \mathrm{R_b^2}\right)}{2\eta} \text{ or } \mathrm{Re} = \frac{\rho\Omega(\mathrm{R_c} - \mathrm{R_b})\mathrm{R_c}}{\eta}. \tag{2.19}$$

Taylor (Taylor, 1923c), demonstrated the stability of the fluid (in his case: water) in the annulus and proved that at specific speeds Taylor vortices are introduced into the system, thereby increasing the torque and producing an apparent shear thickening behaviour (Collyer and Clegg, 1998). The criterion is given by the equation (Taylor, 1936):

$$\mathrm{P} = 0.0571\left(1 - 0.652\frac{\Delta}{\mathrm{R_b}}\right) + 0.00056\left(1 - 0.652\frac{\Delta}{\mathrm{R_b}}\right)^{-1}, \tag{2.20}$$

where,

$$\mathrm{P} = \frac{\pi^4\nu^2(\mathrm{R_c} + \mathrm{R_b})}{2\Omega^2\Delta^3\mathrm{R_b^2}}. \tag{2.21}$$

This criterion helped the formulation of the Taylor Number (Ta) (Macosko, 1994) employed in calculating the criterion of stability. Defined as:

$$\mathrm{Ta} = \frac{\rho^2\Omega^2(\mathrm{R_c} - \mathrm{R_b})^3\mathrm{R_b}}{\eta^2}, \tag{2.22}$$

the Taylor Number predicts the onset of Taylor vortices for inner cylinder rotating concentric cylinders technique, even when the flow is laminar in nature. (Atkinson, 2008) list the importance of dimensionless numbers in predicting flow behaviour.

- For inner cylinder rotating: Ta > 3400 – introduction of Taylor vortices; flow laminar.
- For outer cylinder rotating: Re > 50000 – laminar to turbulent transition; no vortices.

It should be noted that presence of Taylor vortices within a fluid system is not the same as "turbulent". These vortices exist in a laminar flow condition within the fluid in question. Some researchers often use the term "turbulent flow" despite their results demonstrating the presence of Taylor vortices. This must be avoided since the two terms are not the same.

In comparison to the flow between the cylinders when the inner cylinder rotates, when the outer cylinder is rotated, the inertial forces stabilize the flow through the centrifugal action, thus leading to the transition from laminar to the turbulent state at a much greater Reynolds number than for the inner cylinder rotating (given in page 46). This is demonstrated by the Andereck diagram (Fig. 2.15). Traversing along the x-axis, the Reynolds number of the outer cylinder is increased, keeping the inner cylinder fixed; whereas traversing along the y-axis the Reynolds number of the inner cylinder is increased, keeping the outer cylinder fixed. Fig. 2.15 clearly represents the wide range of vortices which are introduced when the inner cylinder rotates compared to the absence of vortices when the outer cylinder rotates.

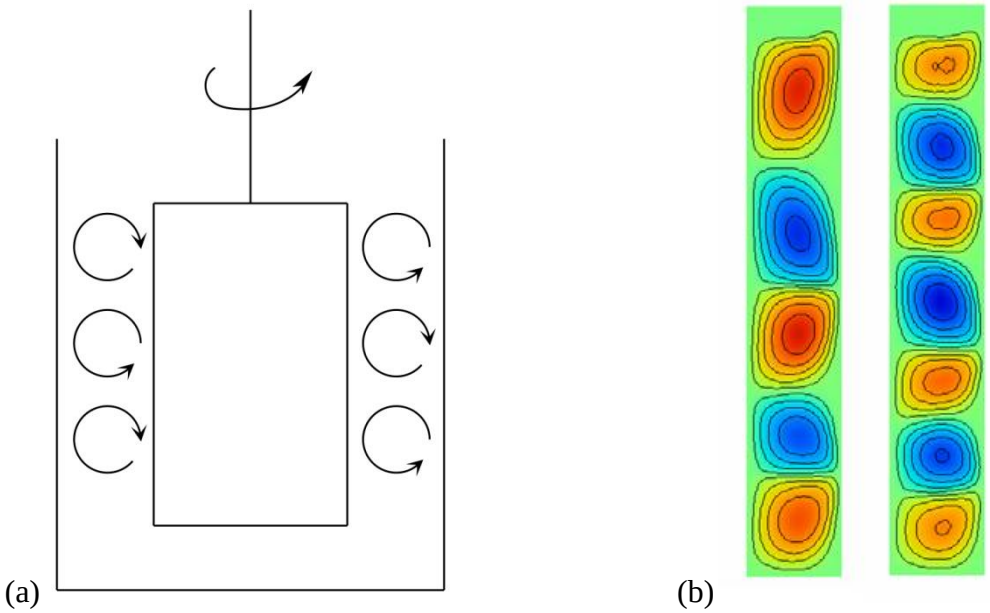

Fig. 2.20. (a) Schematic representation of Taylor vortices in the annular gap of concentric cylinders during rotation of the inner cylinder. (b) Taylor vortices in annular gap with 5-cell and 7-cell mode during rotation of inner cylinder (Watanabe, Toya and Nakamura, 2005).

2.5.4 Viscous heating

The fluid in the annulus of the concentric cylinders is under a shearing action when the cylinder rotates. This shearing action generates heat due to the mechanical energy dissipation

involved. Thus there is a temperature rise within the fluid. Since viscosity of the fluid decreases exponentially with temperature (Andrade, 1952), this temperature rise leads to a decrease in torque measured and thus decrease in the shear stress. To avert this issue in concentric cylinders, the following steps can be taken:

(a) Decreasing the annulus thickness enables the fluid in the gap to dissipate the heat generated throughout the fluid uniformly despite the low thermal conductivity of some fluids.

(b) Constructing isothermal walls for the cylinder to enable the dissipation of heat from the fluid to the body of the machine and subsequently cooling the body would help remove the excess heat from the system.

(c) Calculating the exact contribution from the viscous heating to the change in torque measurements. Palma et al.(Palma, Pezzin and Busulini, 1967), have presented the change in torque readings in a fluid obeying the power law (also applicable for Newtonian fluids) as a function of its radii.

$$T_{R_b} - T_r = \frac{M^2}{8\pi^2 h_0^2 k R_b^2 \eta}\left[\ln\left(\frac{r}{R_b}\right) - \frac{1}{2}\left(\frac{r^2 - R_b^2}{r^2}\right)\right] \qquad (2.23)$$

Other calculations using Brinkman number (Papathanasiou, 1998; Macosko, 1994), have also been employed to correct the torque values obtained.

2.5.5 Presence of solid particles

Measuring the viscosity of fluids employing concentric cylinders, does not take into consideration the presence of solid particles within the system. The presence of such solid particles affects the torque readings; the particles may coagulate leading to blockage in

narrow annuli. In this study involving molten metals, considerable care has been taken to prepare samples as free from oxides as possible. But completely removing oxide particles from the melt is extremely unlikely. Thus some thought must be given to the effect of these solid particles on fluid viscosity.

The first theoretical study of the viscosity of solid suspensions in a fluid medium was performed by Einstein in 1906 (Einstein, 1906). Under the assumption that the particles were spherical in shape and their volume was very small compared to the media in which they were dispersed, Einstein calculated the effective viscosity of the suspension as:

$$\eta = \eta_o \left\{1 + 2.5 \frac{\upsilon}{V}\right\} \qquad (2.24)$$

Further to Einstein's work, Booth extended the work to higher number of terms within the parentheses, thereby increasing the accuracy of the equation (Booth, 1950). The equation 2.24 suggests that with increase in volume content of the solid particles, the viscosity of the suspension will rise. This suggestion was confirmed in the results by Arkharov et al. who studied the effect of inclusions in molten steel employing an oscillating type viscometer to conduct the experiments (Arkharov, Yershov and Novokhatskiy, 1971). They demonstrated the rise in viscosity values of the molten steel by addition of both corundum and vitreous silica. By using different amounts of inclusions they have shown the rise of viscosity with increase in the amount of inclusions. Also, the effect of the structure of the inclusion on the viscosity of the melt has been demonstrated by comparing addition of corundum and silica.

In the above mentioned studies, the inclusions are unchanged by the melt in both their content and mean size. These inclusions exist as solid particles suspended in a fluid phase. But, at times, the inclusion reacts with the fluid medium leading to change in viscosity. The paper by Vignau et al. (Vignau, Azou and Bastien, 1967), demonstrated the effect of flux on

molten aluminium. The reduction of viscosity with the flux is crucial for the aluminium industry, owing to the change of 20% in viscosity values demonstrated by Vignau et al. This change in viscosity readings with the presence of flux indicates a dependence of the viscosity measurement on the surface characteristics of the melt.

Apart from the experimental study involving viscosity measurements, owing to the importance of viscosity of liquids in this study, a deeper understanding of the viscosity from an atomic perspective is necessary. In particular, a look at the viscosity of molten metals from the atomistic point of view is also important.

2.6 Structure of molten state metals and viscosity

The viscosity of molten metals can also be studied microscopically. Molten metals are monoatomic liquids in which the physical property of viscosity is due to a communication of momentum from one layer of liquid to another (analogy of considering that a liquid consists of layers, Fig. 2.1). Andrade believes that unlike Maxwell's theory of gaseous viscosity, which states that the momentum transfer in gases occurs due to movement of the equilibrium position of atoms from one layer to another, the liquid viscosity arises due to the momentum transfer by a temporary union at the periphery of molecules in adjacent layers owing to the large amplitude of the atomic vibrational motion (Andrade, 1934).

Andrade then went on to derive the viscosity of the molten metals from terms which are not related with viscosity measurements. His formula:

$$\eta = 5.1 \times 10^{-4} \frac{(A_m T_m)^{1/2}}{V_A^{2/3}} \tag{2.25}$$

was successfully employed to obtain viscosity values for molten Hg, Pb, Sn and Cu to a high degree of accuracy. From equation 2.25, it is evident that the viscosity of the metal would depend on its atomic weight, melting point and atomic volume. This work was later extended by numerous authors (Eyring *et al.*, 1964; Breitling and Eyring, 1972), details of which are illustrated in (Iida and Guthrie, 1988).

Iida and Guthrie (Iida and Guthrie, 1988) have also employed the theory of pair distribution function to propose an expression for the viscosity of molten metals in terms of more fundamental physical parameters such as the pair distribution function and the average interatomic frequency. Obtaining the necessary expressions for each term, Iida and Guthrie gave the following equation:

$$\eta = 4.5\ \nu_o\ P(T) m^a\ n_o^2\ g(r_m)\ r_m^5\ \left(1 - \frac{r_o}{r_m}\right) \qquad (2.26)$$

Tin and lead are taken as examples for comparing equations 2.25 and 2.26. The values for the equations have been obtained from (Iida and Guthrie, 1988). Both tin and lead have approximately close packed crystal structure, enabling comparison of their viscosities.

$A_{m,Sn}$ = 118.71, $T_{m,Sn}$ = 505.08 K, $V_{m,Sn}$ = 16.98 (atomic weight, melting point and atomic volume of tin respectively). $A_{m,Pb}$ = 207.2, $T_{m,Pb}$ = 600.6 K, $V_{m,\ Pb}$ = 19.44 (atomic weight, melting point and atomic volume of lead respectively).

Hence, from equation 2.25, it is calculated that viscosity of lead at its melting point is higher than the viscosity of tin at its corresponding melting point. From equation 2.26, the above conclusion is also reached by obtaining values of the terms in equation 2.26 from Table 2.1 and Table 6.5 in (Iida and Guthrie, 1988). Experimentally, the viscosity of lead is 2.61 mPa.s as compared to 1.81 mPa.s of molten tin (Iida *et al.*, 1975).

Thus, both equations 2.25 and 2.26 are helpful in predicting the viscosity of molten metals by obtaining the terms in their corresponding equation. But, these terms are difficult to obtain at times and involve several assumptions which bring the accuracies of these equations to about ±10%.

In conclusion, while measuring the rheological properties of a fluid medium with concentric cylinders apparatus, the above mentioned factors: eccentricity, end effects, inertial forces, viscous heating and presence of solid particles, must be carefully considered. Corrections or modifications in the results and equipment, respectively, must be undertaken wherever possible, to ensure that errors due to the measurement technique do not affect the results. Based on these factors, the following chapter describes the equipment employed for conducting experiments in this study illustrating the various modifications. The procedure followed to obtain a rheological understanding of the flow behaviour of molten metals in shear has been described step-by-step, giving details wherever necessary.

Chapter 3

Methodology

Two viscometers have been employed in this study to observe the behaviour of metals in their molten state under shear with different shearing mechanisms. Designed at Brunel University in collaboration with Ravenfield Designs, UK, these instruments are both based on the concentric cylinders mechanism. The factors affecting measurements of liquid metals with concentric cylinders, discussed in the previous chapter, have been carefully considered while designing and developing the equipment and the experimental procedure respectively.

3.1 Equipment used

(a) Searle type viscometer.

- Actual equipment (Fig. 3.1, a); Schematic representation (Fig. 3.1, b).
- Rotating inner cylinder.
- Outer cylinder fixed.
- Increasing speed of rotation of inner cylinder ≡ traversing along y-axis of the Andereck Diagram (Fig. 2.15): prone to Taylor vortices.

(b) Couette type viscometer.

- Actual equipment (Fig. 3.2, a); Schematic representation (Fig. 3.2, b).
- Rotating outer cylinder.
- Inner cylinder suspended by torsion wire.
- Increasing speed of rotation of outer cylinder ≡ traversing along x-axis of the Andereck Diagram (Fig. 2.15): Taylor vortices absent.
- 5 sets of inner and outer cylinders geometry considered (Fig. 3.3, a - e).

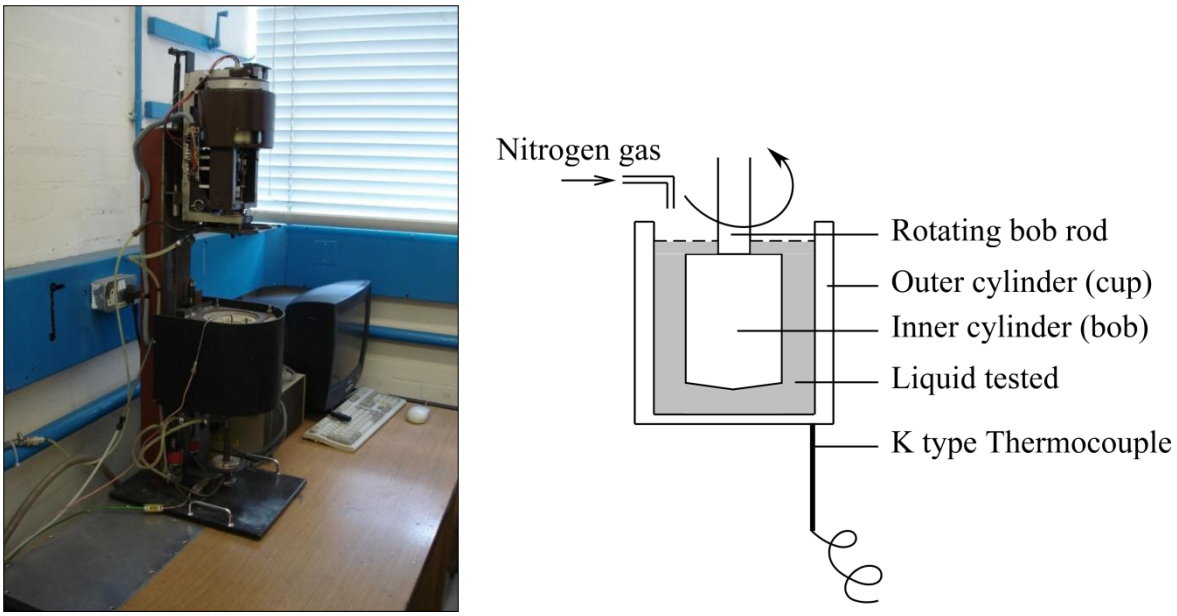

Fig. 3.1. (a) *left*, Actual Searle equipment; (b) *right*, Schematic representation – Searle type. The rotating bob rod is connected with the torque measuring unit which is connected to the computer which records the raw data.

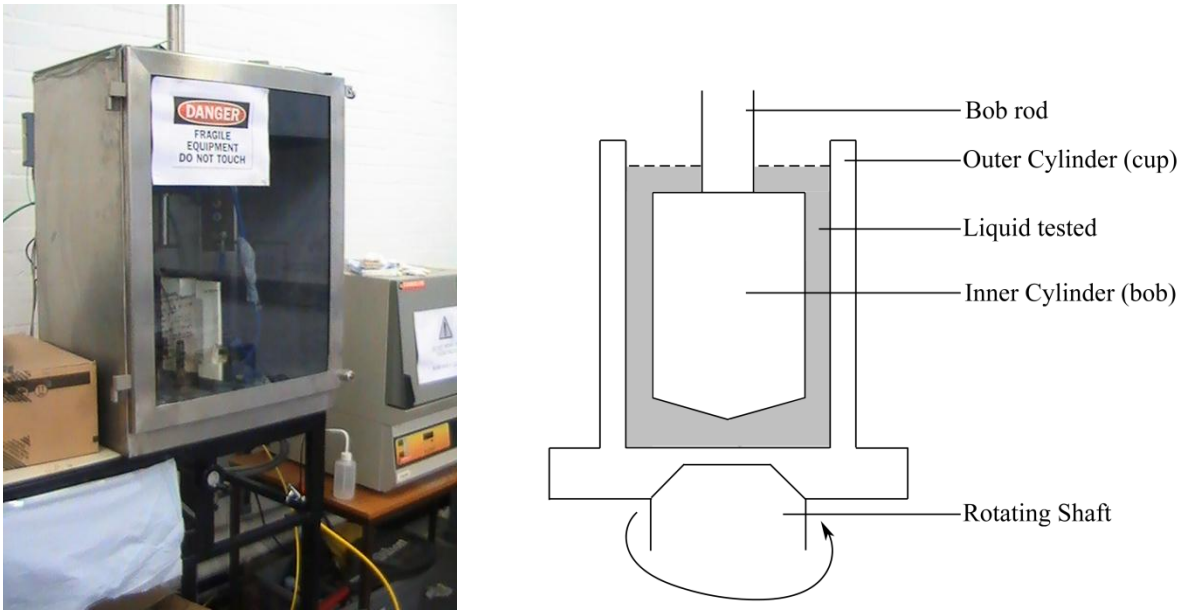

Fig. 3.2. (a) *left*, actual Couette equipment; (b) *right*, Schematic representation – Couette type. The bob rod is attached with the torsion wire which is connected to the torque measuring unit on top of a vertical air bearing. The torque measuring unit is connected to the computer which records the raw data. The arrangement is enclosed in a steel cabinet with a glass front door (inset in left picture) which enables evacuation of the chamber and filling with nitrogen gas during experiments at elevated temperatures.

(a) i. 

ii. 

(b) i. 

ii. 

(c) i. 

ii. 

(d) i.  ii. 

(e) i.  ii. 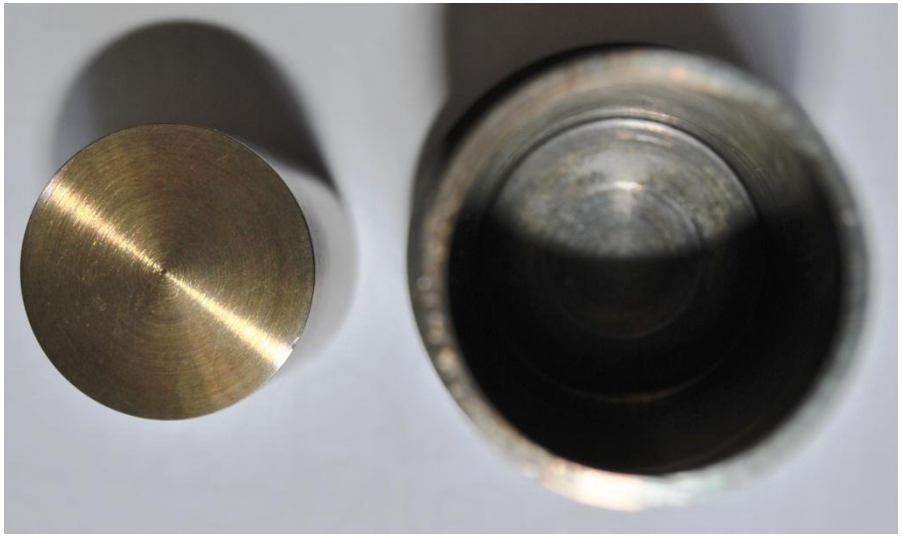

Fig. 3.3. i – Side view, ii – top view for (a) Set 1, (b) Set 2, (c) Set 3, (d) Set 4 and (e) Set 5 employed in the Couette apparatus. The cylinders have been manufactured from Stainless steel grade 316 which has greater corrosion resistance compared to the grade 304.

Description of the Searle and the Couette type viscometers

Along with the summary of the equipment and their components in Table 3.1, a detailed analysis of the equipment is equally necessary.

(a) Searle type viscometer

The Searle type viscometer is primary equipment which consists of a torque measuring unit, which is housed with the motor rotating the inner cylinder. Connected through a steel tube to the inner cylinder, the steel tube along with the inner cylinder can be detached from the torque measuring unit to adjust the concentricity of the inner cylinder with a dial test indicator. The torque measuring unit is connected to the computer through cable wires which transmit the data after passing through an A-D converter. The motor is in a cage supported on precision bearings. The inner and outer cylinders are housed in a muffle furnace open at both ends. Through one end of the furnace, the outer cylinder is raised into position and through the other; the inner cylinder is lowered into position. The lowering and raising of the cylinders is made possible by gears. Attached with the viscometer and the computer is a control box which provides the temperature control, adjustment of the speed of rotation (both increasing from zero and reducing to zero) and control on the duration of rotation. Other details of the equipment can be obtained in (Varsani, 2006).

(b) Couette type viscometer

The Couette type viscometer is primary equipment which consists of a cabinet housed on an iron framework. The cabinet (Table 3.2) consists of steel panels on 5 sides and a glass door in the front. At the bottom of the cabinet, is an opening through which the steel shaft connected to the motor underneath, passes through. The motor, an asynchronous servo motor, enables the rotation of the outer cylinder. The steel shaft

ends in a conical taper which enables fitting the outer cylinder to the shaft. Inside the cabinet, a vertical air bearing, mounted on an iron frame, supports the torque measuring unit. Employing a bob-spider, the bob-rod with the inner cylinder (bob) at one end, is fitted to the air bearing and the torsion wire. On top of the air bearing is the A-D converter and other electronic components. The electronics are also connected to the torsion wire, whose deflection due to the deflection of the inner cylinder immersed in the liquid, measures the torque. Under the glass door of the cabinet, is the control panel of the equipment which controls the temperature, speed of rotation and the option to evacuate the chamber to fill with nitrogen gas: purge. The electronics associated with the control unit, is connected to the computer controller which then monitors the variables through the software. The inner and outer cylinders are enclosed in two halves of the induction electric furnace during an experiment. The copper chilling unit under the vertical air bearing helps prevent the bearing from overheating when the furnace is switched on. The chilling unit cools the air bearing through the continuous flow of water circulating in the chilling unit. The cabinet enclosure when shut, has provision to evacuate the chamber and fill with nitrogen gas during experiments with molten metals.

The software associated with this equipment is in MySQL and enables the user to record the raw torque measured, the speed of rotation of the outer cylinder, control the speed of rotation before an experiment, calibrate the equipment by generating the torque scale and modify temperature of the furnace when the furnace halves are closed. The raw torque data in the software is generated as 1 data point per second. This is the average value of 10 data points which has been collected by the equipment in that 1 second. To avoid an overload of data, the raw torque data generated as 1 data per second has been employed in all calculations of shear stress with the Couette type

viscometer. The speed of rotation of the outer cylinder recorded by the equipment is employed to measure the shear rate within the concentric cylinder walls. The apparent viscosity of the liquid at any given point is a ratio of the shear stress and shear rate at the inner cylinder at that point. The software enables the user to increase the speed of rotation gradually over a fixed duration - ramping up experiment or increase the speed rapidly to a certain value and maintain this speed of rotation for a fixed duration - fixed speed experiment, but is unable to reduce the speed of rotation from a desired value gradually to zero.

Table 3.2. Detailed list describing the components of the Couette type viscometer.

A-D Converter	12 bit converter
Computer controller	Viglen, 2 GB RAM, 2.1 GHz processor
Data acquisition rate	1 data point per second produced (averaged over 10 data points collected in 1 second)
Dimensions of cabinet enclosure	60cm x 60cm x 90cm
Flowing nitrogen gas pressure	5 bar pressure
Materials employed for components	Stainless steel 316 for cylinders, copper for chillers.
Oxygen sensor	International Technologies, GmbH (Type I-01, 480014)
Software base for measurement	MySQL Language
Speed of rotation	0 to 400 rpm
Torsion wires employed	Spring steel. Thin (0.254 mm dia.), Thick (0.4 mm dia.)
Torque constants	Thin (0.045 gm.cm/deg), Thick (0.282gm.cm/deg)
Taper angle at end of bob	2.6 to 2.9^{o}
Torque measuring range	0.839E-04 Nm (thin wire); 9.55E-04 Nm (thick wire)
Volumetric water flow-rate	2 litres/second
Working temperature range	15^{o}C to 450^{o}C

Table 3.1. Comparative summary enlisting the important differences between the Searle and the Couette type viscometers.

Name	Principle of Operation	Outer Cylinder (cup)	Inner Cylinder (bob)	Annular gap = R_c - R_b	Aspect Ratio = Height of bob/annular gap	Height of bob/Radius of bob	Shear Rates (s^{-1})	Name of the set as referenced in text
Searle type viscometer or Rotating bob (inner cylinder) viscometer	Inner cylinder rotating with the outer cylinder fixed. Torque measured at the inner cylinder.	25.5 mm radius 36.0 mm height	24.5 mm radius* 32.0 mm height	1.0 mm	32.0	1.3	0 – 2200	Set A
Couette type viscometer or Rotating cup (outer cylinder) viscometer	Outer cylinder rotates with the inner cylinder freely suspended from a torsion wire. Viscous forces cause torque deflections on the inner cylinder which is recorded.	Radius: (i) 13.0 mm (ii) 31.86 mm (iii) 31.86 mm (iv) 10.0 mm (v) 15.0 mm	Radius: (i) 9.5 mm (ii) 30.65 mm (iii) 30.45 mm (iv) 9.0 mm (v) 14.0 mm	(i) 3.5mm (ii) 1.2 mm (iii) 1.4 mm (iv) 1.0 mm (v) 1.0 mm	(i) 2.9 (ii) 19.5 (iii) 16.7 (iv) 50.5 (v) 42.5	(i) 1.05 (ii) 0.77 (iii) 0.77 (iv) 5.61 (v) 3.04	0 – 700	Set 1 Set 2 Set 3 Set 4 Set 5

*Note that the dimensions sets in Searle type and Couette type viscometer are different since experiments with Searle had to be halted after the motor stopped functioning.

3.2 Sequence of experiments

Irrespective of type of instrument employed, the following flowchart (Fig. 3.4) depicts the sequence of experiments conducted for obtaining experimental values for the viscosity of metals in molten state.

Fig. 3.4. Flowchart illustrating the steps involved during the experimental procedure.

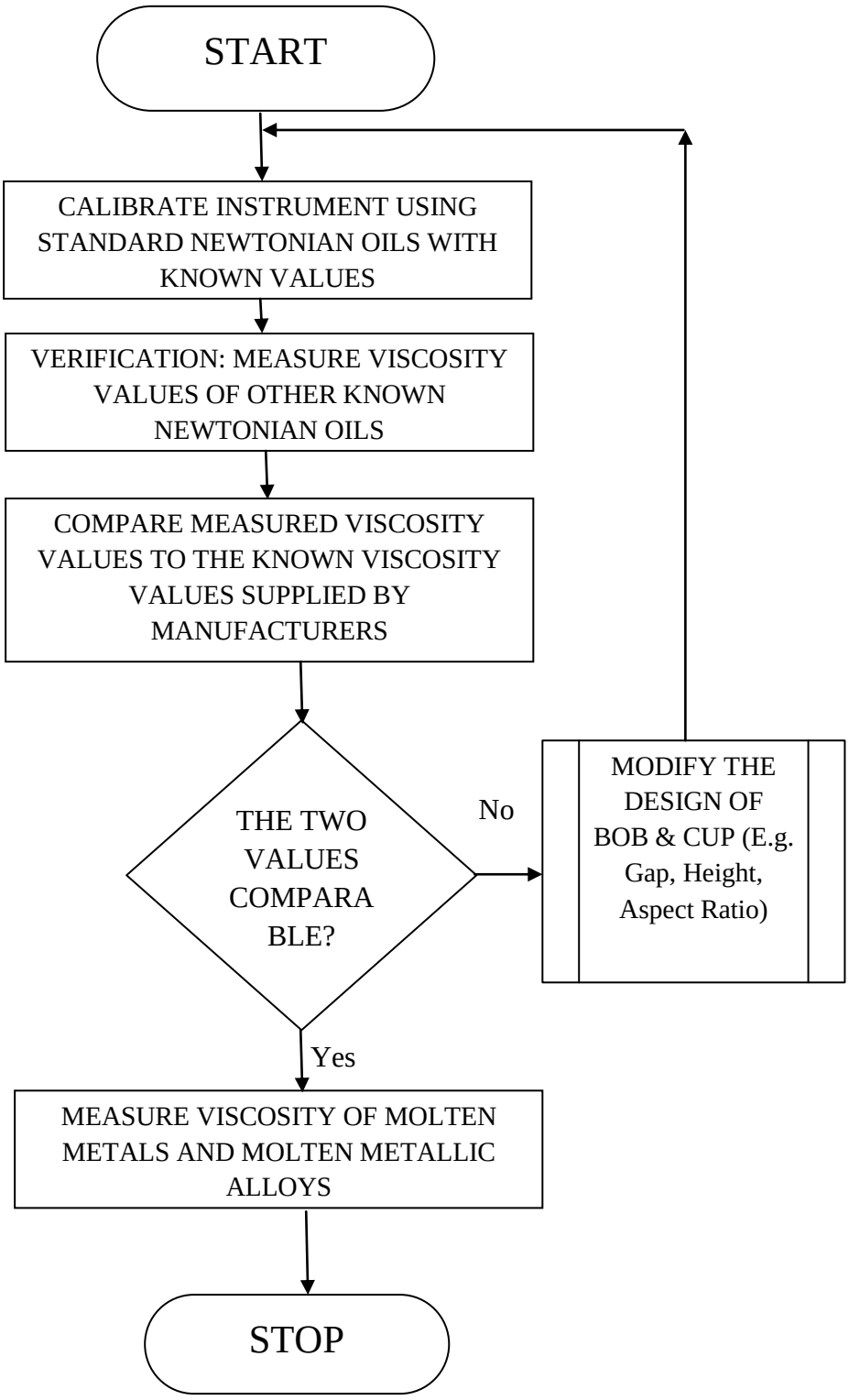

3.3 Materials used for testing

As mentioned in the flowchart above, several standard Newtonian oils have been employed for calibrating and later verifying the instruments. These Newtonian oils were chosen from several others based on their dynamic viscosities. Most metals in their molten state have viscosities ranging from 1 mPa.s to 7 mPa.s. Thus, Newtonian oils with dynamic viscosity close to 3 mPa.s are chosen (Table 3.3). The calibration procedure followed for the Couette type instrument with these standard Newtonian Oils has been described in detail in Appendix I. Certificates of the oils provided by the suppliers are presented in Appendix II.

Table 3.3. List of standard Newtonian oils employed.

Standard Newtonian Oils (code names)	Supplier	Dynamic Viscosity at 20 ^{o}C (mPa.s)	Uncertainty (set by manufacturer)
G3	Ravenfield Designs,UK	3.7	±0.22%
G6	Ravenfield Designs,UK	30.1	±0.22%
D5	Ravenfield Designs,UK	5.8	±0.22%
S3	PSL,UK	3.3	±0.22%
S6	PSL,UK	8.1	±0.22%
PTB Oil 1	PTB, Germany	0.9	-
PTB Oil 2	PTB, Germany	54.2	-

Once satisfactory results were obtained with the oils, metals in their molten state were tested in the equipment. Table 3.4 lists the metals (Sn, Pb) tested in this study, chosen for the wide difference in their densities and similarities in their surface tension values at their melting points (Table 6.1), their low melting points due to low working temperature of the Couette type viscometer (15^{o}C-450^{o}C) and the possibility of the two metals to form a low temperature eutectic alloy (Fig. 3.5). Tin doped with 50ppm germanium (Master Alloy from Imperial College, courtesy Dr. Chris Gourlay) was also tested to observe the effect of altering the surface properties of the melt on the viscosity measurements. Despite their similarities, tin and lead differ significantly also in their atomic weights, which enable comparison between their viscosities based on the works by Andrade (section 2.6). The temperature of the experi-

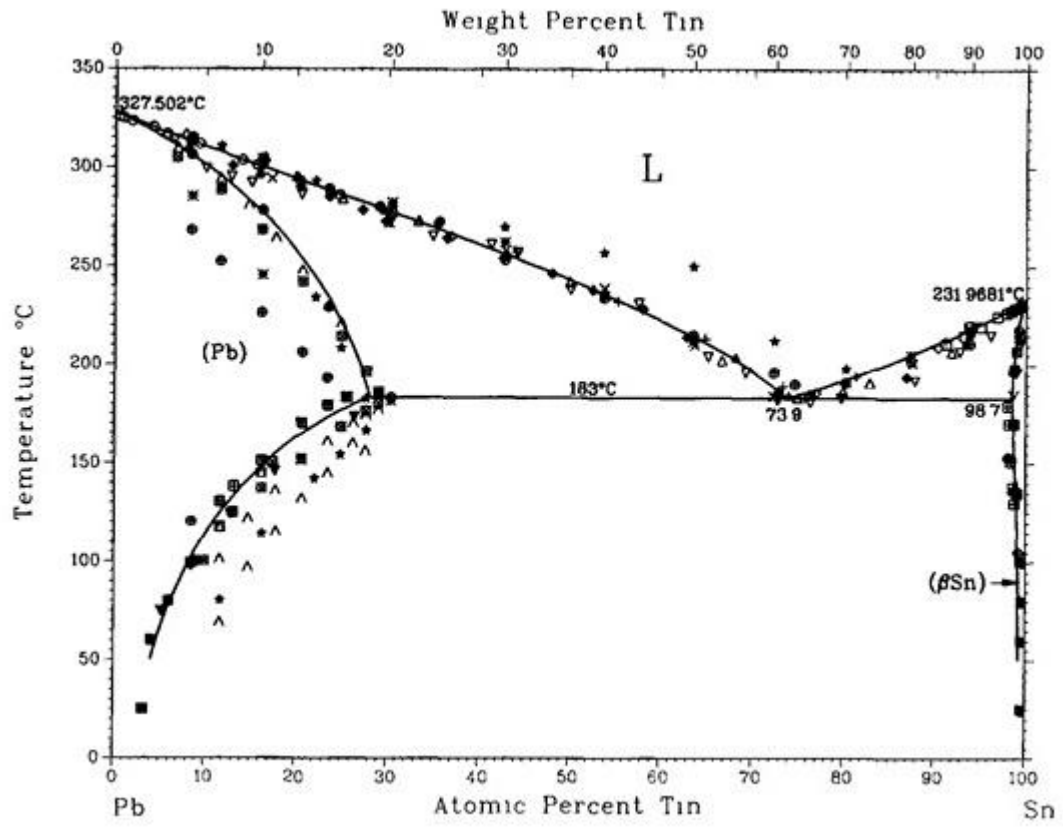

Fig. 3.5. Lead-tin phase diagram (Karakaya and Thompson, 1988)

Table 3.4. List of metals tested in this study.

Name	Viscosity at melting point (mPa.s)	Manufacturer (Purity)
Tin	**1.85**(Thresh and Crawley, 1970), **1.81** (Iida and Guthrie, 1988)	Lowden Metals (99.9%)
Lead	**2.59**(Thresh and Crawley, 1970), **2.61** (Iida and Guthrie, 1988)	Lowden Metals (99%)
Lead – Tin Eutectic Alloy	NA*	Prepared in the lab from the tin and lead from Lowden M.
Tin doped with germanium	NA*	Prepared in the lab from tin from Lowden Metals.

*NA-not available.

-ments was chosen to be 385^{o}C ± 2^{o}C to maintain the molten melt samples at the same temperature to enable comparison. Once the selection of the materials was completed, it was observed that the oxidation of the molten state metals occurs immediately when the melt is exposed to the atmosphere. As mentioned in Table 3.1, the gap between the concentric cylinders at times is 1 mm. When using a narrow gap viscometer, such as the one in this

study, measurements are difficult if the liquid has solid particles, which tend to agglomerate. Since metals in molten state and molten metallic alloys form oxides when exposed to atmosphere, special care has been taken to prepare the raw samples for experiments. The following section describes the steps undertaken during sample preparation.

3.4 Sample preparation for experiments

1. Pieces of raw materials are weighed based on the volume of liquid required to immerse the inner cylinder (bob) surface in the molten melt. This volume varies from one set of concentric cylinders to the next.

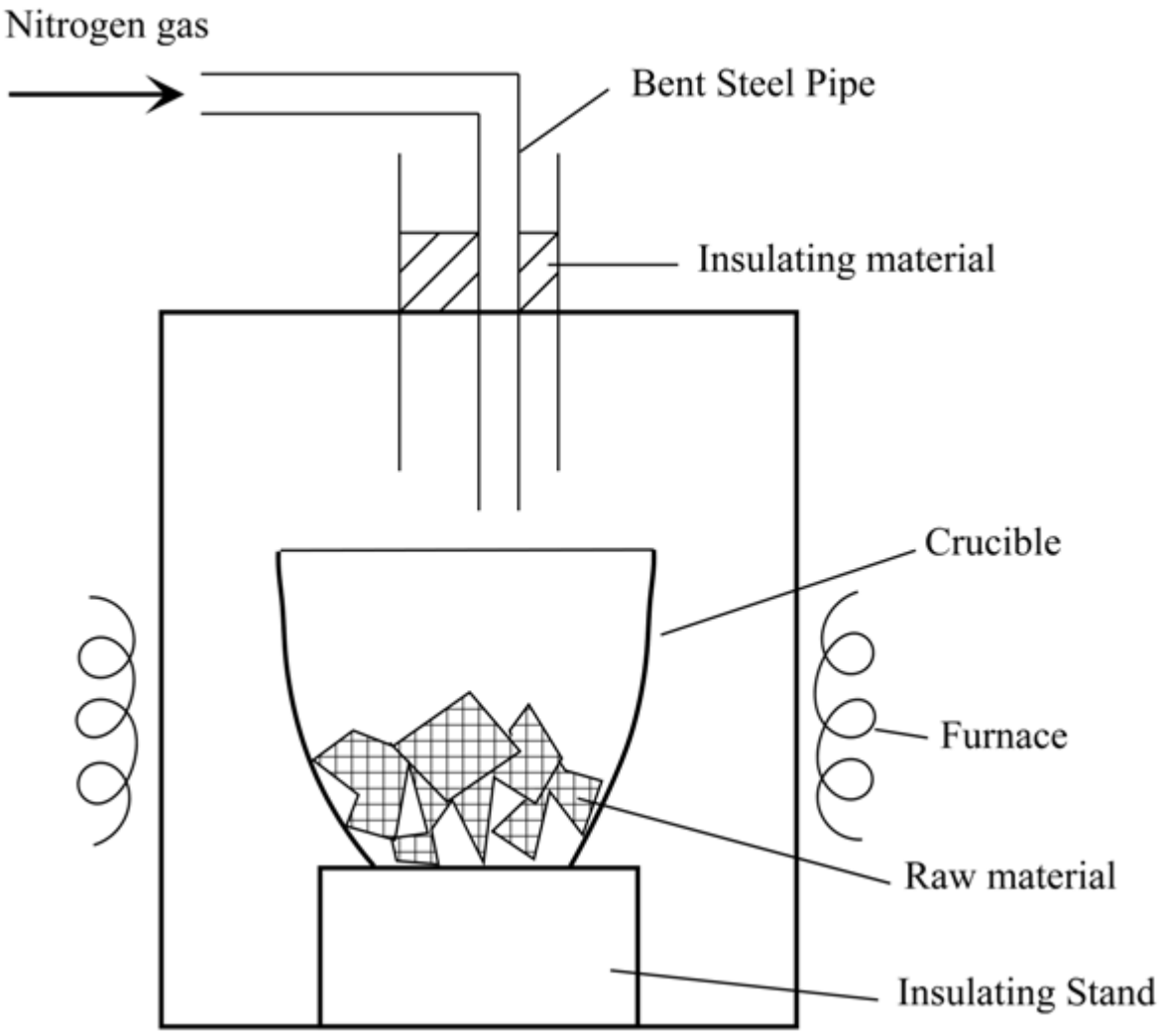

Fig. 3.6. Illustration of experimental arrangement while casting the samples for testing viscosity of molten state metals or their alloys.

2. An additional 5% by weight of the raw materials are prepared to compensate the loss of material due to oxidation during preparation of the sample.
3. The raw materials are placed in a graphite clay crucible which has been pre-heated to 200^{o}C for 1 hour to remove any moisture from the crucible.
4. The crucible is then put into an electric furnace with the temperature set to 100^{o}C above the liquidus temperature of the raw material being melted.
5. A bent steel pipe carrying Nitrogen gas (99.998 % purity, oxygen free nitrogen, BOC Limited, UK) is introduced to the mouth of the crucible to enable nitrogen gas to flow constantly to the surface of the melt to provide an inert atmosphere. A schematic representation of this arrangement is given in Fig. 3.6.
6. Once the raw materials are melted, the crucible is removed from the furnace with the pipe carrying the nitrogen gas still at the mouth of the crucible. Under the atmosphere of Nitrogen gas, the surface of the melt is skimmed to remove the dark oxide residue from the melt.
7. After skimming the surface, the melt is poured into the preheated stainless steel outer cylinder (heated to 200^{o}C for 1 hour to remove moisture) which would be later employed for conducting the rheological experiment.
8. The sample is cooled down to room temperature in the Nitrogen atmosphere, both the outer cylinder and the sample are separated and cleaned thoroughly with ethanol and dried in an oven set at 105^{o}C for 1 hour.
9. After the sample is dried, the inner and outer cylinders are cleaned thoroughly with soap and 4000 grit carbide paper to remove any residue which may affect the flow of molten melt during the experiments.
10. The cylinders are then immersed in a bath of ethanol and cleaned with an ultrasonic cleaner. Once removed from the ethanol bath, the cylinders are dried in an oven, set at

105^{o}C, for 1 hour to remove any moisture and are then setup for calibration or verification of the instrument.

This practise was followed before every experimental run to ensure the cleanliness of the surfaces which is crucial for experiments involving viscosity measurements.

3.5 Calculations

This section describes the formulae employed in this study to calculate shear rate and shear stress from the input variables: speed of rotation and the torque, which are measured as raw data from the equipment.

For the Searle system: Since torque is measured at the inner cylinder, the shear stress and shear rate are measured at the inner cylinder too. For the Couette system: despite the outer cylinder being rotated, the torque is measured at the inner cylinder. Thus the shear rate and shear stress must be calculated at the inner cylinder.

Hence, for both the instruments, the shear stress and the shear rate are to be calculated the inner cylinder only.

Shear stress,

$$\tau = \frac{M}{2\pi\, l_b\, R_b^2}, \tag{3.1}$$

Shear rate,

$$\dot{\gamma} = \frac{2R_c^2}{\left(R_c^2 - R_b^2\right)} * \frac{2\pi}{60} * \omega \tag{3.2}$$

(Mezger, 2006; Whorlow, 1980; Van Wazer, 1963).

Thus the viscosity is calculated from the ratio of the shear stress and shear rate (equation 2.14) (Van Wazer, 1963).

3.6 Types of tests

To observe the difference in rheological behaviour in the molten state metals, two different types of tests have been conducted with the liquids in this study. Each test has its own merits, demerits and type of result which are necessary for comparison.

(1) **Fixed Speed Test**: The cylinder capable of rotating is rotated at a fixed speed defined in the software for certain duration of time, usually 2-5 minutes.

Result: The data collected is the torque and speed measured every second. This data is employed to calculate the shear stress and shear rate respectively and then the apparent viscosity (equation 2.14). The average values are obtained over the duration along with their standard deviations.

Merits: The fixed speed test enables the equipment to generate steady and more accurate torque measurements at a set speed of rotation. The steady torque reading thus generates a more accurate shear stress and thus apparent viscosity value along with the standard deviation on that value.

(2) **Ramping Up Test**: The cylinder capable of rotating is rotated from zero to a designated rotation speed (set in the software), in a fixed duration of time. It is also referred as a 'transient state' test since the speed of rotation of the cylinder keeps increasing throughout this test.

Result: Data in the form of the torque on the inner cylinder and speed of rotation is collected every second until the designated speed is attained.

Merits: Due to the variation of speed, the torque readings can be obtained for a wide range of speed of rotations in one test. **Demerit**: Since this test is a transient state test, the inner cylinder is unable to reach a steady state thereby restricting repeatability.

3.7 Temperature calibration of furnace in Couette type viscometer

One of the difficulties of the Couette type viscometer (outer cylinder rotating), with a narrow annulus gap, is the measurement of temperature of the sample held within the two concentric cylinders. Since viscosity of the liquids is dependent on the temperature of the liquid (Andrade, 1952), a temperature calibration experiment of the furnace in the Couette viscometer was conducted. Altering the temperature of the furnace, the actual temperature inside the outer cylinder was measured employing a K-type thermocouple. From this, a plot comparing the set temperature of the furnace and the actual temperature of the sample was prepared. This plot (Fig.3.7) was constructed to enable the user to set a temperature for the furnace during an experiment and calculate the temperature of the sample of molten melt without opening the glass-steel cabinet, which, during an experiment is usually filled with nitrogen.

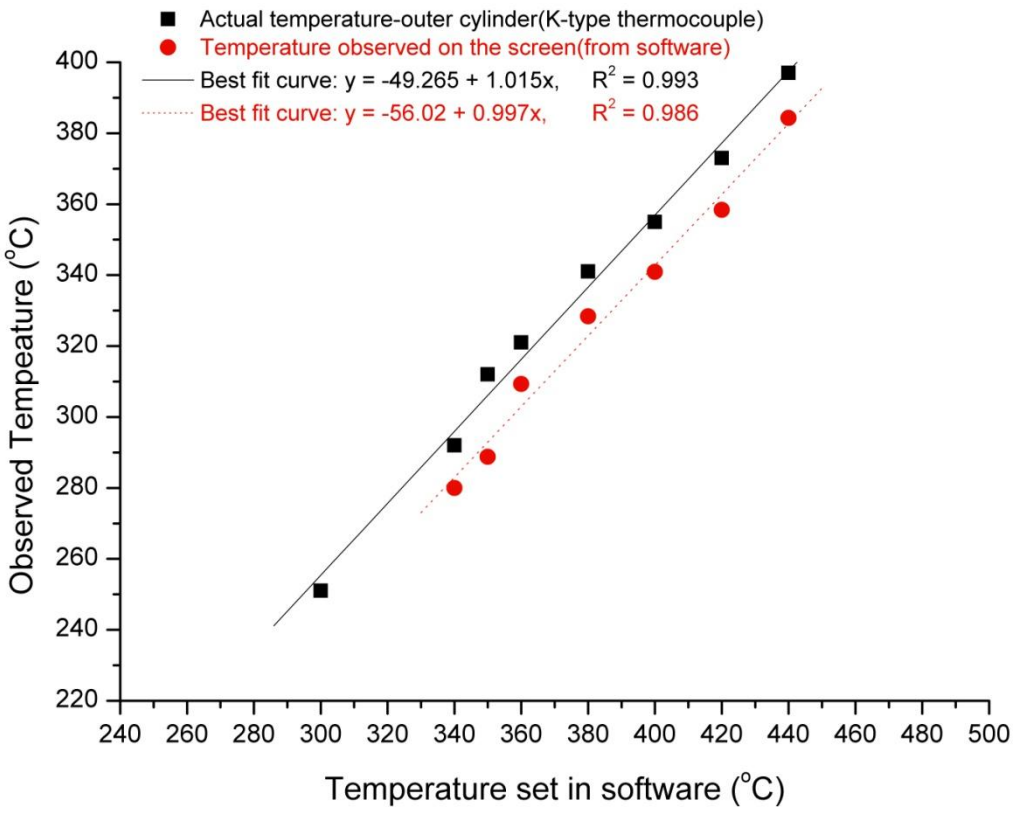

Fig. 3.7. Graphical representation summarizing the variation of the furnace temperature by the user and the corresponding observed actual temperature in the outer cylinder of the Couette type viscometer, measured employing a K-type thermocouple. The temperature was stabilised for 2 hours before measuring the temperature. This plot was employed in the molten metal experiments later on.

3.8 Speed calibration in Couette type viscometer

To ensure the speed of rotation of the outer cylinder set in the software is accurate at any given speed, the rotating cup was tested at various speeds with a photo type Tachometer (Specifications: Eurisem Technics EP – 611). With an empty cup attached to the rotating shaft, the tachometer recorded the speed by measuring the speed of rotation of a piece of illuminated white paper tag attached on the cup, in a series of fixed speed tests. The speed calibration result illustrated in Fig. 3.8 confirms that the motor is accurately generating the desired speed set in the software.

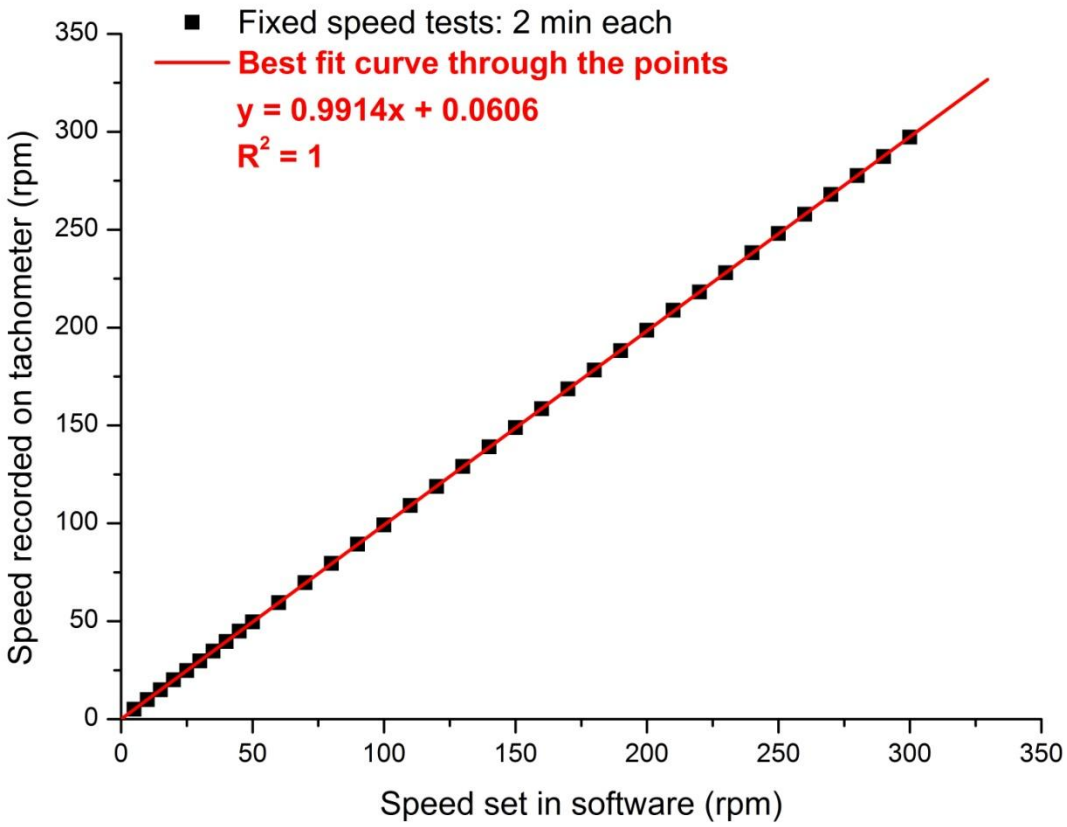

Fig. 3.8. Speed calibration test with a photo type tachometer. Comparative plot of the speed set in the software of the Couette type viscometer against the speed being actually generated by the motor.

The next section discusses the important modifications on the Couette type viscometer which enabled measuring the viscosity of molten state metals.

3.9 Modifications to the Couette type viscometer.

The following modifications improved the measurement technique in the apparatus.

(1) Replacing a mechanical pulley system with a horizontal air bearing.

a.  b. 

c.  d. 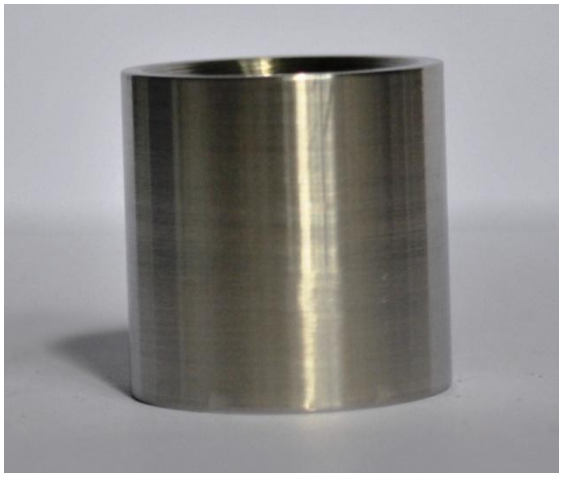

Fig. 3.9. (a). Mechanical pulley system employed to obtain torque scale previously. (b). Main body of the horizontal air bearing. Note the orifices on its body through which nitrogen gas at 3.5 bar atmospheric pressure was passed to elevate outer ring (c). top view, (d). side view, thereby enabling the thread to pass over it while obtaining the torque scale.

A horizontal air bearing was installed in the Couette type viscometer to reduce the internal friction observed in a mechanical pulley used earlier (Fig. 3.9, a). The horizontal air bearing (courtesy Dr. Martin Rides, National Physical Laboratory, London) provided a contactless

technique to obtain accurate and repeatable torque measurements for the torque scale generated during calibration of the machine with weighted washers (Appendix I).

(2) Addition of a mirror to observe liquid surface.

A mirror mounted on a bent steel strip (Fig. 3.10), was attached to the body of the machine to enable the user to observe the surface of the liquid being tested when the two halves of the furnace are closed during experiments with molten state metals or their alloys (Fig. 3.11).

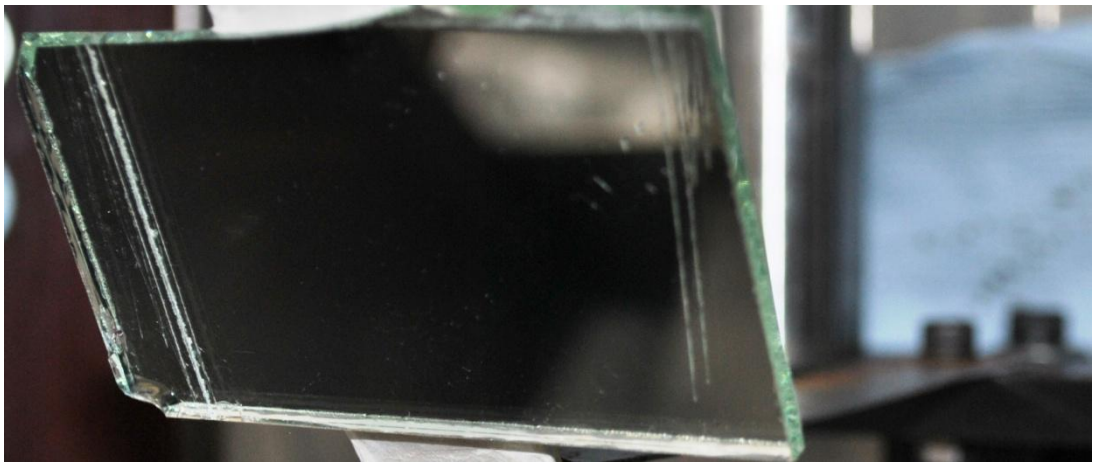

Fig. 3.10. Mirror attached with a steel strip, one end of which is bent at an angle of 45° and the other attached with the body of the Couette type viscometer, seen in the figure as a blue paper towel. With the mirror firmly attached to the body of the viscometer, the surface of the liquid could be observed and recorded during experiments even if the furnace doors were closed.

The mirror enabled the user to view the surface of the molten state metal or alloy with a video recorder for any evidence of vortices or detect reasons for instabilities and noises in the results. This practice has proven crucial for determining causes for any instability in the data recorded during the experiment. Presence of eccentric cylinders, overflow into the motor, misalignment of the cylinders at an angle and spillage (Fig. 3.11, a) could be observed during the experiments thereby enabling the user to stop the experiment and restart after fixing the error. The mirror also enables the user to observe the start of the experiment with molten metal to detect any wall-slip at the molten metal-cylinder wall interface with the naked eye.

(a) 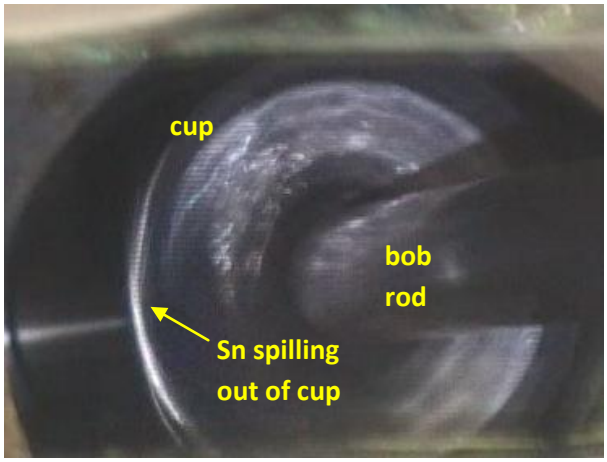

(b) 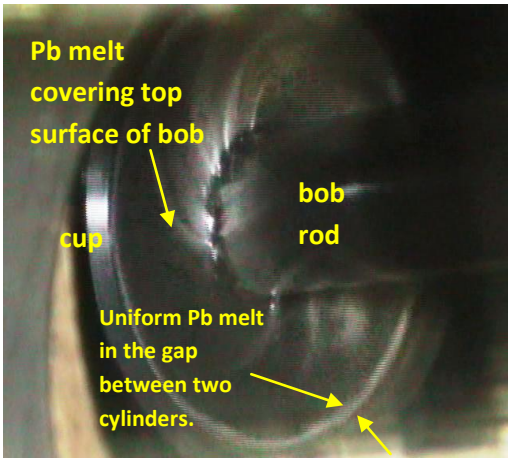

Fig. 3.11. (a) Molten tin experiment in Set 5 inner and outer cylinder with the Couette type viscometer illustrating a spillage incident during an experiment. This view was recorded on video and explained the noise obtained during the experimental run. (b) Molten lead experiment in Set 5 inner and outer cylinder with the Couette type viscometer illustrating the presence of uniform molten melt in the annular gap between the concentric cylinders.

(3) Modified chiller system

The copper chilling unit of the machine, used to prevent the vertical air bearing and the electronics on top of it from getting heated excessively, has been modified from its original design (Fig. 3.12). In the previous design, a copper collar attached to the bob rod dipped into the liquid (usually a standard Newtonian oil) held in the U-shaped trough. But this did not prevent the heat being conducted to the vertical air bearing (Fig. 3.13, marked '1') through the bob rod which was connected to the vertical air bearing at one end. To avoid this, a new copper base (Fig. 3.13, marked '2') was machined and attached directly to the base of the vertical air bearing. This copper base has provisions for cooling water to enter and leave the base (Fig. 3.13, marked '3'), thereby extracting any heat conducted to the air bearing. This ensured a better cooling environment for the air bearing which previously had a tendency to overheat to temperatures above 100^{o}C during experiments with molten state metals and alloys.

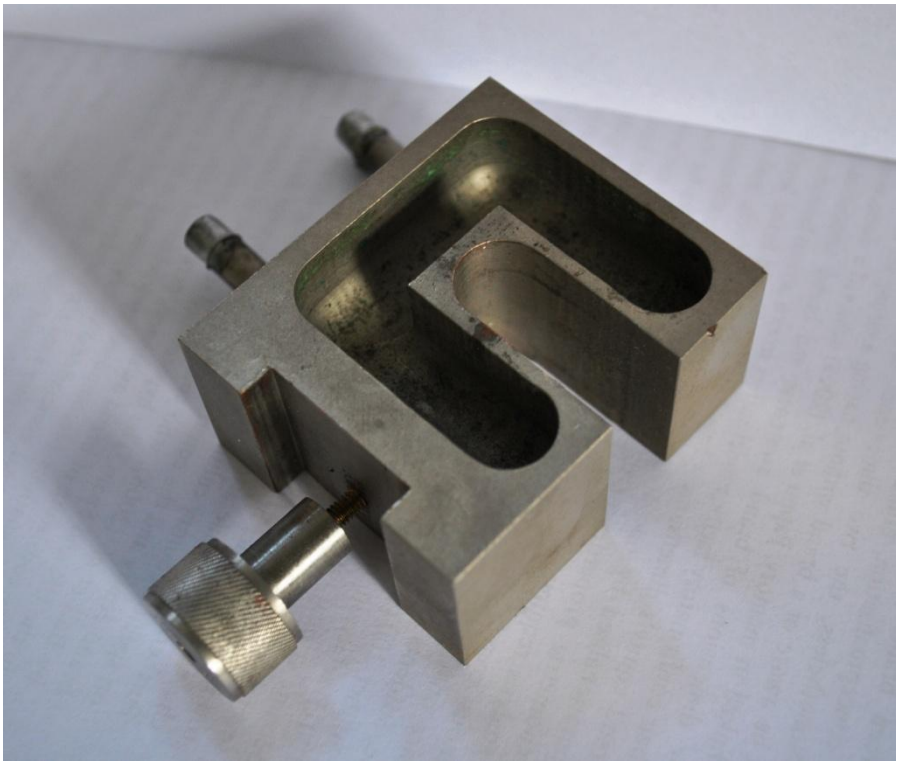

Fig. 3.12. Older version of the chilling unit. The bob-rod had a copper piece which fit in the U-shaped groove, which contained kerosene based oil to provide cooling to the bob.

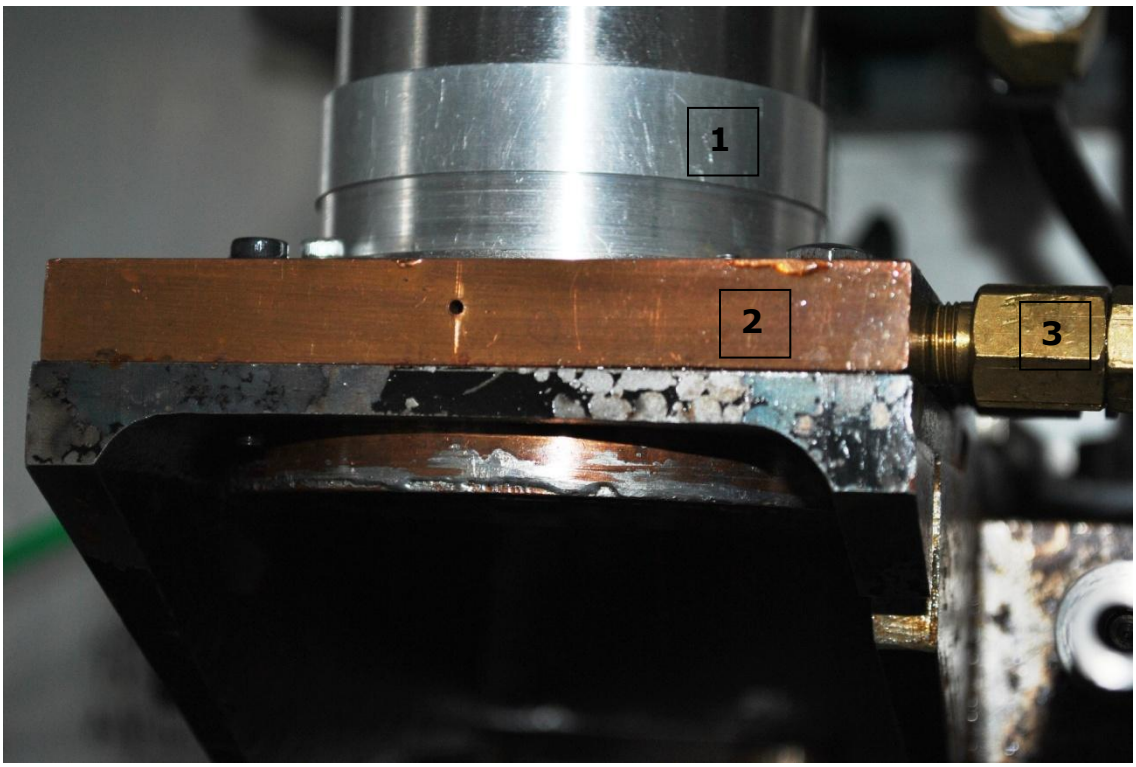

Fig. 3.13. Copper base chiller unit (marked '2') attached to the base of the vertical bearing (marked '1'). Water enters and leaves the unit through pipes connected to the unit (marked '3').

(4) Replacement of the old oxygen sensor with a new version.

During experiments with molten state metals and alloys, the steel-glass cabinet is evacuated and filled with nitrogen gas employing an oxygen sensor attached with a solenoid. The sensor records the oxygen content inside the cabinet in terms of voltage generated. An illustration of the new oxygen sensor is given in Fig. 3.14 (a). The new sensor improved the accuracy of oxygen percentage reading by the software. The variation observed in the % of oxygen is the variation in the voltage reading (in mV) by the oxygen sensor.

Table 3.5. Variation of oxygen content inside the cabinet with the old and new oxygen sensors; assuming a linear relationship between the voltage measured with the solenoid and the oxygen content.

Sensor name	Voltage when cabinet open	Oxygen % when cabinet open (assuming the % of oxygen in atmosphere)	Voltage when cabinet closed, evacuated and filled with N_2	Oxygen % - when cabinet evacuated (assuming the linear relation Appendix II)
Old oxygen sensor	8.14	21 %	1.2 ± 0.2	3.1 ± 0.5 %
New oxygen sensor	8.54	21 %	0.35 ± 0.2	0.86 ± 0.4 %

(a) 

(b) 

(c)  (d) 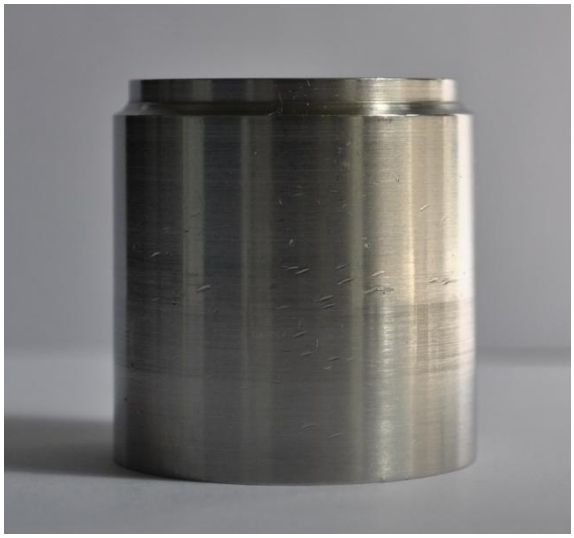

Fig. 3.14. (a) New oxygen sensor. (b) Bob-spider piece (side view) with taper at one end, the other end is attached to the bob rod. (c) Top view of bob-spider piece, the 4 small holes (about 0.5 mm dia) enable attaching the bob rod with 4 screws to the siper. (d) Calibration piece for alligning the inner and outer cylinder of the Couette type viscometer.

(5) Due to incorrect taper angle on the bob-spider (Fig. 3.14 (b), usage described in Appendix I), alignment of the inner cylinder (bob) with the outer cylinder (cup) was impossible. If the bob-spider moved inside the calibrating piece (Fig. 3.14, d) during the alignment of the inner cylinder (bob), the whole procedure had to be repeated from start. This led to the manufacture of a new calibration piece (Fig. 3.14, d) by Hodge Industries, Middlesex, UK after which a more accurate alignment of the inner cylinder with the outer cylinder was made possible.

Apart from the modifications to the Couette type viscometer, several changes were made to the procedure followed for conducting experiments, both during the calibration of the equipment as well as when testing molten state metals. Some of these changes are below:

(i) During the calibration of the equipment (described in detail in Appendix I) the pre-weighted washers employed to obtain the torque scale, were added randomly at first to obtain three readings: 1st with no weights on, 2nd with a random weight and 3rd reading at maximum torque. This procedure increased the error in the torque scale

since a best-fit line through those three points might lay far from the actual desired linear scale, as illustrated in Fig. 3.15.

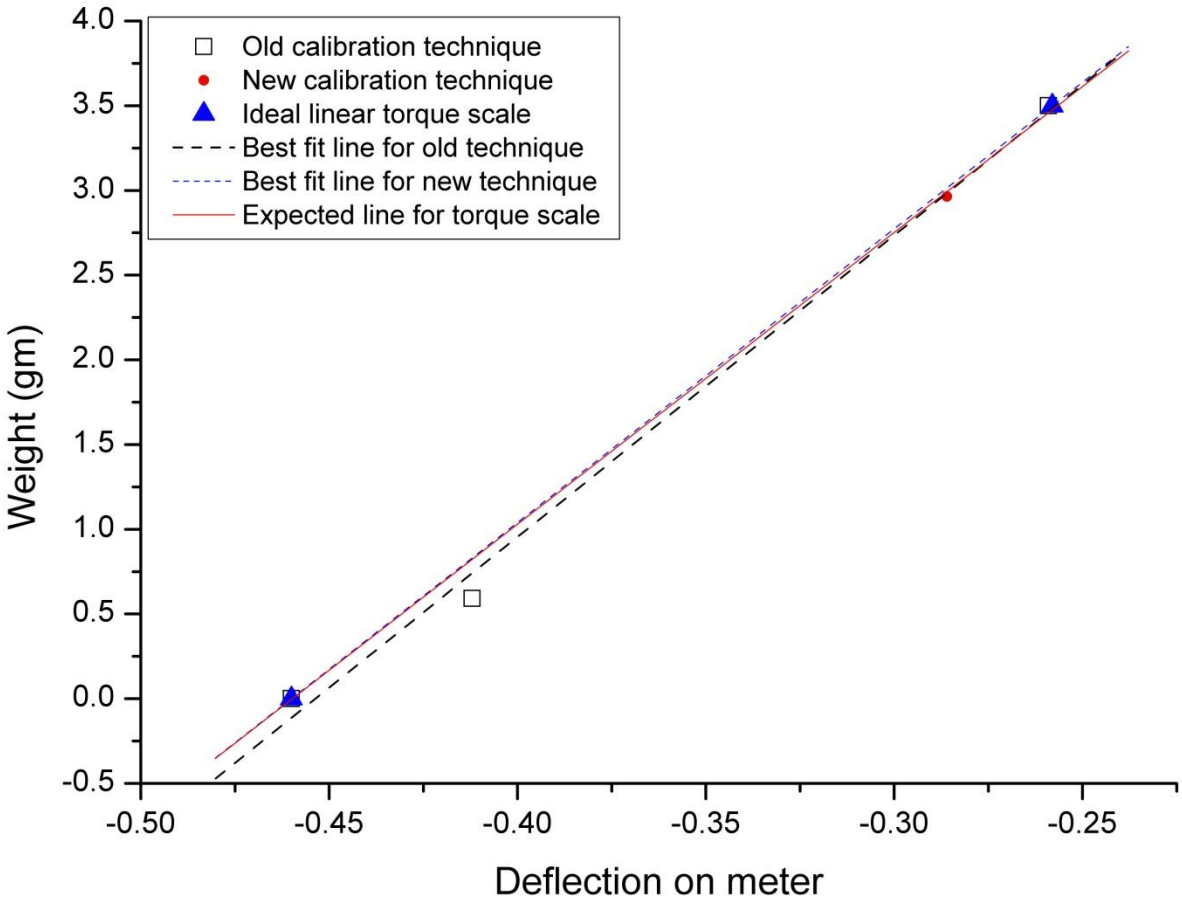

Fig. 3.15. Comparing the old torque scale generation technique with the new version which improved the accuracy of the torque scale obtaining values close to the ideal torque scale (blue curve).

To obtain a more accurate torque scale, the weight added to obtain the second point was such chosen that the torque value from that weight was as close as possible to the maximum torque (Fig. 3.15). This increased the accuracy of the torque scale enabling a better verification result with standard oils and later more accurate results with molten state metals. The improvement in torque scale is illustrated in Fig. 3.15.

With the above mentioned changes and modifications in the Couette type viscometer, experiments were conducted at conditions suitable for measuring the viscosity values of the metals and their alloys in the molten state at high rates of shear. Once these modifications

were done, calibration of the equipment followed by verification, were conducted. This is described in the following chapter. Apart from verification, it is also important to choose the correct geometry for the inner and outer cylinders to measure the viscosity of low viscosity liquids like molten state metals. Also, the factors affecting the measurements in concentric cylinders (described in Chapter 2), have been kept in context while conducting the verification tests discussed in the following chapter.

Chapter 4

Obtaining the right setup: calibration & verification

After completing the modifications in the equipment, it is important to determine the correct measurement procedure and geometry for molten metal viscosity measurements. Generally rheometers employed in studying fluids can generate data in two ways: absolute and relative. Concentric cylinders belong to the relative measuring class. Thus the equipment must first be calibrated, then verified, after which experiments with unknown fluids, in this case molten metals, should be conducted.

4.1 Calibration

Calibration of the equipment is done with Newtonian oils, details of which are given in Chapter 3 of the thesis.

4.1.1 For the Searle type viscometer

- Usual choice of Newtonian oil: D5. Details of procedure in Appendix I.

4.1.2 For the Couette type viscometer

- Usual choice of Newtonian oil: G3. Details of procedure in Appendix I.

Based on the flowchart described in Chapter 3, after any modifications in the components of the Couette apparatus; the equipment was calibrated again to ensure that the torque scale was consistent between runs. The procedure was maintained throughout the study to keep the torque scale repeatable and reproducible.

4.2 Verification

After calibrating the equipment, it is necessary to 'verify' the equipment. For this purpose, other standard Newtonian oils, other than the ones already employed for the calibration of the machine, were employed to check the results generated by the equipment.

4.2.1 Searle type viscometer

The verification of the Searle type viscometer with Set A (Table 3.1), was conducted with the standard Newtonian liquid G6. A ramping up experiment was conducted increasing the speed of rotation to 1000 rpm.

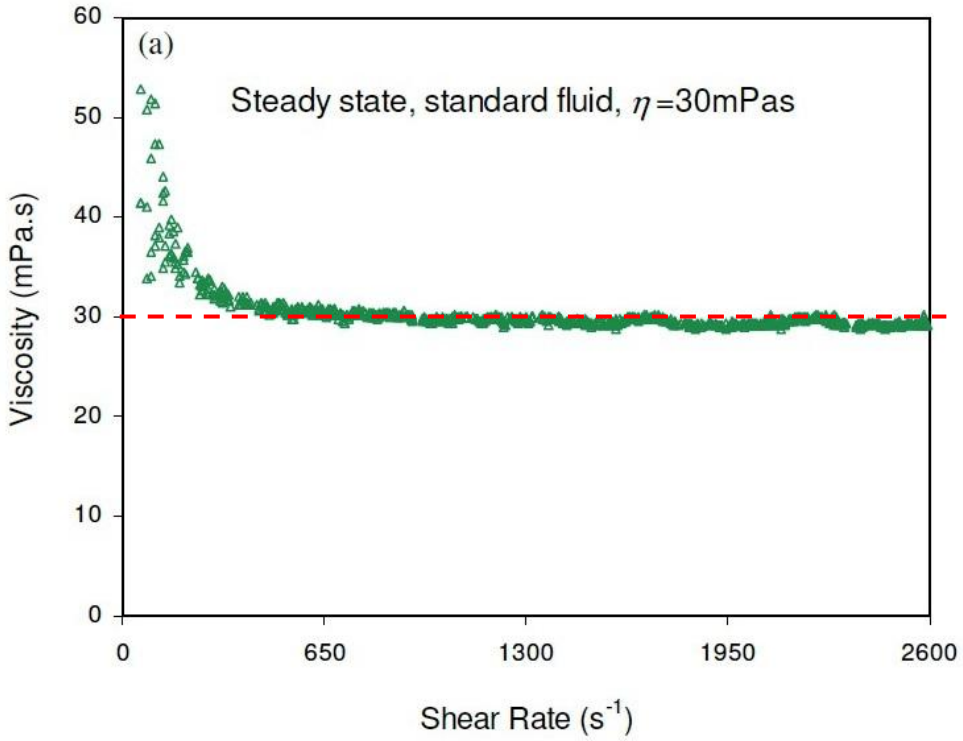

Fig. 4.1 Verification of the Searle type viscometer with standard Newtonian liquid G6 (20°C), by plotting the variation of dynamic viscosity with shear rate. The red line indicates the dynamic viscosity of the liquid G6 at 20°C, as stated by the supplier.

It is important to note the high viscosity readings at low shear rates. This behaviour has been attributed to the effect of eccentricity between the inner and outer cylinder which is diminished at higher speeds of rotation due to the self-centring effect of the bob.

4.2.2 Couette type viscometer

Compared to the Searle type viscometer, a more thorough checking of the Couette type viscometer has been undertaken in this study. Numerous changes, each of which aimed at improving the measurement technique, were monitored with verification results of standard Newtonian oils in the old sets (Set 1 to 3 inner and outer cylinders in particular, Fig. 3.3). Sets 1, 2 and 3 inner and outer cylinders had lower aspect ratio (height of inner cylinder to annular gap) of 2.9, 19.5 and 16.7 respectively. Also the three sets had lower length of inner cylinder to radius of inner cylinder ratio (1.05, 0.77 and 0.77) which led to incorrect verification results with standard Newtonian oils. One such example was the verification of PTB Oil 1 which was obtained from Dr. Martin Rides (NPL). Dr. Rides tested the oil with a cone-plate viscometer and demonstrated that the oil is Newtonian over a wide range of shear rates (Fig. 4.2) owing to the shear independent nature of the dynamic viscosity.

But the oil, which has a dynamic viscosity of 0.911 mPa.s at 20^{o}C, also demonstrated problems with measurements at low (< 10 s^{-1}) and high (>1000 s^{-1}) shear rates even in the cone-plate viscometer. Irregularities in the results at lower shear rates have been attributed to eccentricity between the geometry and inability of the torque measuring transducer to record low torque values. At higher shear rates, instabilities set in the sample lead to deviation of the torque values from Newtonian behaviour. Despite the deviations at low and high shear rates, in the regime of 10 to 1000 s^{-1} shear rates, the PTB Oil 1 is confirmed to be Newtonian.

But, testing the PTB Oil 1 in the Set 3 inner and outer cylinder geometry of the Couette type viscometer (31.86 mm outer cylinder, 30.45 mm inner cylinder radius) lead to an increase of the dynamic viscosity measured with shear rate. This behaviour is illustrated in Fig. 4.3 where the torque values measured by the equipment at different speeds of rotation in a set of fixed speed experiments, are converted into dynamic viscosity values (equation 2.14).

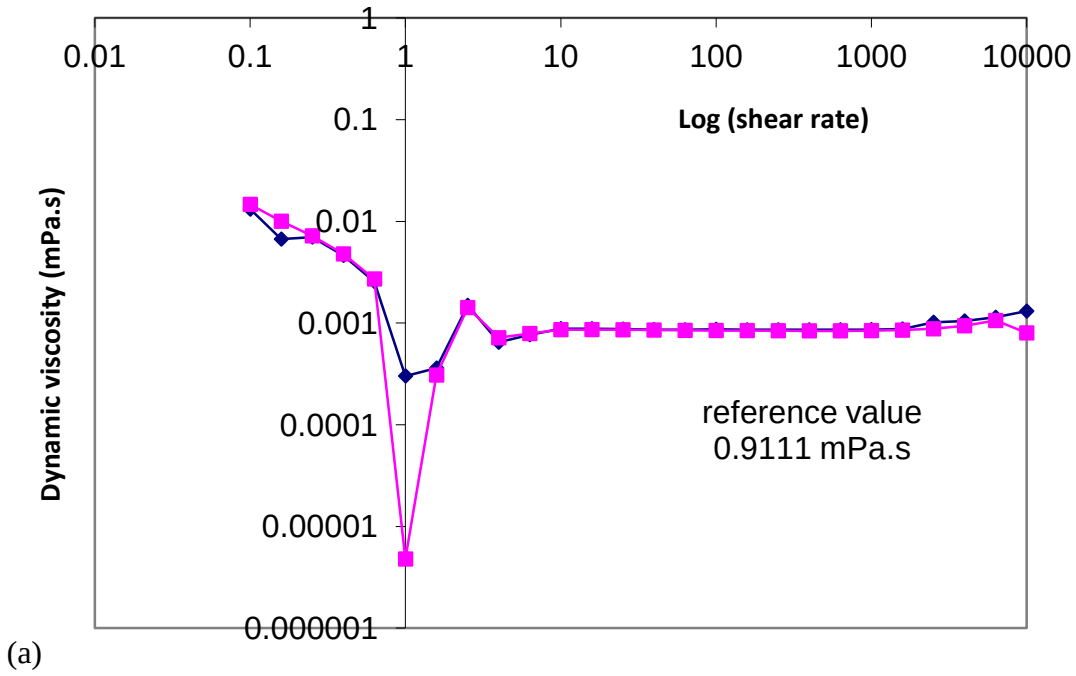

(a)

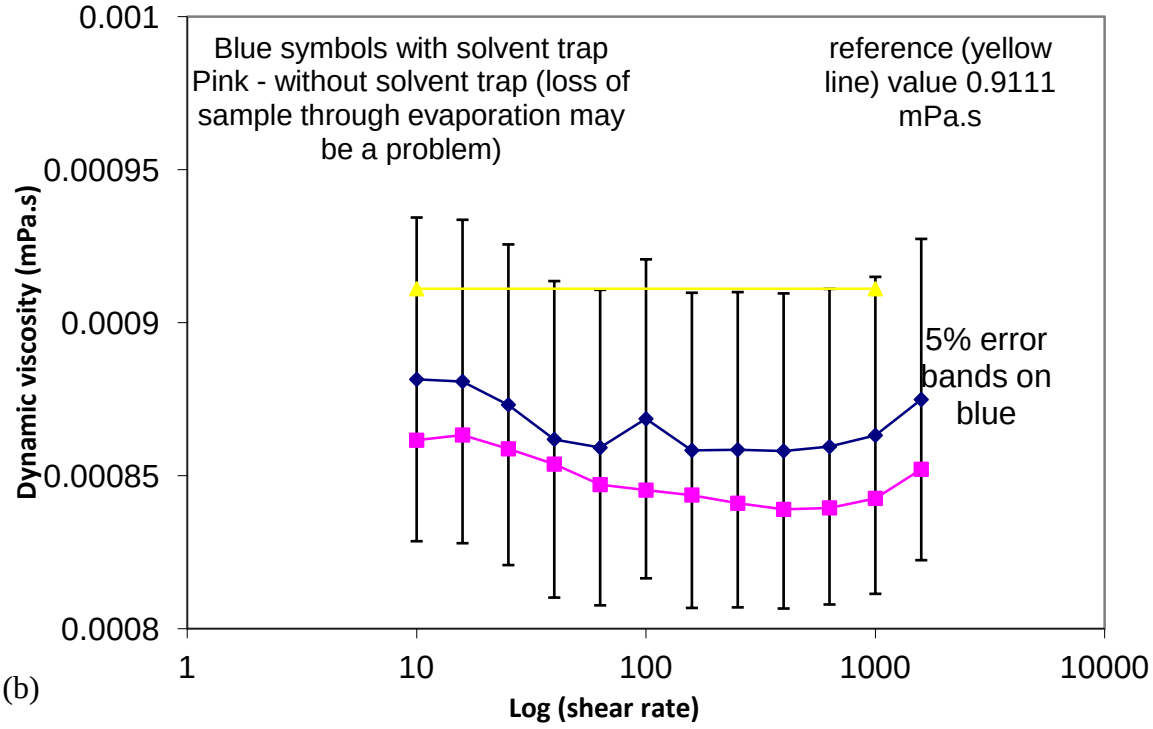

(b)

Fig. 4.2. Results with PTB Oil 1 in a cone-plate viscometer, obtained from Dr. Martin Rides, NPL, London. (a) Variation of dynamic viscosity with shear rate. (b) Magnified view of the result. The difference between using a solvent trap and without it, have been demonstrated.

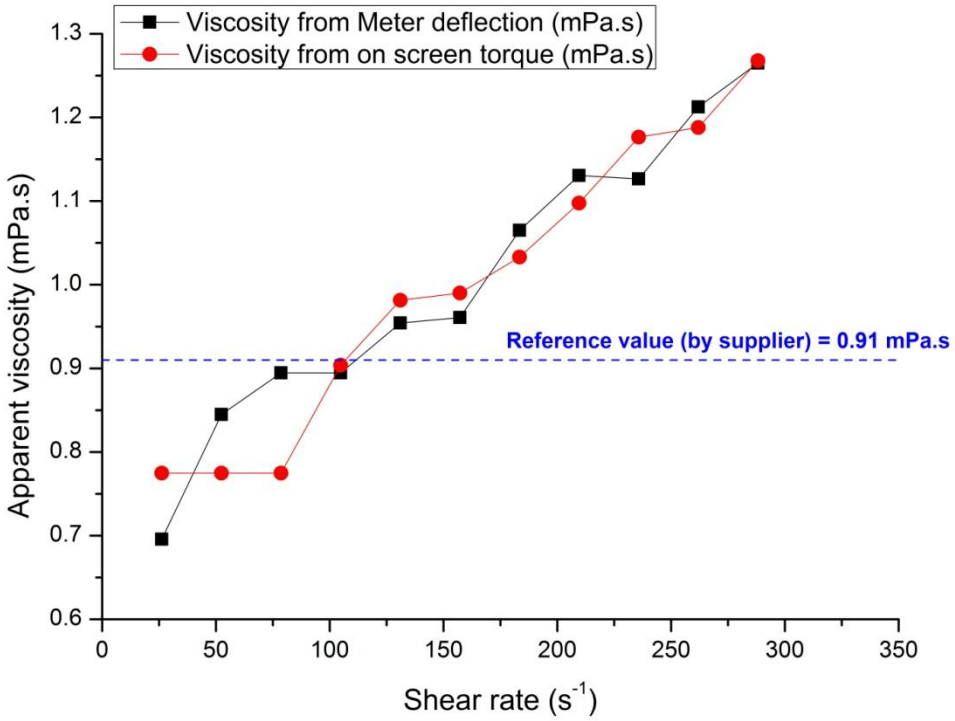

Fig. 4.3. Variation of dynamic viscosity obtained from the software (red) and calculated from torque data (black) in PTB Oil 1 (20°C) with shear rate, in a series of fixed speed experiments with Set 3. The reference value by the supplier is 0.91 mPa.s at 20°C.

Fig. 4.3 illustrates that the dynamic viscosity values obtained at fixed speeds are dependent on the shear rate when using Set 3 inner and outer cylinder geometry. The author believes that the low height of inner cylinder to radius ratio of the sets 1, 2 and 3 led to significant end effects which facilitated the rise of apparent viscosity in these sets when testing Newtonian oils. After manufacturing Set 4 (10 mm outer cylinder and 9 mm inner cylinder radius) and Set 5 (15 mm outer cylinder and 14 mm inner cylinder radius), calibration of these sets was followed by verification. To compare the difference in geometry between Sets 3, 4 and 5, samples from the same liquid (Newtonian S3) were tested in the three geometries at the same temperature. A series of fixed speed experiments were conducted at different speeds leading to a series of average torque values measured, which were then used for calculating the dynamic viscosities. Fig. 4.4 illustrates the difference between the three sets, with the error

bars representing the standard deviation on the average values for the dynamic viscosity calculated at each point.

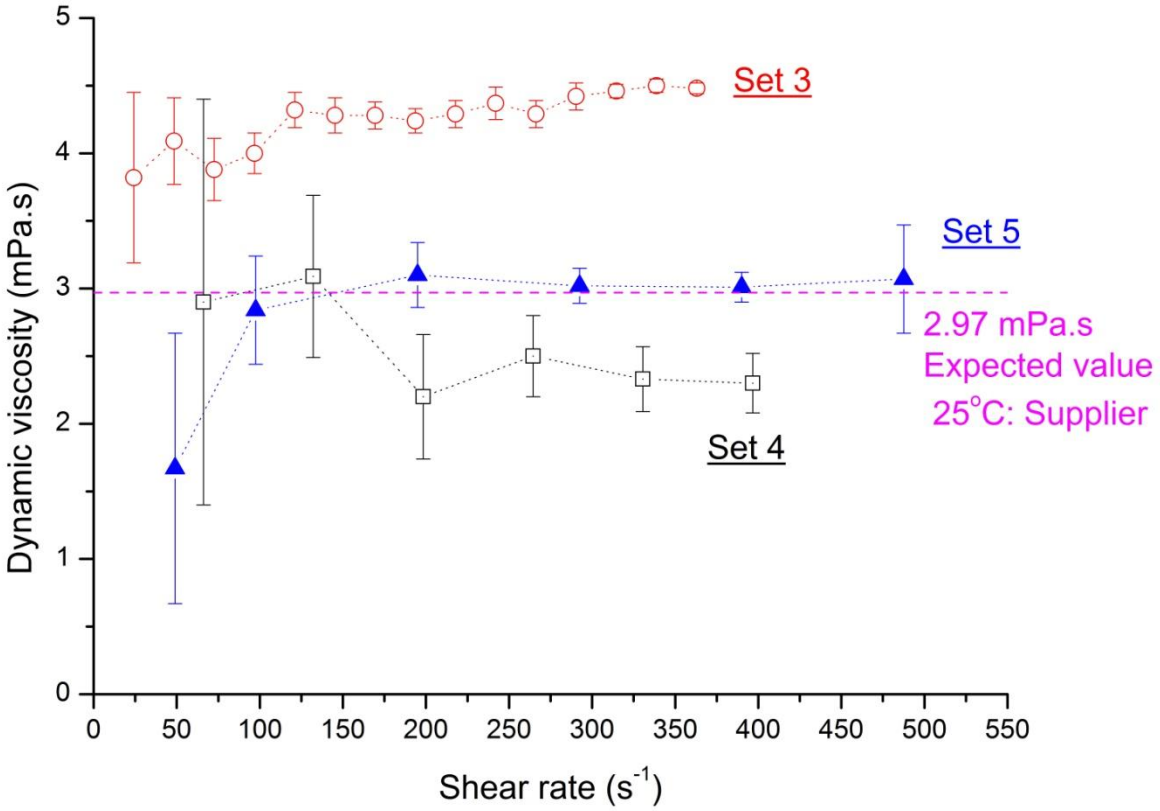

Fig. 4.4. Variation of dynamic viscosity in the standard Newtonian oil S3 held at 25°C. Each point represents averaged values from fixed speed tests with different sets of inner and outer cylinders (set 3, 4 and 5) employed in the Couette apparatus.

Fig. 4.4 confirms that Set 3 geometry is unsuitable for measuring the dynamic viscosity of low viscosity liquids. The steady rise in viscosity with shear rate render any results from this set invalid. When using Set 4 and 5, at low shear rates (< 100 s^{-1}) both sets demonstrate a large deviation from the expected dynamic viscosity of S3. The Set 4, which measures the torque value on the inner cylinder without completely submerging the inner cylinder inside the liquid sample, shows a higher standard deviation at lower shear rates. These results are similar to the behaviour illustrated in Fig. 4.2 (a) by the cone-plate viscometer at lower shear rates when testing the Newtonian liquid PTB Oil 1. Perhaps, this deviation from the standard

expected value is due to eccentricity effects manifesting at low speeds of rotation. As the speed increases (and so does shear rate), both Sets 4 and 5 demonstrate a steadier shear rate independent viscosity value, although values with Set 4 are lower than the value supplied in the certificate. To test the temperature dependence of dynamic viscosity of S3 oil in Set 4, fixed speed experiments were also conducted at a different temperature and the results were compared with the corresponding expected values; one such example is illustrated in Fig. 4.5.

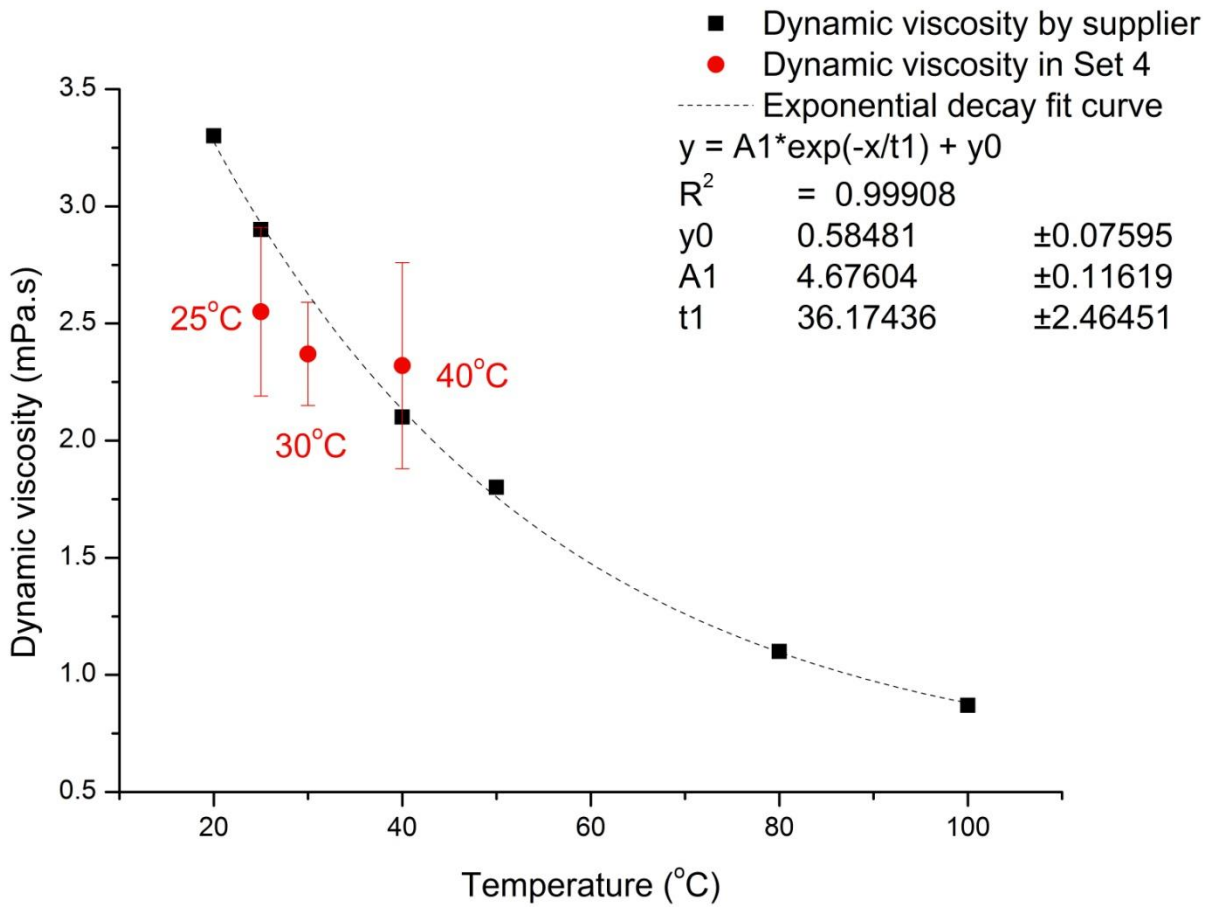

Fig. 4.5. Variation of dynamic viscosity with shear rate in a sample of S3 standard Newtonian oil maintained at different temperatures (25°C, 30°C and 40°C) to observe the temperature dependence of dynamic viscosity. Error bars at each point represent the standard deviation on the average dynamic viscosity values obtained in the fixed speed experiment.

To check the accuracy of the equipment's torque scale at much lower viscosities, Set 4 geometry for inner and outer cylinders was also employed in an experiment with water (Fig. 4.6), a well known Newtonian liquid with a dynamic viscosity of 1.0 mPa.s (Taylor, 1923c).

Due to the large variation in dynamic viscosity results at shear rates lower than 100 s^{-1} (Fig. 4.4 and 4.5), the test was conducted at shear rates above 100 s^{-1}.

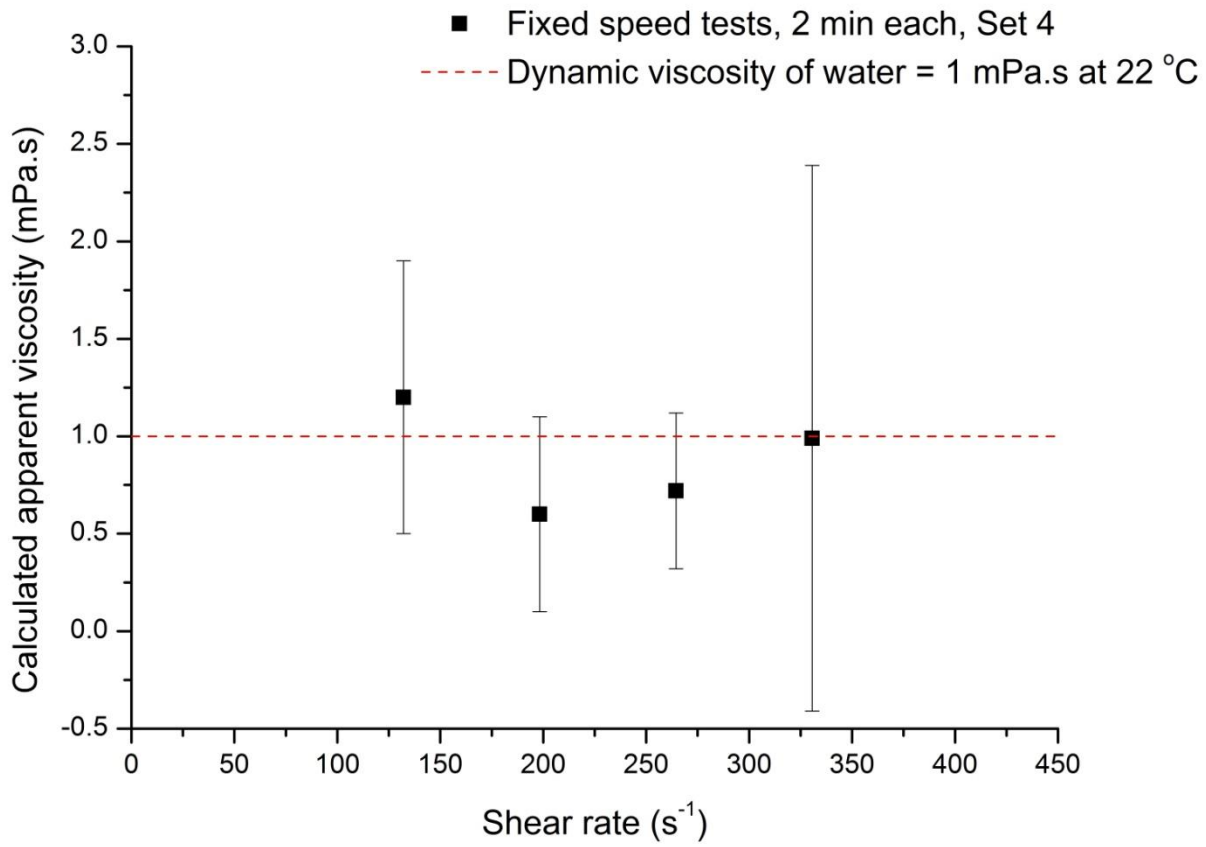

Fig. 4.6. Variation of dynamic viscosity with shear rate in a water sample held at 22°C within Set 4 geometry of inner and outer cylinders. For shear rates over 100s^{-1} to 350s^{-1}, the Set 4 geometry demonstrates an almost Newtonian behaviour for water.

From Fig 4.4 to Fig. 4.6, it was observed that Set 4 geometry for inner and outer cylinders demonstrated an almost Newtonian behaviour for known Newtonian liquids. After the verification, the Set 4 was used to measure the apparent viscosities of molten tin and lead. With the molten metal present in the gap (Fig. 4.7, a), the outer cylinder (cup) was rotated and the torque values collected as the molten tin was sheared.

But, observing the data obtained and comparing with the video of the experiment recorded, instabilities are noted every time there is a formation of a 'globular mass' (Fig. 4.7, b) which was analysed with a Scanning Electron Microscope and EDAX (Fig. 4.7, d, e).

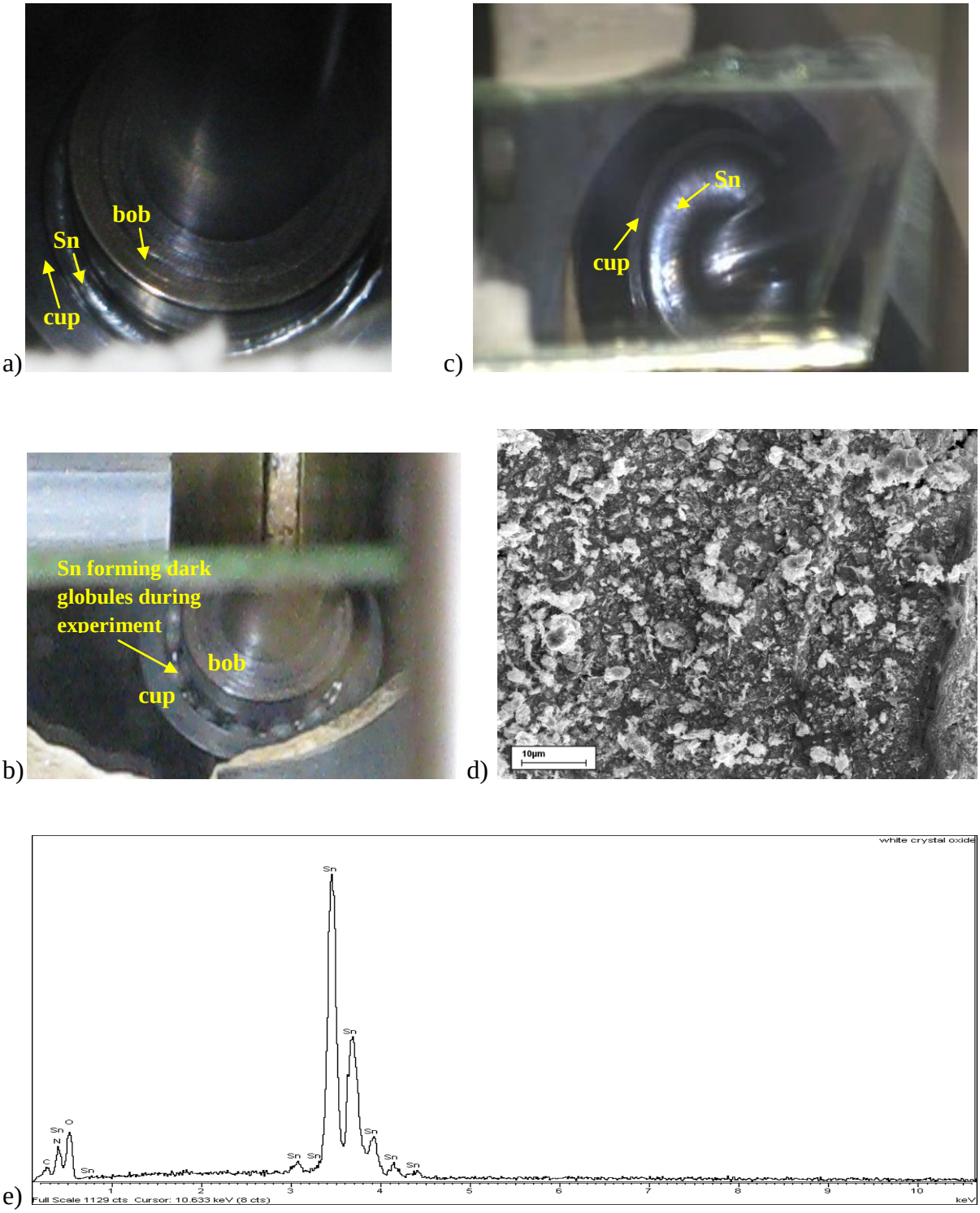

Fig. 4.7. (a), Experiment with molten Sn in Set 4 inner (bob) and outer (cup) cylinder. Here the bob is visible above the melt and is not fully immersed at rest. (b), Molten tin with Set 4, outer cylinder rotating. Note the non-continuous melt shaped as 'globules' around the inner cylinder which leads to irregular oscillations of the inner cylinder during experiments, thereby leading to a failed experiment. (c), Experiment with molten tin in Set 5 inner and outer cylinder. In this case the inner cylinder (bob) is submerged completely to a depth of 3mm from the melt surface. This ensured the presence of a continuous film of melt in the annular gap. (d), SEM image of the discontinuous film present in (b). (e), EDAX analysis confirms the presence of tin oxide in the film.

The analysis revealed the mass to be tin oxide. Such instabilities in the data were also observed when experiments with Pb were conducted (Fig. 4.8). The oxidation of the samples during the experiments, led to the formation of this discontinuous film which adversely affected the torque readings during any experiments. Oxide accumulation in the narrow gap between the inner (bob) and outer (cup) cylinders led to unstable torque measurements during fixed speed and ramping up tests, making the Set 4 unsuitable for measuring molten metal or alloy.

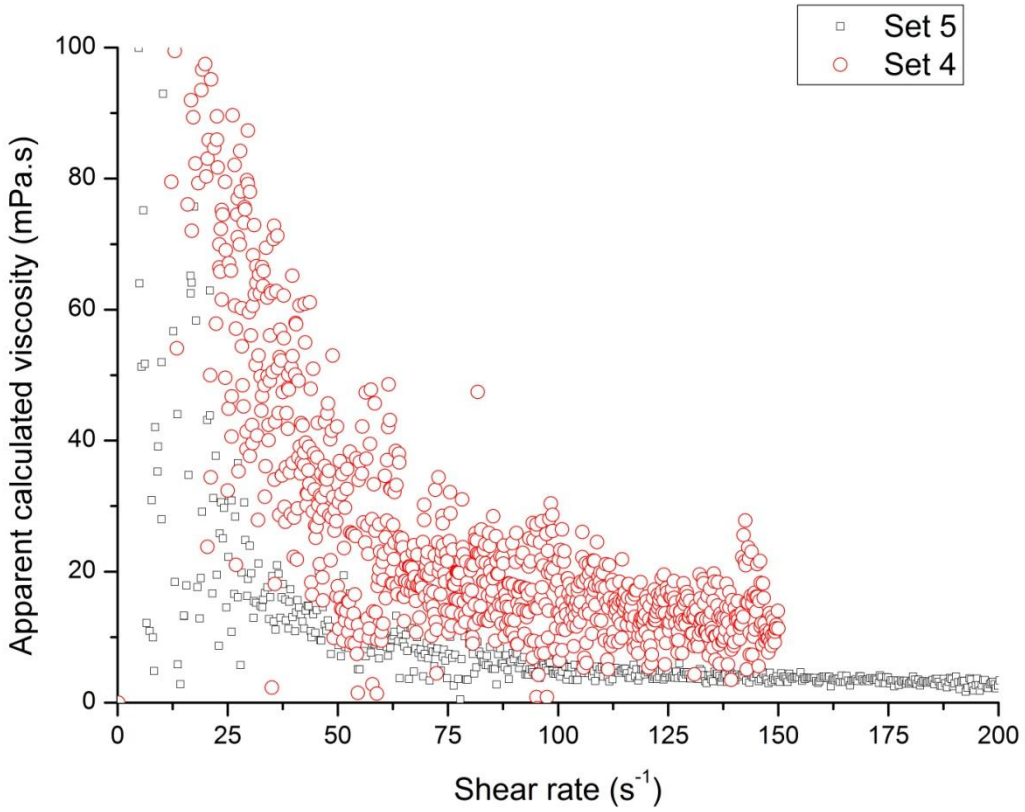

Fig. 4.8. Variation of apparent viscosity with shear rate in molten lead (384°C ± 2°C) demonstrating the effect of oxides in the annular gap when using the Set 4 geometry for inner and outer cylinder with the Couette type viscometer. Note the scatter in the data obtained compared to the experiment with Set 5 geometry for inner and outer cylinder.

This led to the development of Set 5 cup and bob arrangement. The Set 5 geometry is similar in design to the Set 4 geometry. It differs in the dimensions of the cup and bob, the shear rates to which the liquid can be tested to (Appendix III) and the practice of completely submerging the inner cylinder (bob) into the sample of molten state metal or alloy (Fig. 4.7,

c) to avoid the oxide film on the sample in the gap affecting the torque measurements during an experiment, as observed in Set 4. After calibrating the Set 5 geometry, fixed speed verification tests with S3 oil were conducted (Fig. 4.9). The Set 5 geometry for inner and outer cylinder, which measures the torque value on the inner cylinder with the inner cylinder completely submerged inside the liquid sample, shows a lower dynamic viscosity value than the expected dynamic viscosity at shear rates below $100s^{-1}$. At shear rates above $100s^{-1}$, the geometry illustrates a close agreement with the dynamic viscosity given in the certificate (Appendix II).

The Newtonian oil S3 was also employed in a ramping up test to observe the difference, if any, in the results obtained from the fixed speed tests. The torque values obtained instantaneously during the transient state ramping up test were used to measure the shear stress and the speed of rotation of the outer cylinder was employed to measure the shear rate in the liquid. The ratio of the shear stress and shear rate gave the dynamic viscosity of the liquid. Fig. 4.9 illustrates the ramping up test where the flow curve has been presented. From the shear stress–shear rate plot (green), a best fit line through the data points provides the dynamic viscosity of the liquid. Slope of the shear stress–shear rate best fit plot is given by,

$$\frac{\Delta\sigma}{\Delta\dot{\gamma}} = 0.00298$$

Hence, dynamic viscosity for a Newtonian liquid,

$$\eta = \frac{\Delta\sigma}{\Delta\dot{\gamma}} = 0.00298 \text{Pa.s}$$

$$\therefore \eta = 2.98 \text{ mPa.s}$$

Dynamic viscosity of the S3 oil = 2.966 mPa.s at 25^{o}C (Appendix II).

$$\text{Error} = \frac{(2.98 - 2.966)}{2.966} \text{ x } 100\% = 0.47\ \%$$

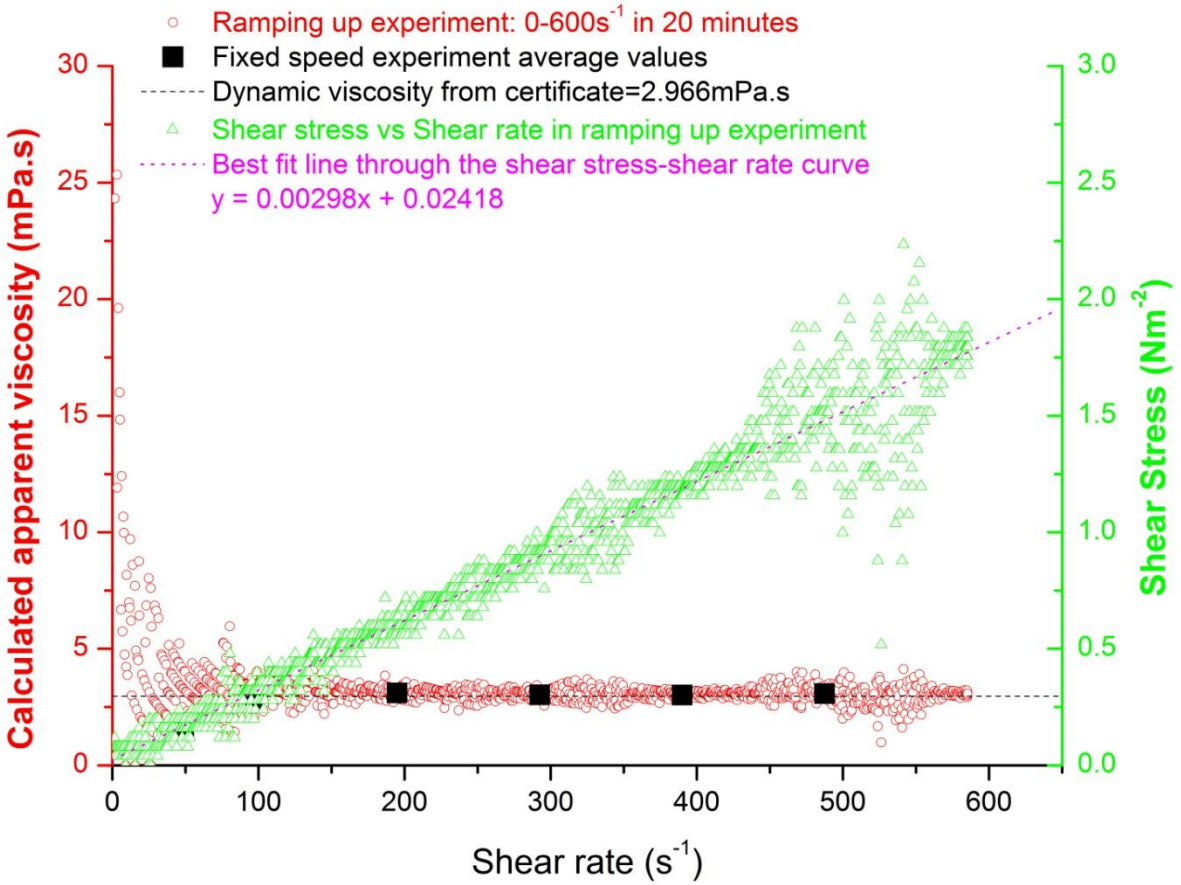

Fig. 4.9. A combined plot showing the variation of dynamic viscosity with shear rate from the ramping up test (as red dots) and fixed speed tests (as black dots) for the oil S3 held in set 5 geometry of inner and outer cylinders at 25°C. Despite the transient nature of the ramping up test, the dynamic viscosity values from the ramping test coincide with the results from the fixed speed tests (stable state test).

The deviation in dynamic viscosity for low shear rates is consistent with the behaviour observed previously in Set 4 and may be due effects of eccentricity between the cylinders at low rotation speeds, which leads to errors at lower shear rates. Scatter in the raw data at high shear rates is attributed to resonant vibrations within the equipment due to high speeds of rotation of the outer cylinder. But owing to the symmetric nature of the scatter (around $500s^{-1}$ shear rate), it has been retained in the plot. Plotting the fixed speed results with S3 against the results from ramping up experiments (Fig. 4.9), indicate the similarity in the results from both types of experiments. Thus Fig. 4.9 demonstrates the successful verification of the Set 5

geometry of inner and outer cylinders in the Couette type viscometer. For a Newtonian system, the Set 5 demonstrates a shear independent behaviour in the dynamic viscosity.

Thus, from the above experiments the following conclusions can be derived:

(1) With Set A, the Searle type viscometer demonstrates a reduction of apparent viscosity with shear rate in Newtonian systems at low speeds of rotation. At higher rates of rotation, the equipment demonstrates a shear-independent behaviour in apparent viscosity for the Newtonian system, indicating that results at low shear rates are questionable.

(2) In the Couette type viscometer, Sets 1, 2 and 3 with lower aspect ratio (length of inner cylinder to annular gap ratio) and length to radius ratio for inner cylinder lower than 3, are unsuitable for measuring the dynamic viscosity of low viscosity liquids (Mezger, 2006).

(3) Set 4 in the Couette type viscometer, despite a higher aspect ratio and a length to radius ratio for the inner cylinder greater than 3, is unsuitable for measuring the apparent dynamic viscosities for molten state metals and its alloys, owing to the accumulation of oxide particles in the narrow annular gap which leads to irregular torque data and oscillation of the inner cylinder.

(4) Set 5 geometry of inner and outer cylinder in the Couette type viscometer, is suitable for measuring the dynamic viscosity of low viscosity liquids accurately (Fig. 4.4) with error less than 1% for the Newtonian oils.

(5) The Set 5 geometry in the Couette type viscometer illustrates shear-independent dynamic viscosity behaviour for Newtonian oil in ‘transient state’ ramping up experiments and the ‘steady state’ fixed speed experiments (Fig. 4.9). It is thus the most suitable geometry for testing the dynamic viscosities of molten state metals and its alloys.

Chapter 5

Results with molten metals and alloys

After obtaining satisfactory results with the standard Newtonian oils, above a certain shear rate, experiments were conducted with metallic melts and molten metallic alloys. Temperature control in the experiments with metals is crucial. When using the Couette type viscometer, temperature calibration tests (section 3.6) were conducted once every 3 months to check the repeatability of the curves. Since no significant difference was observed in several tests, the original plot was followed (Fig. 3.6). After ensuring that the temperature of the furnace in the Couette type viscometer was stable, the equipment was set up to conduct experiments with metals.

5.1 Materials tested

The metals and alloys tested in this study are (from Table 3.4):

(i) Sn.

(ii) Pb.

(iii) Pb-Sn eutectic.

(iv) Sn doped with Sn-Ge master alloy.

The sample preparation from the raw materials has been described in section 3.3. To compare the results from the Searle type and the Couette type viscometer the experiments with both the equipment were conducted at similar temperatures. The temperature of conducting experiments with Sn and Pb was chosen as to be the same, namely $385^{o}C \pm 2^{o}C$, so as to ensure that there is a superheat of at least $60^{o}C$ to the molten Pb sample. In both types of equipment, the same raw materials have been employed to prepare the samples, thereby maintaining consistency. The following section present results obtained from Set A in the

Searle type viscometer. With the Couette type viscometer, the Set 5 geometry, of inner and outer cylinders, has been employed for studying the molten state metals and the alloys. Since Sets 1 to 3 failed the verification step with Newtonian oils and Set 4 geometry led to accumulation of oxides in the narrow annular gap, only the results from Set 5 geometry in the Couette type viscometer have been presented. The speed of rotation of the outer cylinder, along with the type of experiment: ramping up or fixed speed, is set in the software. Upon commencing the experiment, torque values are recorded due to twist in the torsion wire. These torque values are employed in calculating the shear stress on the inner cylinder and the speed of rotation of the outer cylinder enables calculation of the shear rate at the inner cylinder.

5.2 Preparation for experiment

Appendix IV.

5.3 Results with tin

Molten tin has been a popular choice of several authors for demonstrating the dynamic viscosity values for metals (Sun *et al.*, 2007; Battezzati and Greer, 1989; Thresh and Crawley, 1970; Culpin, 1957; Lewis, 1936). Known to be reactive, careful experimental procedure has been followed in this study to measure the viscosity of the molten tin. To minimise the contamination of the molten tin sample during experiments with the viscometers, two major steps were undertaken before conducting experiments:

(a) Stainless steel grade 316 was used for manufacturing the inner and outer cylinders in all sets. This grade of stainless steel is known to have good corrosion resistance for longer durations of time at elevated temperatures.

(b) Numerous studies have been conducted demonstrating the effect of oxygen and fluxes on surface tension of molten tin (Passerone, Ricci and Sangiorgi, 1990; Howie and Hondros, 1982).

Also, Protsenko et al. (Protsenko *et al.,* 2001) demonstrated the influence of container material on the wetting characteristics of tin. Comparing the spreading time for Sn on pure Fe and FeCr steel, Protsenko et al. demonstrated that due to interaction of Sn with pure Fe, the contact angle of Sn reduces from an initial 40^o-90^o to 25^o in a spreading time of 500s due to formation of $FeSn_2$ intermetallic. In comparison, the spreading time of Sn on FeCr steel to 25^o is 10000s. In other words, Sn reacts with the FeCr steel more actively beyond 10000s. To avoid this phenomenon in the experiments with tin or other alloys in this study, a time limit of 10000s or 2 hours 47 minutes was strictly followed in every molten state metal experiment. Beyond this time limit, the rate of contamination is expected to escalate to proportions which would be damaging to the surface of the cylinders as well as altering the wetting characteristics of the liquid. Hence, the two important steps followed were:

- Material for cylinders – Stainless Steel 316 grade, for all components.
- Time limit for experiments – 2 hours 47 minutes.

Before conducting any experiments with tin, a mass spectrometer analysis of the raw tin employed in this study was conducted to analyse the various constituents (courtesy Dr. Christopher Gourlay, Imperial College London).

Table 5.1. Mass spectrometer analysis of the commercial tin employed in this study. The numbers are weight percentages. * ND = 'Not detected'. The detection limit for this test is 0.0002 wt%. Balance is tin.

Cu	Pb	Ag	Sb	Bi	Zn	Fe	Al	As	Cd	Ni	Ge
0.006	0.021	0.004	0.026	0.009	ND*	0.008	ND*	0.003	ND*	0.004	0.0000

5.3.1 Reference data

A literature review of the data on viscosity of tin was conducted to compare with the experimental values obtained in this study. Fig. 5.1 has been created by collecting the experimental results of authors from literature, most of whom employed an oscillating type

equipment to measure the dynamic viscosity. As discussed earlier in Chapter 2, the shear rates in oscillating type viscometers are very low (less than $1s^{-1}$). Thus most studies have been based on measuring the dynamic viscosity of tin at different temperatures and then obtaining the constants in Andrade's Equation (Rothwell, 1961; Andrade, 1952; Andrade and Chiong, 1936) , since most scientists assume "*All molten metals are Newtonian*". To observe the behaviour of molten tin with shear, experimental results with the Searle type (inner cylinder rotating) and Couette type (outer cylinder rotating) viscometers are presented below.

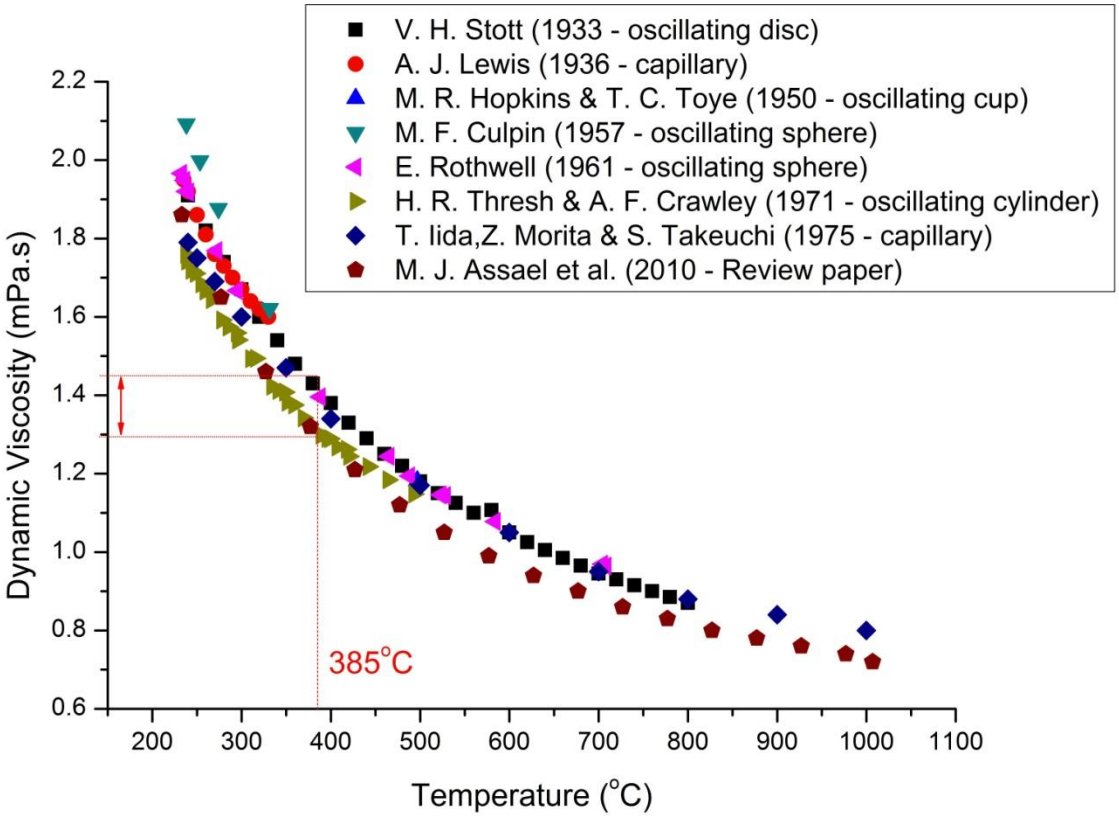

Fig. 5.1. The variation of dynamic viscosity of molten tin with temperature obtained from different authors (inset) who had presented prior experimental results with different measurement techniques, included in the figure within brackets (shear rates < $1s^{-1}$).

5.3.2 Results with Searle type viscometer

In the Searle type viscometer, ramping up tests were conducted with the sample of molten tin by increasing the speed of rotation of the inner cylinder from zero to 1000rpm, measuring the

torque on the inner cylinder. The torque obtained, along with the speed of rotation, was employed in measuring the instantaneous apparent viscosity which was then plotted against shear rate. From Fig. 5.2, the apparent viscosity is observed to first decrease with shear rate until shear rate 250 s^{-1} is reached. Then on, the apparent viscosity increases steadily with shear rate until the experimental run terminates. The corresponding variation of shear stress with shear rate is also plotted on the same graph (Fig. 5.2).

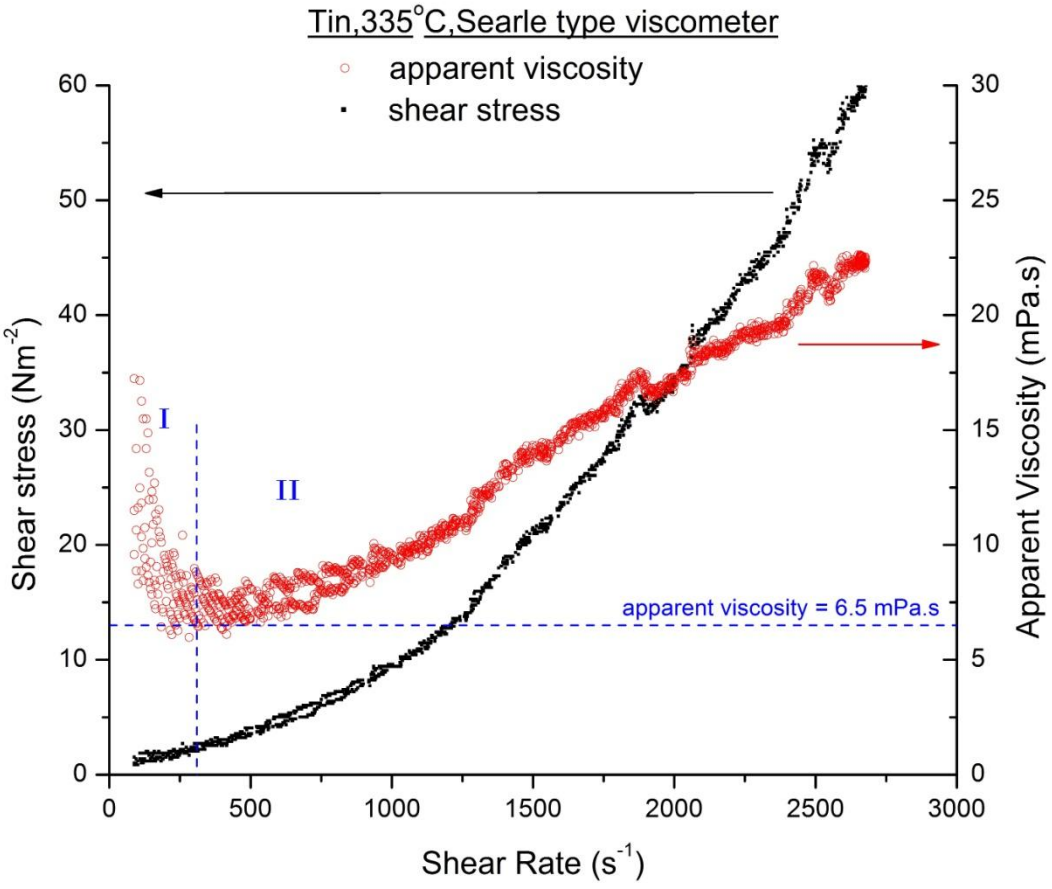

Fig. 5.2. Variation of apparent viscosity for molten tin with shear rate, in the Set A of Searle type viscometer – marked as open red dots; variation of corresponding shear stress with shear rate – marked as closed black squares. The temperature has been maintained at 335°C to compare with results at other temperatures and with Couette type viscometer.

The flow curve of apparent viscosity against shear rate can be divided into two zones:

(I) Until shear rate 300s^{-1}: Decrease in apparent viscosity with shear rate.

(II) Above shear rate 300s^{-1}: Increase in apparent viscosity with shear rate.

One plausible explanation for the rise in apparent viscosity above $300s^{-1}$ might be the presence of oxides within the melt. So to test this hypothesis, an experiment was conducted with a sample of molten tin where four consecutive ramping up experiments were undertaken with the same sample held in the gap of Set A. This was conducted to oxidise the sample to the maximum extent possible and simultaneously observe the effect on apparent viscosity.

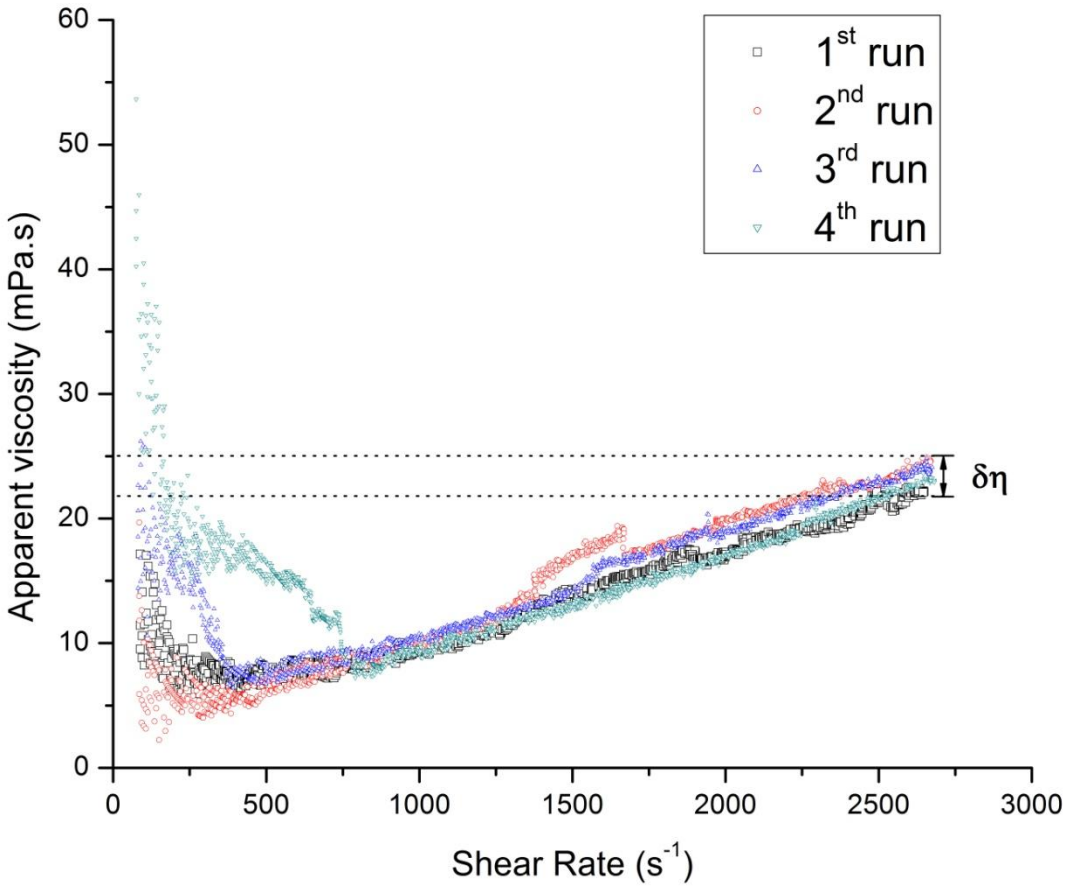

Fig. 5.3. Variation of apparent viscosity with shear rate after four consecutive ramping ups in molten tin held at 385°C, ramping up experiment 0 to 1000 rpm in 20 minutes (Set A of the Searle type viscometer). Temperature kept similar to Couette type viscometer.

Fig. 5.3 clearly illustrates the similarity in the profile of the four curves which almost superimpose on one another and are also similar to Fig. 5.2. This proves that the four consecutive ramping up experiments show similar variation of apparent viscosity with shear rate. Upon analysing the four curves carefully, it is observed that there are instabilities in the dynamic viscosity values obtained at times, especially in the 4th run. This can be attributed to

the presence of oxide particles saturating inside the melt. But the increase in the apparent viscosity, at the maximum shear rate, from the 1st to the 4th run, **(δη) < 5 mPa.s**. This means, even after saturating the melt with oxides, the actual increase in apparent viscosity due to the oxide particles (< 5 mPa.s) is still less than the rise in apparent viscosity from $300s^{-1}$observed in the plots (> 15 mPa.s). Experiments were then conducted with the Couette apparatus.

5.3.3 Results with Couette type viscometer

As mentioned before, only the results with Set 5 geometry of inner and outer cylinder are presented. During the setting up of the equipment for the experiment with molten metal, it is important to make the cylinders concentric with each other. This important practice is observed strictly, since presence of significant eccentricity leads to the inner cylinder to be pushed against the outer cylinder due to the high surface tension of liquid state metal thereby leading to irregular oscillations of the inner cylinder and a failed experiment (Fig. 5.4).

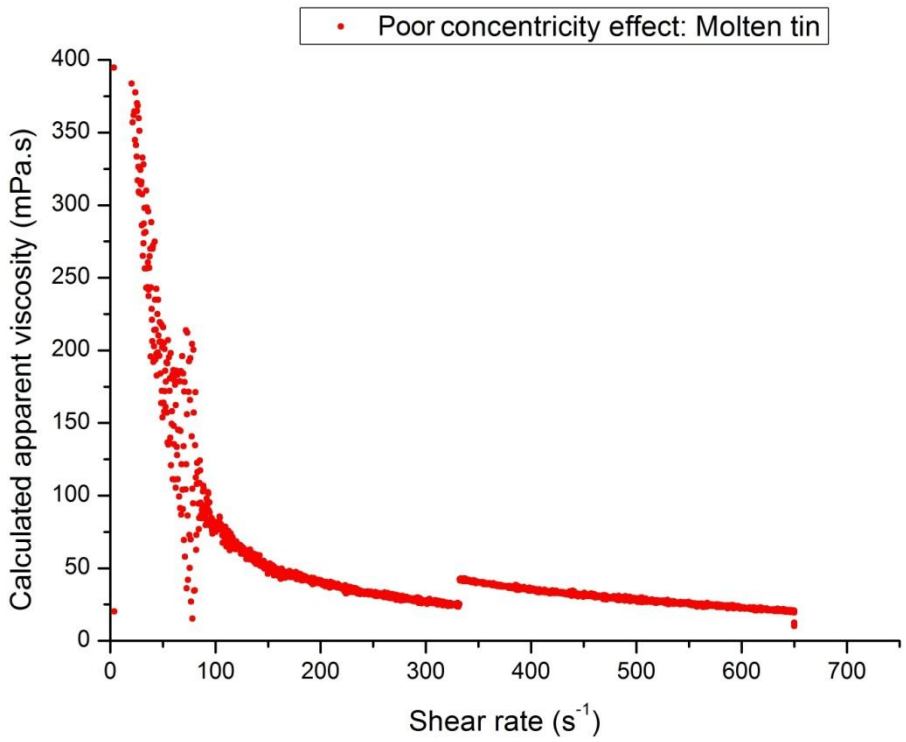

Fig. 5.4. Eccentricity effect during experiment with molten tin (384°C) with Set 5 geometry of the Couette type viscometer, when ramping up from 0 to 650 s^{-1} shear rate in twenty minutes. Notice the effect of poor concentricity between the cylinders which led to the inner cylinder touching the outer cylinder wall during the experimental run.

Ramping up experiments with molten tin was conducted to observe the transient state behaviour of viscosity with shear rate. As discussed in Appendix IV, the cabinet of the Couette type viscometer is evacuated and filled with N_2 gas to provide a protective atmosphere to minimize oxidation of the sample. To compare with the results obtained with the transient state ramping up experiments, fixed speed experiments with samples of molten Sn were also conducted at the same temperature. The results from both types of experiments are illustrated in Fig. 5.5.

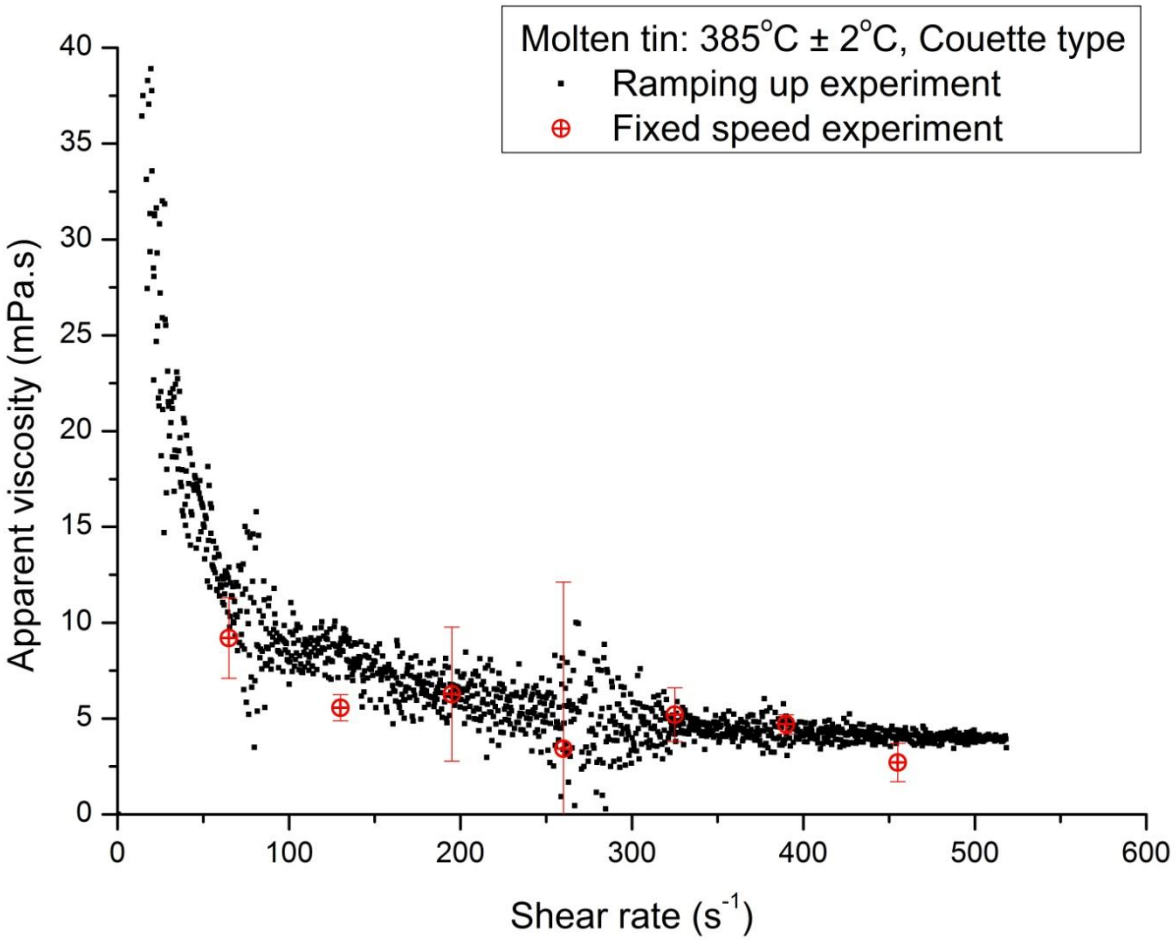

Fig. 5.5. Variation of apparent viscosity with shear rate in molten tin (385°C ± 2°C) during ramping up and fixed speed experiments in Set 5 geometry of the Couette type viscometer. Each of the fixed speed experimental results presented are obtained by averaging the apparent viscosity values obtained from atleast 3 experimental runs where the speed of rotation of the outer cylinder is kept constant at the designated speed. The error bars represent the standard deviations on the average values of the viscosity calculated for each fixed speed.

Most of the experiments with molten metal or alloy in the Couette type viscometer were conducted in the presence of an atmosphere of N_2. But many industrial processes do not employ any protective medium. To observe the difference between the presence of N_2 as a protective medium and its absence, experiments with tin were also conducted as fixed speed tests in the absence of N_2 within the cabinet of the Couette type viscometer (Fig. 5.6). As in previous fixed speed experiments, apparent viscosity from atleast 3 experimental runs is averaged and the standard deviation on these averages are presented as error bars.

Without N_2 gas

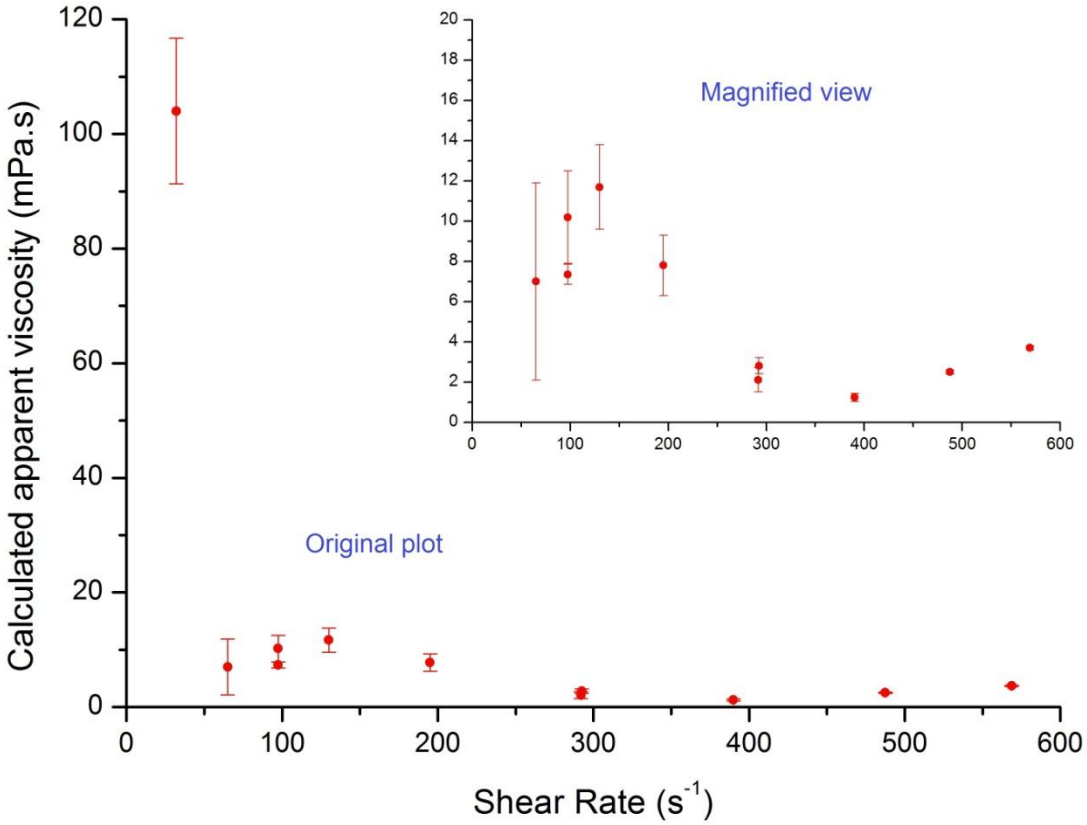

Fig. 5.6. Fixed speed tests with molten tin at 386°C ± 2°C. Error bars are the standard deviations on the average apparent viscosity values measured for the corresponding fixed speed. The metal was held for 1 minute for each of the fixed speed tests. *Inset, magnified view of the graph with modified scales.*

5.4 Results with lead

Molten lead is known to be less reactive than molten tin (Protsenko *et al.*, 2001). Besides the usual practices followed while conducting experiments with molten metal, great care in handling the raw material and lead samples was observed for health & safety reasons.

5.4.1 Reference data

Numerous studies of molten lead have been conducted over the years and some of the results can be obtained from (Tsai, Hwang and Chou, 2009; Sobolev, 2007; Sun *et al.*, 2007; Thresh and Crawley, 1970). Some are illustrated in Fig. 5.7. As discussed in section 2.6, Pb has a higher viscosity than molten tin at their respective melting points, owing to its large atomic number and higher melting temperature.

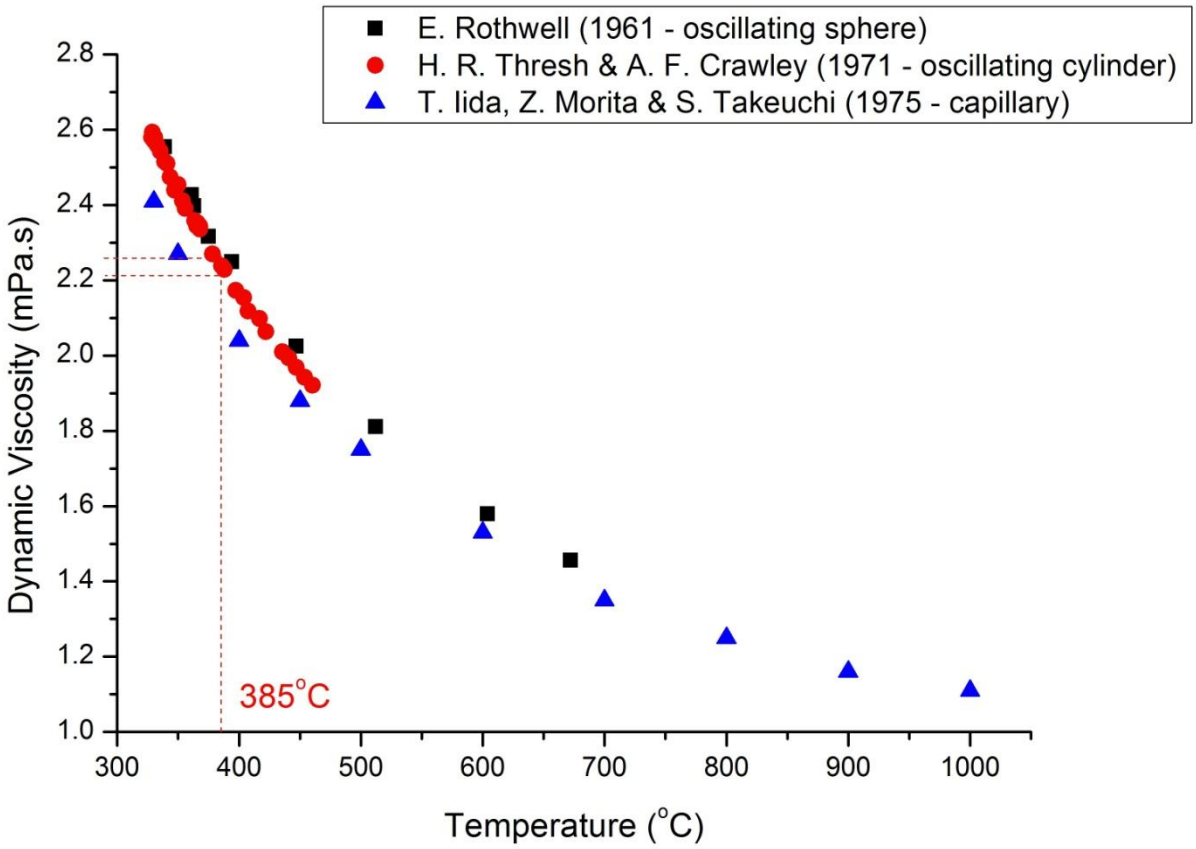

Fig. 5.7. Some literature values demonstrating the variation of dynamic viscosity of molten Pb with temperature. (Sobolev, 2007) presents a comprehensive Arrhenius type equation defining the temperature dependence of dynamic viscosity in molten lead, $\eta\,[\mathrm{Pa.s}] = 4.55 \times 10^{-4} \times e^{(8888/RT)}$, where T is the temperature of the lead sample in Kelvin. As discussed in Chapter 2, oscillating type viscometers only generate shear rates of less than $1s^{-1}$ within the sample of molten Pb.

5.4.2 Results with Searle type viscometer

As in molten tin, ramping up experiments with molten lead was conducted in the Searle type viscometer and the apparent viscosity plotted against shear rate. The variation of shear stress and apparent viscosity with shear rate was also plotted on the same graph (Fig.5.8) to illustrate the rheological behaviour of molten lead in a Searle type viscometer.

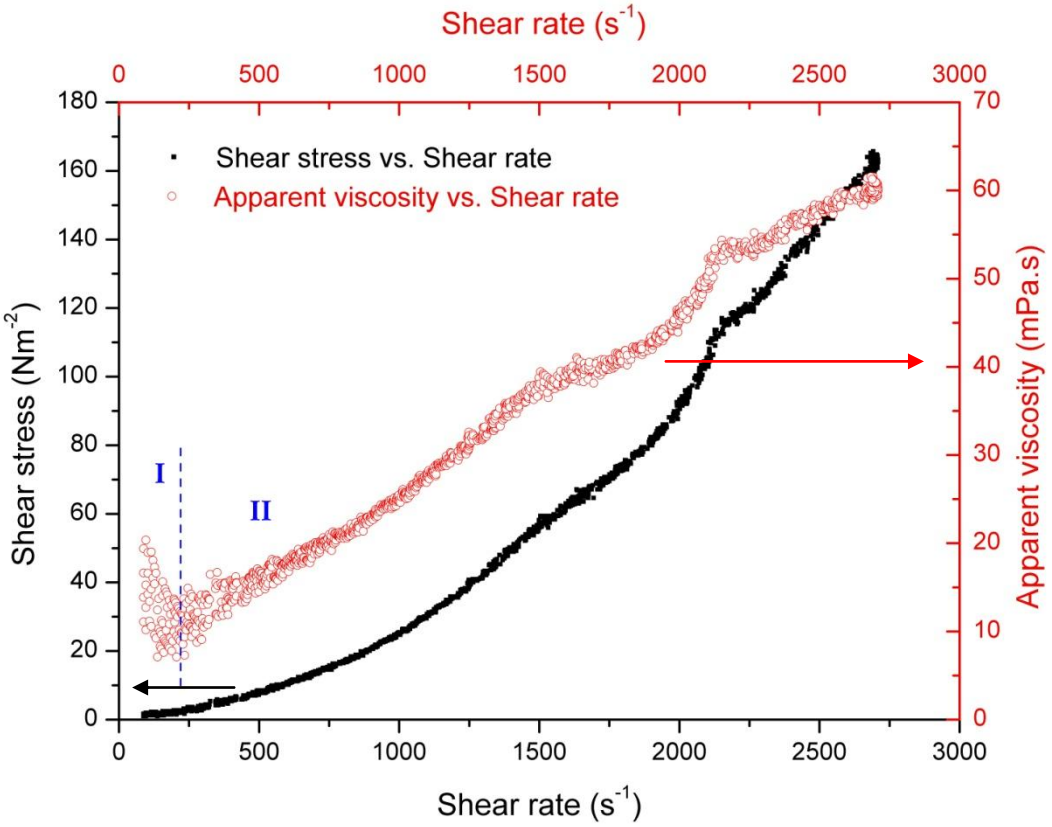

Fig. 5.8. Variation of apparent viscosity with shear rate (in red) and shear stress with shear rate (in black) in Set A of the Searle type viscometer with molten lead held at 387°C ± 3°C, during a ramping up experiment from 0 to 1000rpm in 30 minutes.

Similar to molten tin (Fig. 5.2), the flow curve for molten lead (Fig. 5.8) has two zones:

(I) Until shear rates of $220s^{-1}$: Decrease of apparent viscosity with shear rate.

(II) Above shear rates $220s^{-1}$: Continuous increase of apparent viscosity with shear rate.

To analyse this rise in viscosity with shear, it was important to test the same material with the Couette type viscometer and observe any difference in the results. The difference in flow behaviour in the two systems is expected to bring some difference in the flow curve.

5.4.3 Results with Couette type viscometer

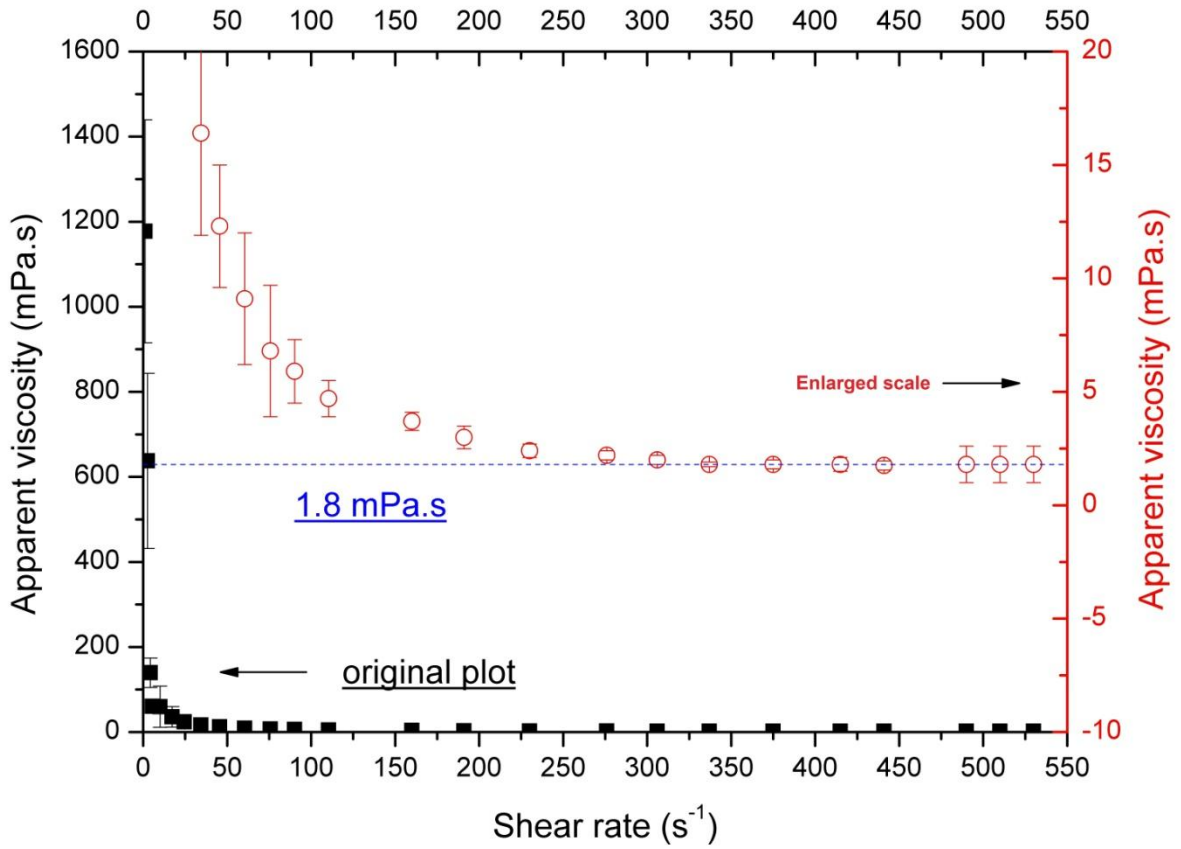

Fig. 5.9. Variation of apparent viscosity with shear rate in molten lead at 385°C ± 2°C, in Set 5 geometry of the Couette type viscometer. The original plot, along with an enlarged version, illustrates the variation of apparent viscosity with shear in this figure. The plateau value for apparent viscosity of lead, 1.8mPa.s is also presented as a dashed line.

In the Fig. 5.9, fixed speed experiments with a sample of molten lead are presented. In the fixed speed tests, each of which is repeated at least 3 times, the melt has been held for 1 minute at the speed during which the torque has been measured. This torque has been averaged and employed to measure the apparent viscosity. The error bars on the plots represent the standard deviations on the average apparent viscosity values for those speeds. Observing the Fig. 5.9, two distinct zones can be identified:

(I) Until shear rates of $250s^{-1}$: apparent viscosity reduces with shear rate.

(II) Above shear rates of $250s^{-1}$: apparent viscosity stays shear independent.

This observation is quite distinctly different from the Searle type viscometer.

5.5 Results with lead-tin eutectic alloy

Apart from metals, binary alloys are an important segment of the industrial processes involving metals. Thus, understanding the flow of molten binary alloys is equally important. In thus study, the lead-tin binary eutectic alloy has been studied with the Set 5 geometry of inner and outer cylinders of the Couette type viscometer. Samples from the same batch of lead-tin eutectic alloy are tested in a series of ramping up experiments with different final speed of rotation of the outer cylinder (100 rpm, 250 rpm and 400 rpm). Despite the difference in final speed (and final shear rate), the profile of the curves (Fig. 5.10) are similar to one another and show a similar profile to those for molten Sn and Pb.

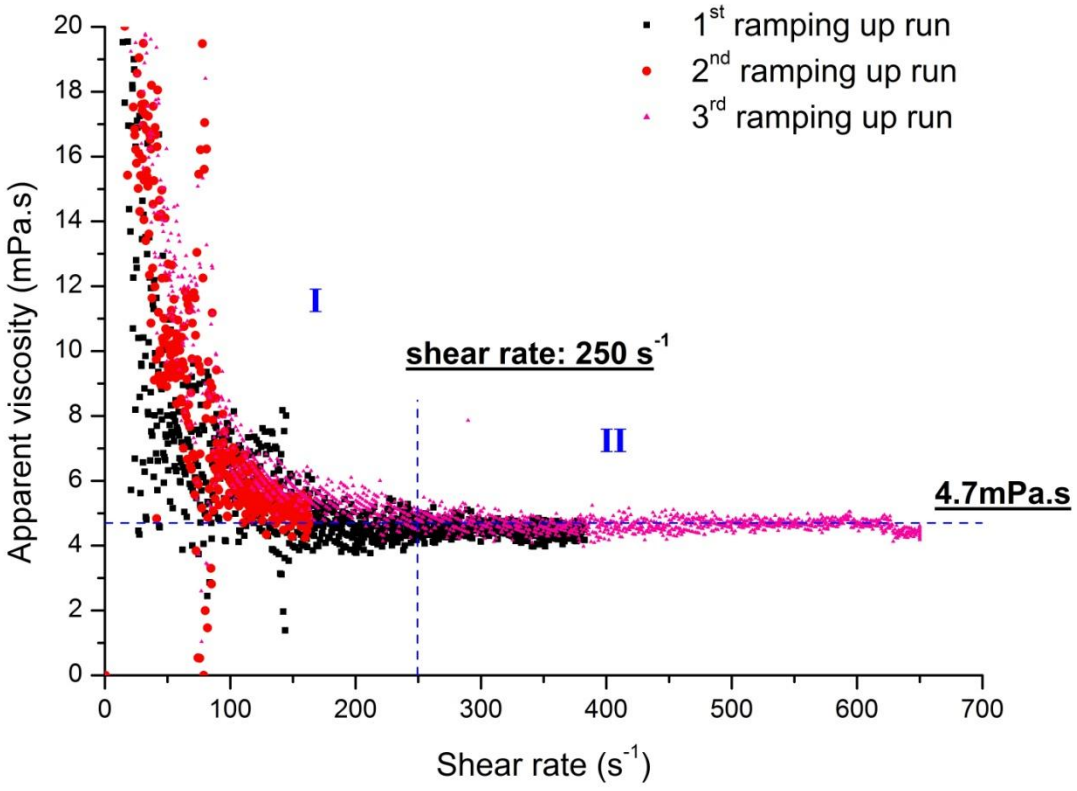

Fig. 5.10. Apparent viscosity against shear rate for Pb-Sn eutectic alloy (384°C±2°C) in three consecutive ramping up runs with different final speeds reached in the same time interval of 5 minutes. Note that despite the difference in final speed of rotation, the profiles of the flow curves are similar to one another. Also, like molten Sn and Pb, the plot can be divided into zone I: reduction of apparent viscosity with shear rate and zone II: shear independent behaviour for apparent viscosity.

5.6 Results with tin doped with Sn-Ge master alloy

Germanium is known to alter the surface properties of the tin melt. (Wan Cho *et al.*, 2006) conducted X-ray photoelectron spectroscopy (XPS) studies on Sn-Ag-Cu and Sn-Ag-Cu-Ge solder alloys after passing the solder samples through the reflow oven 2 to 5 times. The oxygen atomic density during the XPS depth profiling indicated that the Sn-Ag-Cu alloy had twice-thicker oxide layer as compared to the Sn-Ag-Cu-Ge alloy after 5-time reflow. It is believed that the Ge, which does not form any intermetallic with tin (Naidich and Perevertailo, 1971), forms GeO_x on the surface of the melt, thus preventing oxidation of the lead-free solder sample and ensuring a good contact with the substrate after the soldering procedure. Thus to observe the change in viscosity measurement, by altering the surface properties of the melt, a Sn-Ge master alloy (courtesy Dr. Christopher Gourlay, Imperial College, London, UK) was added to the tin melt to obtain 50ppm of Ge in the melt.

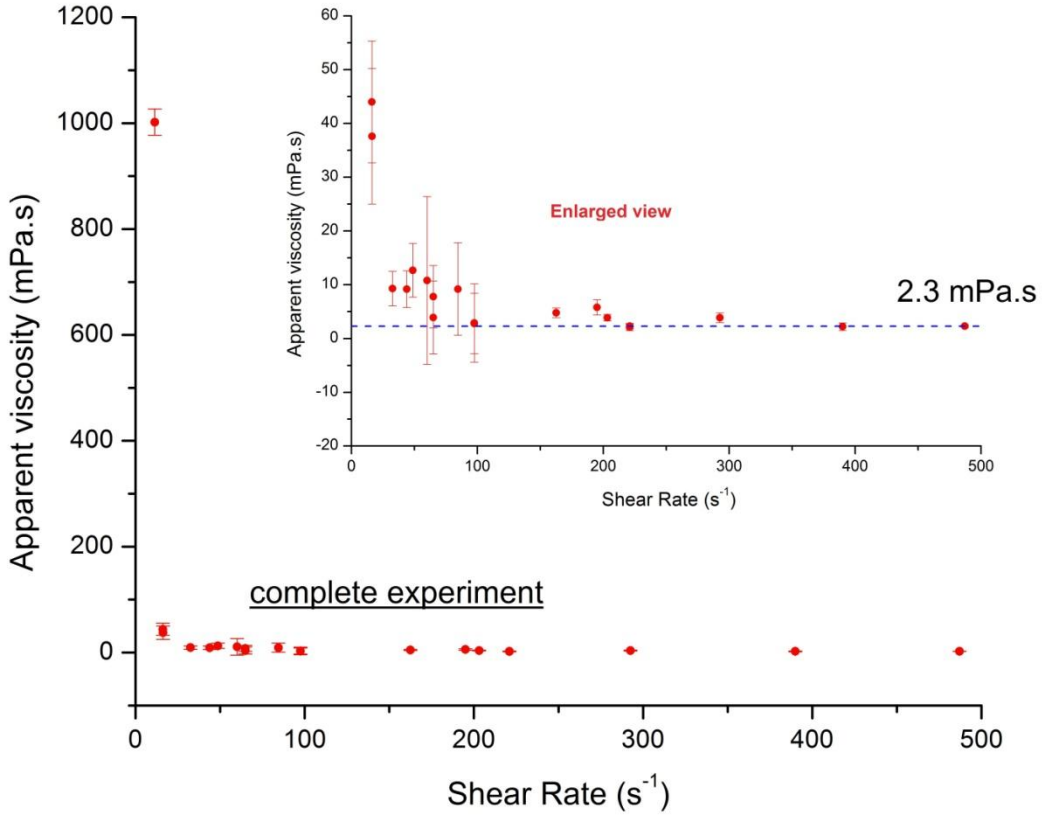

Fig. 5.11. Variation of apparent viscosity with shear rate in Sn doped with Sn-Ge master alloy in a series of fixed speed experiments holding the melt at each fixed speed for 1 minute each. Temperature was held at 385°C ± 2°C during the experiment.

Thus based on the results presented so far, the following observations can be made:

(1) Distinct difference in the rheological behaviour of molten tin and molten lead when tested with a Searle type and a Couette type viscometer.

(2) Molten state Sn and Pb tested in a Searle type viscometer show two zones in their flow curves:

    (i) Until shear rates of 200-300s^{-1}: decrease of apparent viscosity with shear rate.

    (ii) Above shear rates of 200-300s^{-1}: increase of apparent viscosity with shear rate.

(3) Molten state Sn, Pb and Sn-Pb eutectic tested in the Set 5 geometry of the Couette type viscometer also show two zones in their flow curves:

    (i) Decrease of apparent viscosity with shear rate until a specific shear rate, based on the material tested.

    (ii) A relatively shear independent apparent viscosity with shear rate above a certain shear rate, based on the material being tested.

(4) Metals in their molten state show greater scatter in results of apparent viscosity without the presence of nitrogen than in the presence of the protective nitrogen medium when tested with the Couette type viscometer.

(5) Tin doped with Ge demonstrates a lower apparent viscosity with shear in the Couette type viscometer than pure tin.

Based on these observations, possible causes and explanations for the phenomena have been discussed in the following chapter; along with a critical analysis of some results by other authors on metals in their molten state (Iida and Guthrie, 1988).

Chapter 6

Discussion

This chapter discusses the observations made during the experiments with molten state metals in the Searle type and the Couette type viscometers. For both apparatus, there were two zones observed, at low shear rates: decrease of apparent viscosity with shear and at high shear rate: either increase in apparent viscosity (Searle type) or an almost shear independent behaviour (Couette type). Based on these observations, the following points help discuss the causes:

- Past work.
- Searle type viscometer vs. Couette type viscometer.
- Testing in a protective atmosphere of N_2 and without it.
- Pure tin vs. Tin doped with germanium.
- Low shear rate vs. High shear rate.
- Experimental results vs. Literature values.

Before proceeding to analyse the results, it is important to note the differences in the physical properties of the liquids (density, viscosity and surface tension) tested in this study. This is crucial since the viscosities of these liquids are all similar in magnitude (1–10 mPa.s).

Table 6.1. Physical properties of materials tested in this study.

Liquid	Type	Density[1] (g/cc)	Viscosity[2] (mPa.s)	Surface tension[3] (mN/m)	Working temperature
Molten tin	Metal	7.000	1.85	544	> 232^{o}C
Molten lead	Metal	10.678	2.65	468	> 327^{o}C
S3	Newtonian Oil	0.815	3.347	23 – 32*	> 20^{o}C
Water	Newtonian liquid	1.0	1.0	72	> 20^{o}C

[1,3]Source: material certificates (Appendix II) and (Gale, Totemeier and Smithells, 2004). [2]Source: (Assael *et al.*, 2010; Thresh and Crawley, 1970).*Typical values for kerosene based oils.

6.1 Past work

Some of the past work on molten metal or alloys with concentric cylinder apparatus includes (Malik *et al.*, 2010; Sun *et al.*, 2007; Varsani and Fan, 2007; Bakhtiyarov and Overfelt, 1999; Jones and Bartlett, 1952). A brief summary of the equipment used by them is given in the table below, in a chronological order.

Table 6.2. Summary of concentric cylinder equipment employed for measuring viscosity of metals in the molten state, in the past.

Name of author (year)	Type of equipment	Dimensions of geometry
Jones and Bartlett (1952)	Couette type	R_b = 55mm, R_c = 60mm
Bakhtiyarov and Overfelt (1999)	Searle type	R_b = 12.7mm, R_c = 26.75mm
Varsani and Fan (2007)	Searle type	R_b = 24.5 mm, R_c = 25.5mm
Sun et al. (2007)	Searle type	R_b = 10mm, R_c = 15mm
Malik et al. (2010)	Searle type double concentric	R_1 = 14.5mm, R_2 = 16.5mm, R_3 = 18mm, R_4 = 20.5mm

- Jones and Bartlett (Jones and Bartlett, 1952), do not measure the variation of the apparent viscosity in molten aluminium and its alloys with shear rate. They obtain a temperature dependence of apparent viscosity. Only the other authors vary the shear rate and observe the corresponding effect on the apparent viscosity.
- Bakhtiyarov and Overfelt (Bakhtiyarov and Overfelt, 1999) , measure the viscosity of LMA-158. Schematic representation of their apparatus is illustrated in Fig. 2.15. Although the authors claim the liquid to demonstrate Newtonian behaviour by showing shear independence behaviour of viscosity, careful calculations indicate otherwise. Demonstrated in Appendix V, a reduction of apparent viscosity, from 2.065mPa.s to 1.99mPa.s, with shear rate (0 to 70 s^{-1}) is observed.

- Varsani and Fan (Varsani and Fan, 2007) demonstrate a reduction of apparent viscosity with shear rate at low shear rates like a shear thinning fluid. On further increasing the shear rate, the apparent viscosity measured by them increases linearly, demonstrating a shear thickening behaviour (Fig. 6.1). This result is similar to Fig. 5.2.Varsani and Fan believe "*…this scattering at low shear rate is caused by the mechanical instability of the concentric cylinder mechanism*" (Varsani and Fan, 2007). They reject the values at low shear rates based on the eccentricity effects at these low rotation speeds. Correlating molten metal to a granular fluid, they believe that the liquid shows a non-Newtonian shear thickening behaviour since "*…under shear flow, atoms in the liquid will obtain an extra random velocity sustained by the granular temperature, which in turn increases the friction between atoms, giving rise to an increase in viscosity. The higher the shear rate is, the stronger the friction between atoms, and hence the higher the viscosity*" (Varsani and Fan, 2007).

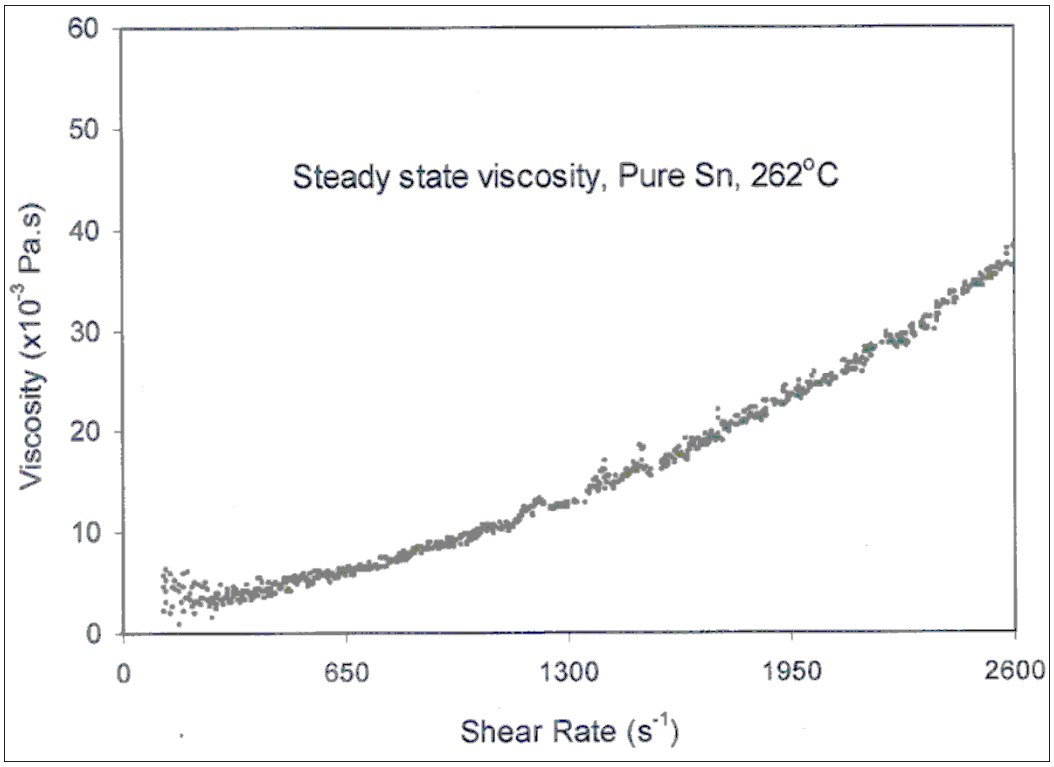

Fig. 6.1. Variation of apparent viscosity with shear rate in molten tin using a Searle type viscometer. Result from Varsani and Fan (Varsani, 2006).

- Sun et al. (Sun *et al.*, 2007), measure the rheological behaviour of Sn, Pb, Bi and Sb and present the non-Newtonian behaviour of molten Sn and Bi. But, calculations of apparent viscosities for Sn at 387.5^{o}C from Fig. 3 in (Sun *et al.*, 2007) yield values of over 8 Pa.s for the dimensions provided (Appendix V). Compared to literature values of 1.85mPa.s (Assael *et al.*, 2010), the values from Sun et al. are over three orders of magnitude higher. This makes their values questionable.
- Malik et al. (Malik *et al.*, 2010), who employ a double-concentric cylinder apparatus to reduce end effects, demonstrate that the apparent viscosity for Al, Zn and tin-based solder alloy reduces with shear rate as a shear thinning fluid. Recent works by the group (Jeyakumar, Hamed and Shankar, 2011), also illustrate this result. Malik et al. believe that the values for apparent viscosity at higher shear rates are complicated by turbulence and the presence of Taylor vortices (Malik *et al.*, 2010). Malik et al. go so far as to dismiss the oscillating cup data because of its inherent assumptions that the material in the cup behaves as a Newtonian liquid and the damping oscillation in the oscillating cup is a decaying sine wave. Employing a Newtonian liquid Cannon S2000 to calibrate their equipment, they demonstrate a shear thinning behaviour in molten Al and Zn in (Malik *et al.*, 2010) and Sn in (Jeyakumar, Hamed and Shankar, 2011). To compare their results for molten Sn, a combined plot of apparent viscosity against shear rate is illustrated in Fig. 6.2, where data has been taken from Fig. 7(b) in (Jeyakumar, Hamed and Shankar, 2011) and compared with data obtained by testing Sn in the Searle and the Couette type viscometers employed in this study. The combined plot in Fig. 6.2, illustrates the following:

(i) In all three types of concentric cylinders apparatus, there is a decrease of apparent viscosity with shear rate at low shear rate values.

(ii) Results by Jeyakumar et al. and Malik et al. (Jeyakumar, Hamed and Shankar, 2011; Malik *et al.*, 2010) show a higher absolute value (1 order of magnitude higher) for the

apparent viscosity than the results in this study, which the author believes is due to the greater surface area of the double concentric cylinder setup wet by the liquid, which in turn increases the surface effect on the torque measurements.

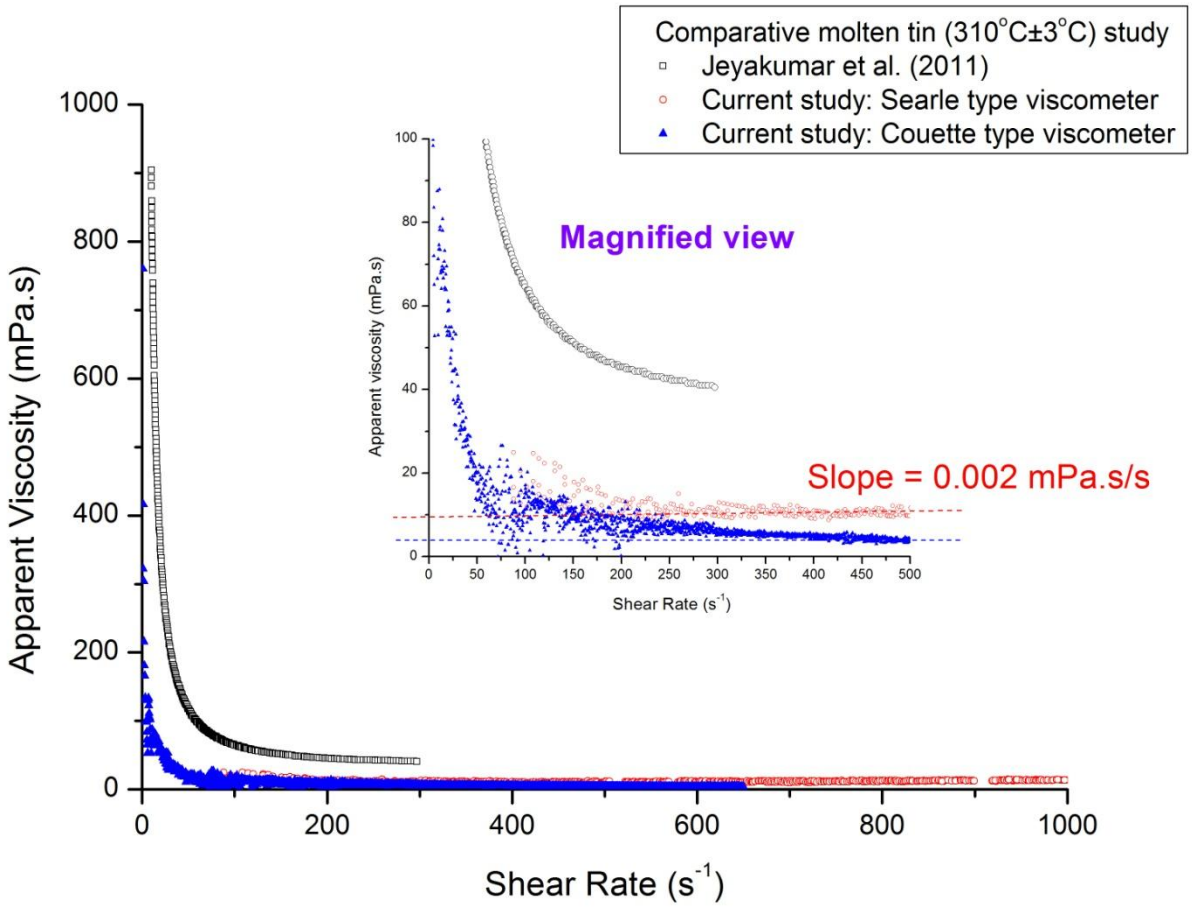

Fig. 6.2. Combined plot of variation of apparent viscosity with shear rate for molten tin held at temperatures 307°C ± 5°C in the Couette type viscometer, 310°C ± 1°C in the Searle type viscometer and 312°C in (Jeyakumar, Hamed and Shankar, 2011).

(iii) Above shear rates of 250s^{-1}, the apparent viscosity in the Searle type viscometer begins to increase with shear rate slowly (slope = 0.002mPa.s.s) whereas the apparent viscosity in the Couette type viscometer gradually reduces to a plateau value.

Since the Searle type viscometer used in this study and the AR2000 rheometer with the DCC geometry employed by Malik et al., both rotate the inner cylinder keeping the outer cylinder fixed, we conclude that the choice of which cylinder rotates has a significant influence on the rheological behaviour displayed by metals. This difference has also been predicted by Stokes,

Rayleigh and Taylor for water (see Chapter 2). To analyse this difference further, an in-depth comparison of the results from the Searle type viscometer and the Couette type viscometer employed in this study is very crucial. Despite the difference in equipment described in Table 6.2, there is a similarity in the shapes of all the curves (Fig. 6.2) at low shear rates.

6.2 Searle type viscometer vs. Couette type viscometer

6.2.1 Comparing Andereck Diagram

The Searle type and the Couette type viscometer differ in the choice of the rotating cylinder. The difference between the instruments can be further appreciated by correlating with the Andereck Diagram (Fig. 6.3). Andereck performed experiments rotating the concentric cylinders by different speeds both in the same direction (co-rotating) and in the opposite direction (counter-rotating) using water. He employed particles in the water to follow the flow of water at various Reynolds number.

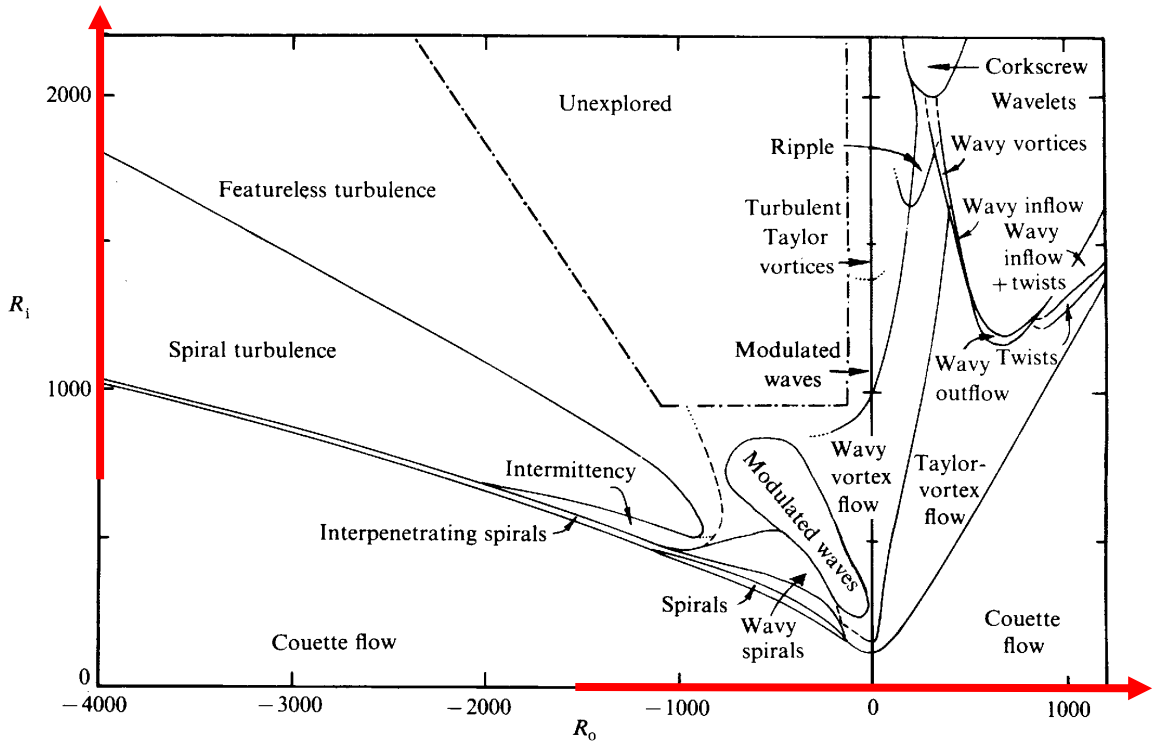

Fig. 6.3. The Andereck Diagram (Andereck, Liu and Swinney, 1986) , illustrating the variation of Reynolds number of the inner cylinder (R_i, y-axis) against the Reynolds number of the outer cylinder (R_o, x-axis). The Searle type viscometer lies along the y-axis and the Couette type viscometer lies on the x-axis of this Andereck Diagram.

In the Andereck Diagram, the Reynolds number of the inner cylinder is plotted against the Reynolds number of the outer cylinder. As the inner cylinder rotates (like the Searle type viscometer), its Reynolds number gradually traverses along the y-axis, in the positive direction. As the outer cylinder rotates (as in the Couette type viscometer), its Reynolds number traverses along the positive x-axis. Thus in the Searle type viscometer, the secondary flows are more prevalent starting with the Taylor vortices; whereas in the Couette type viscometer, the flows between the concentric cylinders are more stable for the given Reynolds number. Thus the following hypothesis explaining the results is given.

[Hypothesis: Presence of Taylor vortices in the Searle type viscometer causes the rise in viscosity at higher shear rates; Taylor vortices are less likely to be present with the Couette type viscometer.]

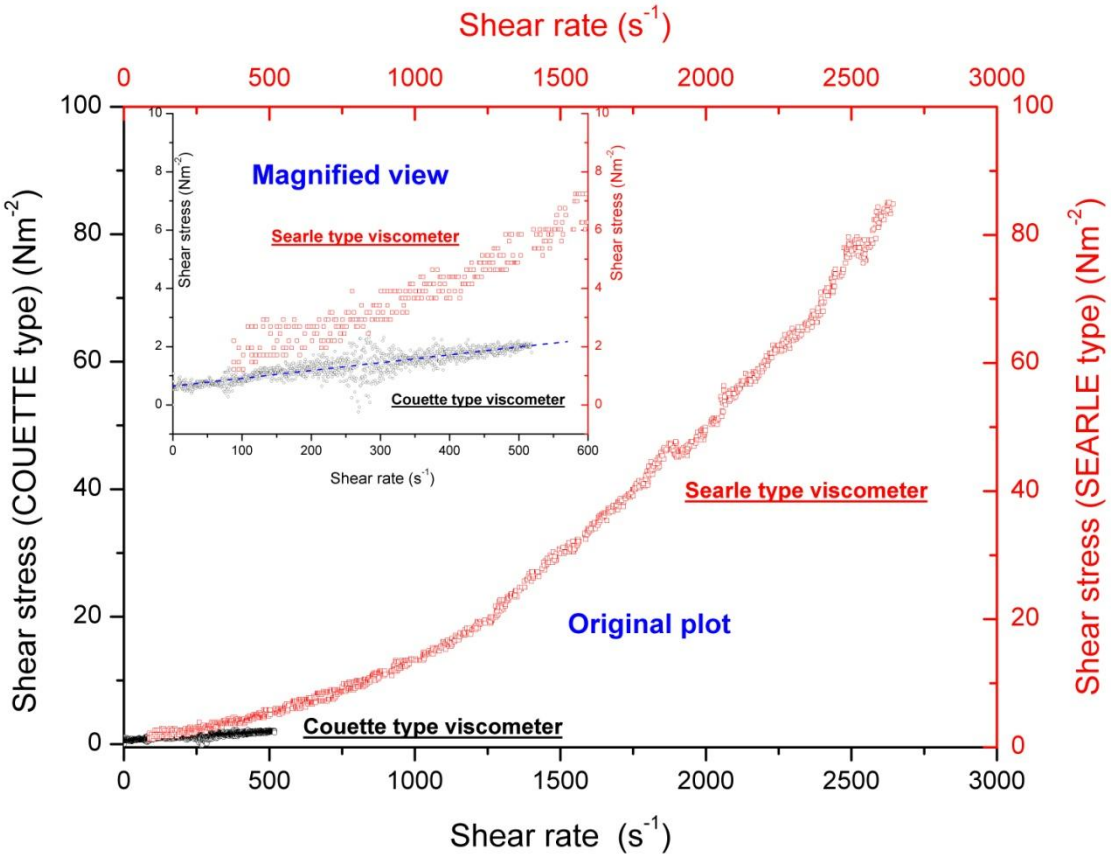

Fig. 6.4. Flow curves in Searle and Couette type viscometers, molten Sn (384^{o}C ± 3^{o}C) during ramping up experiment of 0 to 1000rpm in 10 minutes for the Searle type and 0 to 320rpm for the Couette type. *Inset, magnified view of the flow curves until 600s^{-1} shear*. Blue dashed line (inset) represents best fit line through the points for the Couette type.

6.2.2 Comparing flow curves

Comparing the flow curves for tin for the Searle and Couette type viscometers (Fig. 6.4), a distinct difference in profile is observed. The tin when measured with a Searle type viscometer demonstrates a typical shear thickening fluid's flow curve (Fig. 2.3). Whereas, in the Couette type viscometer, the shear stress shows a linear variation with shear rate, despite the symmetric scatter of data at shear rates $300s^{-1}$. This form of linear variation is consistent with a Newtonian fluid, although studies to higher shear rates are equally necessary. Calculating the slope for the flow curve (best fit line through the data points: blue line);

$$\frac{d\tau}{d\dot{\gamma}} = 0.00268;$$

$$\therefore\ \eta = 0.00268\ \text{Pa.s or } 2.68\ \text{mPa.s}$$

The author suggests that the increase in viscosity for the Searle type viscometer is consistent with the theory, predicting the presence of Taylor vortices and other secondary flow systems within the melt, which are known to increase the apparent viscosity of a fluid. Thus, the author believes that it is the presence of such secondary flows which gives the shear thickening effect in the molten metal and not the true nature of the liquid. Calculation of the Taylors number is also demonstrated in the next section comparing the flow system with molten tin in the Searle type and the Couette type viscometers. The Taylor stability criterion (equation 2.20 and 2.21) is also employed to check the presence of secondary flows in the Searle type viscometer. If the hypothesis of secondary flows in Searle type viscometers is true, the use of equipment with inner cylinder rotating, must be restrained while testing low viscosity liquids since formation of secondary flows may lead to misleading results.

6.2.3 Calculation of Taylor's stability criterion

Obtained from (Taylor, 1936), the criterion was set by Taylor to predict the introduction of Taylor vortices in a Searle type system only (equation 2.20 and 2.21).

For molten tin (335^{o}C ± 2^{o}C) viscosity from Fig. 5.1, density from (Alchagirov and Chochaeva, 2000);

$$\eta = 1.5 \text{ mPa. s};\ \rho = 6.963\text{x}10^{3} \text{ kg/m}^{3}$$

$$\therefore\ \nu = \frac{\eta}{\rho} = 0.2154 \text{ mm}^{2}/\text{s}$$

For the Searle system used (this geometry is the same as used by (Varsani, 2006));

R_c = 25.5 mm; R_b = 24.5 mm; $\Delta = R_c - R_b$ = 1.0 mm

$$\text{P} = 0.0571\left(1 - 0.652\frac{\Delta}{\text{R}_b}\right) + 0.00056\left(1 - 0.652\frac{\Delta}{\text{R}_b}\right)^{-1}$$

Thus P = 0.05615, after entering the terms in the formula above (equation 2.20).

From equation 2.21,

$$\text{P} = \frac{\pi^{4}\nu^{2}(\text{R}_c + \text{R}_b)}{2\Omega^{2}\Delta^{3}\text{R}_b^{2}}.$$

Thus P = 0.188/Ω^2. Comparing the two results,

$$\Omega^{2} = 3.352 \text{ s}^{-2}$$

$$\therefore\ \Omega = 1.83 \text{ s}^{-1} \text{ or } \omega = 17.5 \text{ rpm}$$

This analysis predicts that for the Searle type viscometer used, beyond a speed of 18 rpm, Taylor vortices and later secondary flows are most likely to be present in the molten tin sample held at 335^{o}C (Fig. 5.2) as mentioned by Malik et al. (Malik *et al.*, 2010).

6.2.4 Calculation of Taylor number

From equation 2.22, the Taylor number for the molten tin at 335^{o}C ± 2^{o}C is calculated for the Searle type viscometer. From the data in the previous page, the critical speed beyond which Taylor vortices will be present in the system can be calculated.

$$\mathrm{Ta} = \frac{\rho^2\Omega^2(\mathrm{R_c} - \mathrm{R_b})^3\mathrm{R_b}}{\eta^2} < 3400$$

Entering the data, we obtain: $\Omega^2 < 6.44\ \mathrm{s}^{-2}$.

Thus the critical speed, Ω is 2.54 s^{-1} or ω is 24.2 rpm.

From the Taylor number calculations for the Searle type viscometer employed in this study, there will be Taylor vortices present in molten tin (335^{o}C) beyond a speed of rotation of 25 rpm. This result is of the same order of magnitude as the critical speed obtained from the original Taylor stability criteria (section 6.2.3). Thus, both the calculations in section 6.2.3 and 6.2.4 indicate that at speeds of rotation above 30 rpm (or 82 s^{-1} shear rate) for the Searle type viscometer, there is a strong possibility of the presence of Taylor vortices which is leading to the rise in apparent viscosity.

The Reynolds number is employed to calculate the critical speed for the Couette type viscometer (equation 2.19). Obtained from (Atkinson, 2008; Macosko, 1994; Van Wazer, 1963):

$$\mathrm{Re} = \frac{\rho\Omega(\mathrm{R_c} - \mathrm{R_b})\mathrm{R_c}}{\eta} < 50000 \qquad (6.1)$$

For the Couette type viscometer (R_b = 14mm, R_c = 15mm), calculation of the critical Reynolds number for molten tin at 385^{o}C: density from (Alchagirov and Chochaeva, 2000) and viscosity from Fig. 5.1 yields ρ = 6.9295x10^{3} kg/m^{3} and η = 1.37 mPa.s.

Using these values in the equation 6.1 yields: Ω < 706.1 s^{-1}.

Thus the critical speed of rotation, Ω is $706.1 s^{-1}$ or critical ω is 6742.7 rpm.

The speed of rotation of the outer cylinder has to be of the order of six thousand rpm before the liquid (molten tin in this case) becomes turbulent. Since such high speeds have not been reached in this study, presence of any turbulence or Taylor vortices or secondary flows within the Couette type viscometer can be rejected. Hence, from these calculations, it is confirmed that conducting molten tin experiments (or molten state metals in general) with the Searle type viscometer at high shear rates, will lead to presence of Taylor vortices within the melt during measurements (Ball, 2001).

6.3 Testing in a protective environment of N_2 and without it

The results presented in Fig. 5.5 and 5.6 demonstrate the differences and similarities of measuring the apparent viscosity with and without the presence of nitrogen gas. Although the presence of a protective medium around the melt is crucial for conducting experiments, lack of such a medium does cause variations in the behaviour of the melt. Comparing the two plots, the following observations are made:

1. Both curves demonstrate a reduction of apparent viscosity with shear rate at low shear rate conditions.
2. The absolute value of apparent viscosity at low shear rates is lower for the experiment with the N_2 than the results without the protective medium.
3. The results without the presence of nitrogen gas are more irregular with sudden increase and sudden decrease in apparent viscosities compared to the results with the presence of N_2, where there is a gradual decrease of apparent viscosity to a plateau value.

4. At higher shear rates, there is an increase in apparent viscosity with shear rate in the experiments without N_2. This is consistent with the theory that the presence of solid particles increases the viscosity of the fluid medium.

6.4 Pure tin vs. tin doped with germanium

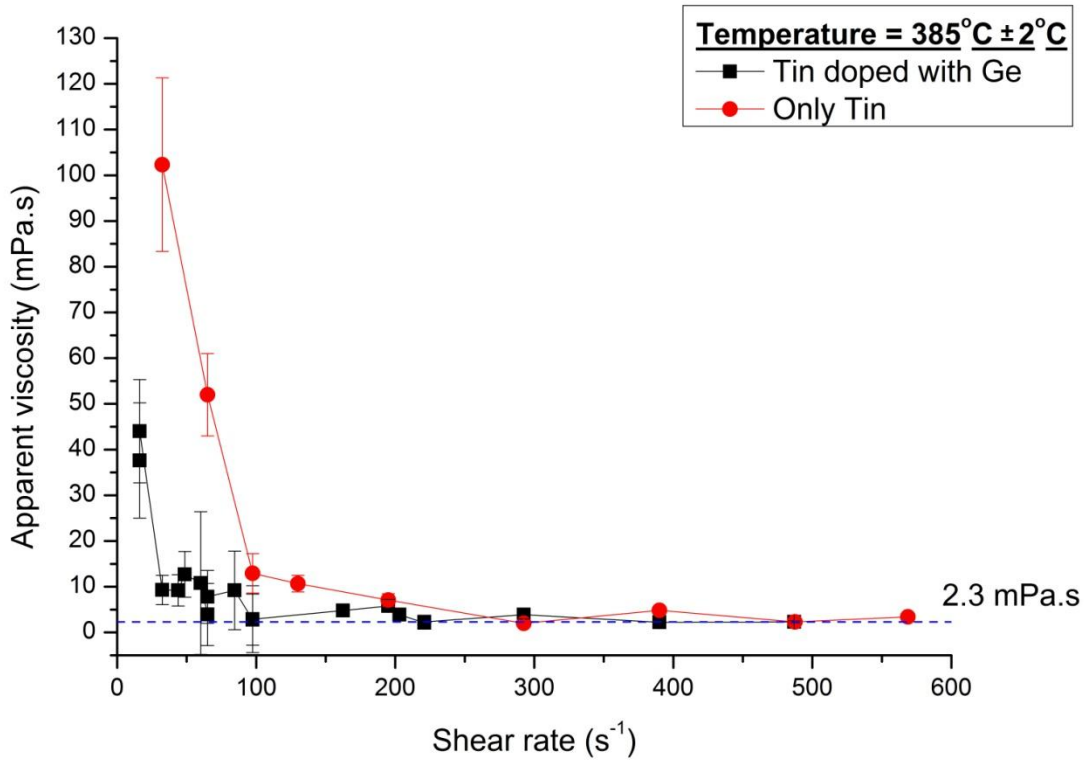

Fig. 6.5. Comparative plot illustrating the effect on viscosity measurements when tin is doped with 50ppm Germanium. The master alloy, obtained from Dr. Christopher Gourlay, Imperial College, London, helped demonstrate the change in apparent viscosity in the melt at low shear rates in a series of fixed speed experiments.

A series of fixed speed experiments with tin (shown in red, Fig. 6.5) illustrated the difference in apparent viscosity values at low shear rates when the melt was doped with germanium (shown in black, Fig. 6.5). The comparative plot illustrates that at low shear rates, the apparent viscosity values are much lower in tin doped with germanium than the undoped tin,

for the same shear rates. Also, as shear rate is increased, both curves gradually come closer and almost overlap over one another. The tin doped with germanium demonstrates a plateau value of 2.3 mPa.s ± 0.2 mPa.s (also, Fig. 5.11); the sample of undoped tin has a plateau value of 2.7mPa.s ± 1.2 mPa.s at the same experimental temperature of $385^{o}C \pm 2^{o}C$. The author believes that the change in surface properties by the addition of 50ppm germanium has altered the wetting characteristics of the tin on the surface of the concentric steel cylinders. This indicates that the surface tension forces on the liquid-cylinder interface are playing a key role in the viscosity measurements since surface properties of the melt greatly affect the surface tension of the melt.

6.5 Low shear rate vs. high shear rate

So far, most plots of apparent viscosity against shear rate for any concentric cylinder (Searle or Couette type) apparatus have demonstrated the following observations:

- At low shear rates apparent viscosity reduces with shear rate
- At high shear rates either apparent viscosity increases or is shear independent, depending on the shear condition of rotating the inner or outer cylinder.

Explanations:

(I) Reasons for such a profile lie in the Reynolds number (equation 2.19) calculations for the low and high shear rates. The calculations can be correlated with the Andereck Diagram (Fig. 2.15) and the table 6.1 illustrating the difference in physical properties of the various liquids tested in this study. From Table 6.1, it is easy to recognise the high density values for tin and lead (by analogy lead-tin eutectic alloy as well). Since density lies in the numerator of the Reynolds number, for two liquids with similar viscosity to have similar Reynolds number, the speed of rotation of the higher density liquid must be

low. In other words, the critical Reynolds number for introducing secondary flows into the system would be at a lower speed of rotation for metals than for low density liquids like water or the silicone oils, which have similar dynamic viscosity as the metals. This means, for metals being rotated at low shear rates, there is greater possibility of vortices (in the annular gap or under the inner cylinder) being generated within the system for the low shear range, than for silicone oils at the same shear rate. This is illustrated when comparing the low shear range of Fig. 4.4 and Fig. 6.5, where in the first case silicone oil S3 is tested and in the latter, tin is tested.

(II) From the German National Standards DIN 53018 (Part 1and 2) and DIN 53019, LeBlanc et al. mention in section 30.1 of (Webster, 1999) that, when the Reynolds number reaches unity in the Couette type viscometer, the vortices under the inner cylinder play a significant role in torque measurements. Despite an absence of Taylor vortices in the annular gap, the vortices under the inner cylinder can have a profound effect on these torque measurements. Since Reynolds number of unity occurs in the Couette type viscometer of this study at speeds << 1 rpm ($\omega = 0.135$rpm; from equation 2.21), it is believed that these vortices might lead to the higher torque measurements at these low shear rates. The higher torque measurements in turn would lead to high apparent viscosity values, as observed for molten metals.

(III) Coupled with this belief, the eccentricity between the concentric cylinders also plays a major role in torque measurements. At low speeds of rotation, the eccentricity between the cylinders is more significant, owing to the inability of the motor to generate smooth rotation of the outer cylinder leading to “jerking”. With high density-low viscosity liquids like molten tin or lead in the gap, any eccentricity between the cylinders is believed to cause significant increase in the torque readings which is manifested in the results of the apparent viscosity at low shear rates. As the speed increases, eccentricity

between the cylinders is minimised owing to the self-centring effect on the rotating outer cylinder. This leads to stable and less scattered results at higher shear rates (Fig. 6.5).

(IV) Surface properties of the liquid play a major role in viscosity measurements. This is demonstrated well in Section 6.4. Addition of 50ppm germanium led to a significant reduction of the apparent viscosity values observed at low shear rates, the values at higher shear rates being similar to undoped tin. Generally surface tension forces, which are based on the surface properties of the liquid, are too small to influence the total torque readings. But in some materials, any change at the free surface might have large effects on the measurements (Macosko, 1994). Addition of germanium to the melt alters the oxidation of the tin-rich section of the melt (Wan Cho *et al.*, 2006). Germanium addition has also been observed to alter the contact angle of molten tin on a germanium substrate from 180^{o} to $20\text{-}60^{o}$ in a mere 10^{-2} s (Fig.4, (Naidich and Perevertailo, 1971)). Thus presence of germanium most certainly alters the surface properties of the tin-rich melt, which is manifested by the low apparent viscosity at lower shear rates compared to the melt with just tin. At the high shear rates, both liquids display similar apparent viscosities.

Based on these possible explanations to the difference in the profile of the apparent viscosity against shear rate curves for metals, it is easy to recognise the intricacies within the liquid metal system during measuring processes. Thus to correlate the results obtained from the experimental measuring processes to real world application scenarios, a comparison must be done with literature values, which are generally accepted in any calculations involving the viscosity of molten metal or alloys. To compare with literature values, an uncertainty budget has been conducted to calculate the uncertainty in the viscosity results obtained from the Set 5 geometry of the Couette type viscometer.

The results from the uncertainty budget are summarised in the next section and details on the calculations involved, are given in Appendix VI.

6.6 Uncertainty budget

Obtaining the basic knowledge of uncertainty from (Bell, 2001), the combined uncertainty of the measurand y (the quantity to be measured), has been determined from the partial derivatives of the function (y = f(x)) and the standard uncertainties in the parameters of that function. Assuming that the individual uncertainty sources are uncorrelated, the combined uncertainty has then been computed using the root sum squares method (mentioned as SQRT in Table 6.3). The combined uncertainty corresponds to one standard deviation and therefore has as associated confidence level of approximately 68%. Assuming a normal distribution, the expanded uncertainty equivalent to a 95% confidence level, can be determined using a coverage factor of 2, i.e. twice the combined uncertainty value.

First, the parameters in the equation employed for obtaining the apparent viscosity of the liquid in this study are identified. The equation employed for calculating viscosity is:

$$\eta = \frac{M}{8\pi^2 l_b \left(\frac{\omega}{60}\right)}\left[\frac{1}{R_b^2} - \frac{1}{R_c^2}\right],$$

The parameters in this equation are: M, l_b, ω, R_b and R_c. Based on the calculations on the uncertainties of these parameters described in Appendix VI, the following table summarises the uncertainties for each parameters and the combined uncertainty from these calculations.

Table 6.3. Uncertainty analysis on the apparent viscosity measurements of different liquids tested with the Couette viscometer.

Name	Type of uncertainty	Value
u(ΔT)	B	1.15 for metals; 0.58 for Newtonian oils.
u(R_c^o)	A	0.004
u(R_b^o)	A	0.005
u(l_b^o)	A	0.008
u(M)	B	0.025 for metals; 0.003 for Newtonian oils
u(ω)	B	0.115

For standard Oil S3					
Name of Input Variable	Value of variable	uncertainty [u(x)]	Sensitivity (dy/dx)	u(x) * (dy/dx)	[u(x)*(dy/dx)]^2
Torque (M) (gm.cm)	0.46	0.003	6.6E-08	2.12E-10	4.5E-20
Length of bob (mm)	42	0.008	-7.3E-10	-6.0E-12	3.6E-23
radius of cup (mm)	15	0.004	2.8E-08	1.1E-10	1.2E-20
radius of bob (mm)	14	0.005	-3.4E-08	-1.8E-10	3.5E-20
rotational speed (w)(rpm)	180	0.115	-1.7E-10	-1.9E-11	3.9E-22
				Total standard uncertainty = SQRT (Σ([u(x)*(dy/dx)]^2))	9.3E-20
				u(η) [Units - mPa.s]	0.03
				U(η)[Expanded uncertainty 95% confidence][Units - mPa.s]	0.06
				η [Units - mPa.s]	3.01
				Relative expanded uncertainty of density (95% confidence level), %	2.0

For Molten metal Tin					
Name of Input Variable	Value of variable	uncertainty [u(x)]	Sensitivity (dy/dx)	u(x) * (dy/dx)	[u(x)*(dy/dx)]^2
Torque (M) (gm.cm)	0.64	0.025	4.2E-08	1.1E-09	1.1E-18
Length of bob (lb) (mm)	42	0.008	-6.5E-10	-5.3E-12	2.8E-23

radius of cup (mm)	15	0.004	2.4E-08	9.8E-11	9.7E-21
radius of bob (mm)	14	0.005	-3.0E-08	-1.7E-10	2.8E-20
rotational speed (w)(rpm)	280	0.115	-9.7E-11	-1.1E-11	1.2E-22
				Total standard uncertainty = SQRT (Σ([u(x)*(dy/dx)]^2))	1.2E-18
				u(η) [mPa.s]	0.1
				U(η)[Expanded uncertainty 95% confidence][mPa.s]	0.2 (coverage factor of 2)
				η [mPa.s]	2.67
				Relative expanded uncertainty of density (95% confidence level), %	8.0
For Molten metal Lead					
Name of Input Variable	Value of variable	uncertainty [u(x)]	Sensitivity (dy/dx)	u(x) * (dy/dx)	[u(x)*(dy/dx)]^2
Torque (M) (gm.cm)	0.32	0.025	5.7E-08	1.4E-09	2.0E-18
Length of bob (lb) (mm)	42	0.008	-4.3E-10	-3.6E-12	1.3E-23
radius of cup (mm)	15	0.004	1.6E-08	6.6E-11	4.4E-21
radius of bob (mm)	14	0.005	-2.0E-08	-1.1E-10	1.2E-20
rotational speed (w)(rpm)	207	0.115	-8.9E-11	-1.0E-11	1.0E-22
				Total standard uncertainty = SQRT (Σ([u(x)*(dy/dx)]^2))	2.1E-18

				u(η) [mPa.s]	0.14
				U(η)[Expanded uncertainty 95% confidence][mPa.s]	0.28(coverage factor of 2)
				η [mPa.s]	1.80
				Relative expanded uncertainty of density (95% confidence level), %	15.8
For molten Tin doped with Germanium (50 ppm)					
For Molten metal					
Name of Input Variable	Value of variable	uncertainty [u(x)]	Sensitivity (dy/dx)	u(x) * (dy/dx)	[u(x)*(dy/dx)]^2
Torque (M) (gm.cm)	0.59	0.025	4E-08	1.0E-09	1.0E-18
Length of bob (lb) (mm)	42	0.008	-5.6E-10	-4.6E-12	2.1E-23
radius of cup (mm)	15	0.004	2.1E-08	8.5E-11	7.3E-21
radius of bob (mm)	14	0.005	-2.67E-08	-1.4E-10	2.1E-20
rotational speed (w)(rpm)	300	0.115	-7.8E-11	-9.0E-12	8.2E-23
				Total standard uncertainty = SQRT (Σ([u(x)*(dy/dx)]^2))	1.03E-18
				u(η)[mPa.s]	0.1
				U(η)[Expanded uncertainty 95% confidence][mPa.s]	0.2(coverage factor of 2)
				η[mPa.s]	2.3
				Relative expanded uncertainty of density (95% confidence level), %	8.6
For Molten metallic alloy Tin-Lead eutectic					
Name of Input Variable	Value of variable	uncertainty [u(x)]	Sensitivity (dy/dx)	u(x) * (dy/dx)	[u(x)*(dy/dx)]^2
Torque (M) (gm.cm)	1.526	0.025	3. 1E-08	7.8E-10	6.1E-19
Length of	42	0.008	-1.1E-09	-9.3E-12	8.7E-23

bob (lb) (mm)					
radius of cup (mm)	15	0.004	4.29E-08	1.7E-10	2.9E-20
radius of bob (mm)	14	0.005	-5.2E-08	-2.9E-10	8.4E-20
rotational speed (w)(rpm)	384	0.115	-1.2E-10	-1.4E-11	2.0E-22
				Total standard uncertainty = SQRT (Σ([u(x)*(dy/dx)]^2))	7.2E-19
				u(η)[mPa.s]	0.083
				U(η)[Expanded uncertainty 95% confidence][mPa.s]	0.17(coverage factor of 2)
				η[mPa.s]	4.6
				Relative expanded uncertainty of density (95% confidence level), %	3.6

Thus from the table, the expanded uncertainty along with the relative uncertainties are employed in the comparison with the literature values for the liquids tested. The expanded uncertainty illustrates the range of the apparent viscosity value of the specific liquid. The comparison is presented in the following section.

6.7 Experimental results vs. literature values

Table 6.4. Comparing the experimental results for oils and molten state metals with the results from certificate and literature respectively. The confidence level for the results is 95% with a coverage factor of 2.

Name of Material	Temperature of Measurement (^{o}C)	Literature Value (mPa.s)	Experimental Value (mPa.s)
S3 standard oil	25	2.966 [1]	3.01 ± 0.06
Molten Tin (without additions)	384.5	1.29 to 1.45 [2]	2.67 ± 0.2
Molten Tin (doped with Germanium)	384.5	1.29 to 1.45 [2]	2.3 ± 0.2
Molten Lead (without additions)	384.5	2.21 to 2.26 [3]	1.8 ± 0.3
Molten Lead – Tin eutectic alloy	288.5	NA*	4.63 ± 0.17

*NA – not available. [1] see: Appendix I, [2] see: Fig. 5.1, [3] see: Fig. 5.7.

The results of apparent viscosity of molten metal and alloys from the experiments in this study are higher for tin and marginally lower for lead, compared to the values quoted in literature (Assael *et al.*, 2010) which have generally employed oscillating type viscometers to measure the apparent viscosity. Yet, these higher values are of the same order of magnitude as the ones from literature and have been measured at shear rates (about 700 s^{-1}) well above the ones mentioned in literature (less than 1 s^{-1}). The differences in the absolute values might be difficult to resolve owing to the measurement limitation of the equipment. Thus, based on the discussions in this chapter and Table 6.4, conclusions can be derived regarding the flow behaviour of molten metal in different measuring systems. These have been summarized in the following chapter.

Chapter 7

Conclusions

This study has revealed that the flow in liquid metals is more complicated than generally assumed. It is clear, further work is needed to untangle the intricacies of flow behaviour under shear.

In this comparative study, two instruments based on the concentric cylinders mechanism, have been employed to study the effects of shear on the flow behaviour of molten metals. A Searle type viscometer with the inner cylinder rotating and a Couette type viscometer with the outer cylinder rotating are used. Both equipment have been calibrated with standard Newtonian oils and verified with Newtonian systems. Different modifications to the Couette type viscometer have enabled the equipment to accurately measure the dynamic viscosity of low viscous oils. Thus a novel piece of equipment (the Couette type viscometer-outer cylinder rotating) has been developed during the course of this study for measuring the viscosity of low viscous liquids. There are not many instruments being used, which are based on a similar measurement technique. Consequently, few experiments with molten Sn and Pb in the Searle type and the Couette type viscometer along with a few more experiments with Sn-Pb eutectic and Sn doped with Ge in the Couette type viscometer have been conducted.

Based on the experimental results obtained, the following conclusions can be made:

(1) From the standard Newtonian oils in the Couette apparatus:

(a) The rheological behaviour observed experimentally depends on the aspect ratio of the geometry of the inner (bob) and outer (cup) cylinder.

(b) A lower aspect ratio of the geometry leads to end effects thereby affecting the verification experiments thereafter.

(c) A higher aspect ratio should always be maintained while designing the inner cylinder (bob) and outer cylinder (cup) of the viscometer. Also, the length of the inner cylinder (bob) should be kept atleast three times longer than its radius.

From these results, the optimised system was: R_c = 15mm, R_b = 14mm, l_b = 42mm, taper at the end of inner cylinder = 2.94^o.

(2) From the results with the molten metals and molten metallic alloys in the Couette apparatus, the plot of apparent viscosity against shear rate can be divided into two zones:

(I) Upto 250 s^{-1} shear rate: Decrease of apparent viscosity with shear rate.

(II) Above 250 s^{-1} shear rate: Apparent viscosity is independent of shear rate.

The zone I of the apparent viscosity against shear rate plot which presents a decrease of apparent viscosity with shear rate may be explained by the following causes:

(i) Eccentricity effect

Due to the greater density of the molten metal or its alloy compared to the standard Newtonian oils, the eccentricity effect is magnified in molten state metals as compared to the oils at the low rates of shear due to jerkiness of the rotating cylinder.

(ii) Surface Tension effect

The surface tension of the molten metals is much higher than the surface tension of the standard Newtonian oils. This enables the wetting characteristics of molten metals to play a significant role at low rates of shear. The results comparing the apparent viscosities of tin doped with germanium and undoped tin support this observation. By altering the surface properties of the melt, a significant change in the thermophysical properties is recorded.

(iii) Oxide effects

Although the results of apparent viscosities obtained from the experiments with molten tin with and without the presence of Nitrogen are similar, results with the presence of Nitrogen show less oscillation in values as compared to the results obtained without the presence of Nitrogen. At higher rates of shear the difference between the two is more significant owing to the presence of greater quantity of oxide particles.

The zone II of the molten metals which presents a more stable and shear independent behaviour of apparent viscosity enables the user to calculate the apparent viscosity of the melt at higher rates of shear and compare them to the values from literature. It is at this zone that the difference in results between the Searle type viscometer (inner cylinder rotating) and the Couette type viscometer (outer cylinder rotating) become more prominent.

(3) Comparing the apparent viscosity against shear rate results from the Searle type viscometer with molten metals and molten metallic alloys against the results from the Couette type viscometer, differences in behaviour in zone II are observed. For the Searle type, there is a rise in apparent viscosity with shear rate as compared to the flat or very slowly decreasing apparent viscosity with shear rate obtained in the Couette type viscometer.

(4) The above results are consistent with the Andereck Diagram developed for water where rotating the inner cylinder with the outer cylinder fixed ($R_o = 0$) would lead to flow instabilities such as Taylor vortices, giving rise to an increase in apparent viscosity. For the Couette type viscometer, with the outer cylinder rotated and the inner cylinder fixed ($R_i = 0$), a region of stable flow will be followed, giving a stable apparent viscosity.

(5) Calculations of the stability criterion given by the calculation of the Reynolds number and Taylor number for the molten metals indicate that Taylor vortices or secondary flows may be present at speeds above 30 rpm when employing the Searle type viscometer employed in this study (inner cylinder rotating). In comparison, only above speeds of 6700 rpm in the Couette type viscometer of this study, can there be turbulent flows within the molten tin system. Since such speed was not achieved in these experiments, the Couette type viscometer demonstrates stable flow behaviour in the absence of secondary flows. Since the presence of Taylor vortices or secondary flows increases viscosity (as observed in the Searle type viscometer), the author believes that it is these secondary flows which facilitate the rise in apparent viscosity rather than the inherent nature of the molten metal.

(6) The experimental values for the molten metals and molten metallic alloys obtained for the Couette type viscometer at higher rates of shear (above 250 s^{-1} shear rate) are of the same order as the results generally accepted in the literature, which had employed the oscillating type viscometers to measure the dynamic viscosity.

Chapter 8

Future work

This study is not a definitive study and further effort towards developing the measuring equipment and developments in the underlying theory must be undertaken. Despite the efforts to accurately measure the viscosity of metals in the molten state at higher shear rates done in this study, there are still many improvements possible which could improve the accuracy and capability of the equipment's data collection.

Improvements in the Couette type viscometer:

(1) The current rotating mechanism could be altered to facilitate counter rotating and co-rotating cylinder mechanisms between the inner and outer cylinders. This would enable observing the change in flow behaviour by altering the shearing mechanism and also lead to development of equipment which has the capability of combining the Searle and the Couette type viscometers.

(2) Modifications to the software in the viscometer to collect data in a transient state. For low speed of rotations, more data points to be collected per second than at higher speeds of rotation when fewer data points can be collected. Compared to the current technique, where ten data points are collected and averaged to give the 1 data value per second, irrespective of speed of rotations, the improvement would be suitable in resolving the flow curves at low shear rates.

(3) To resolve the front end of the apparent viscosity against shear rate curve, experiments in the Couette type viscometer with molten state metals must be conducted with a more sensitive torsion wire than the one used in this study since a sensitive torsion wire would be able to resolve the data points better. But this may lead to problems of measuring at low strain rates which may overload the wire.

(4) Modification of the concept in centring the two cylinders. Currently the procedure followed (described in Appendix I) is quite time consuming and requires a great amount of effort in attempting to reduce eccentricity. Employing a rack and pinion gear system, commonly employed in optical microscopes to move the eye piece in x and y–directions, centring of the cylinders would be much easier and exact dimensions of the eccentricity can also be calculated.

(5) Improved cooling system should be implemented to raise the working temperature of the Couette type viscometer, to enable measuring the viscosity of commercial alloys and metals like LM25, AZ91, aluminium and magnesium.

Improvements in the Searle type viscometer:

(1) In the Searle type viscometer, manufacturing transparent quartz based outer cylinder to observe the formation of Taylor vortices in the molten state metals would conclusively demonstrate the presence of such vortices and would support the calculations presented in this thesis.

(2) Modifications to the dimensions of the inner and outer cylinders employed in the Searle type viscometer, to values similar to the ones employed in the Couette type viscometer, would enable direct comparison. This would demonstrate the change in flow curves when the choice of cylinder rotating is changed.

Simulation work

To support the experimental study, detailed and more in-depth simulations representing the flow systems in the molten state metals in the annular gap, should be conducted to obtain valuable information regarding the flow behaviour.

Appendix I

Couette type viscometer

(1) Switch on the equipment, computer and ensure water is flowing in the cooling system.

(2) Switch on the software, Ravenfield V1.17.

(3) Enter name of torque scale in "torque calibration tab".

(4) Now the software is ready to begin the calibration procedure.

(5) Clean the calibration piece and bob-spider with ethanol and dry them.

(6) Insert the taper end of the bob-spider into the calibration piece and fix it firmly with a M5 screw.

(7) After cleaning the inner cylinder (bob) and bob-rod with ethanol and dying them, the inner cylinder is screwed onto the bob rod.

(8) Now fix the bob rod to the bob-spider with 4 screws. These 4 screws would enable adjusting the concentricity of the inner cylinder.

(9) Using the dial test indicator (DTI) mounted on a horizontal steel plate, the combination of calibration piece, bob-spider and bob-rod with the inner cylinder at one end is rotated manually, adjusting the 4 screws as we go along, making sure that the variation on the circumference of the inner cylinder is less than 1 division of the dial test indicator. Since it is an inch DTI, the smallest unit is $1/1000^{th}$ of an inch = 25μm.

(10) After repeated rotation and checking, the bob-spider combined with the bob-rod and inner cylinder is removed from the calibration piece and is screwed onto the vertical air bearing.

(11) Nitrogen gas is switched on from the gas bottle (BOC Lmt., UK) at a pressure of 5 bars.

(12) The inner cylinder is seen oscillate freely once the gas starts passing through the vertical air bearing at a steady rate.

(13) Nitrogen gas is also passed through to the horizontal air bearing at a pressure of 3.2 bar ± 0.5 bar, to ensure that the outer ring floats on the inner rod without rotating in either direction. At such a state, the ring is suspended frictionless.

(14) When the inner cylinder stops oscillating about its axis, the torque reading at "0 torque" is recorded by pressing the "0 torque" tab on the software. This records the first point on the torque scale.

(15) After the ring of the horizontal air bearing stabilizes, a thread (cotton) attached to the pin of the bob-spider, is passed across half the perimeter of the bob-spider and over the horizontal air bearing.

(16) The thread has a copper pan at the other end which was suspended over the horizontal air bearing. The weight of the copper pan is included in the torque calculations.

(17) Pre-weighed washers are put into the copper pan to record the deflection.

(18) To obtain the weight which would lead to a torque reading close to the maximum torque measurable, different weights are put into the copper pan.

(19) When a weight with torque reading closest to the maximum torque is obtained, the weight is entered into the software and the tab "W weight torque" is pressed on the software. This obtains the second point on the torque scale.

(20) The inner cylinder is swung gently to the maximum limit and held there during which the "maximum torque" tab on the software is pressed. This records the third point on the torque scale.

(21) Obtaining the three points, a torque scale is generated.

(22) Now the equipment is calibrated with Newtonian oil.

(23) The tab "Viscosity Calibration" is pressed and the known viscosity of the liquid is entered into the software.

(24) At this time, the outer cylinder or cup is mounted on the shaft connected to the motor.

(25) The dial test indicator is mounted on the base of the vertical air bearing to centre the outer cylinder with respect to the inner cylinder, which is fixed to the air bearing.

(26) Placing the tip of the indicator, the outer cylinder is slowly rotated at a speed of 4 rpm.

(27) A set of 4 nuts at the base of the shaft are adjusted during this rotation to keep the variation in the dial test indicator at less than 1 division throughout the length of the outer cylinder.

(28) The step 27 is extremely difficult as even the smallest variation at the base of the outer cylinder leads to a huge error at its other open end, due to magnification of error through its length. This leads to several repeats of the adjustment process with attempts to minimize the variation.

(29) In most cases, the variation at the base of the outer cylinder is ± 0.3 divisions of the DTI and the variation at the top end of the outer cylinder is ± 1.5 divisions of the DTI on the circumference.

(30) After this, a sample of the Newtonian oil is poured into the outer cylinder. Based on the end gap (gap between the base of the inner and outer cylinders), the annular gap and the height by which the inner cylinder is inside the outer cylinder, the volume of the sample varies.

(31) The temperature of the liquid is maintained at the desired temperature of calibration.

(32) To ensure that the liquid is at the desired temperature, the system is left undisturbed for an hour after which the temperature of the liquid is measured with a K-type thermocouple.

(33) Once the temperature of the liquid has stabilised, the viscosity calibration tab of the software enables the user to enter the speeds at which the liquid will be rotated.

(34) The speeds are entered in an interactive table. After entering, the “0 torque” tab at the top of the software is pressed.

(35) To start collecting the torque values, the button “Start reading” is pressed, which leads to the motor rotating at the first speed entered in the table.

(36) Once a steady state of rotation is reached, the button “Take Reading” is pressed which records the torque value for that rotating speed in the adjacent table to the speed table.

(37) As the button for “Take Reading” is pressed, the motor goes onto the next speed of rotation automatically.

(38) Just as in the previous run, the steady state of rotation is reached and the “Take Reading” tab is pressed again to record the torque.

(39) In this way, all the speeds record corresponding torque values which are then plotted on a graph in the software.

(40) A best fit line connecting the points of torque against speed measures the constants for “speed” and “torque”. If the keta value, which is the regression coefficient for the curve, is greater than 0.99, the values are accepted else the steps from 34 till 39 is repeated until the value for keta greater than 0.99 is obtained.

(41) Once the values are obtained, the equipment is calibrated with the Newtonian oil and is ready for the verification test.

Searle type viscometer

(1) The torque calibration test was conducted to ensure that the torque values do not fluctuate beyond an acceptable level.

(2) The torque scale was generated by applying known weights to the bob shaft through a string passing over a pulley. The aim was to examine the linearity between the applied force and the measured torque and to examine the variations of the measured torque

whilst gradually increasing or gradually reducing the applied force within the gicen range.

(3) The torque readings were generally 7 times the known weight, 7 being the dimension of the torque measuring head.

(4) After generating the torque scale, the torque calibration test was simply done by running the machine at a fixed shear rate or by ramping the shear rate to maximum ($2724s^{-1}$) over a fixed period of time (usually 15 minutes) and recording the torque values.

(5) If the torque values remained accurate and constant with very little variation over a specified period of time, one can claim that the measured torque was accurate and reliable.

(6) After the torque calibration, the viscosity calibration was conducted. Newtonian oil D5 was employed for this calibration. Ramping up experiments was conducted with the oil and the corresponding torque values were measured.

(7) The torque values were employed in a calculating the constants in the software and there on the constants were employed for measuring torque and speed for unknown fluids.

(8) More details of the procedure can also be obtained from (Varsani, 2006) .

Appendix II

ACCREDITED TO ISO 17025:2005

CERTIFICATE OF CALIBRATION

ISSUED BY THE PSL CALIBRATION LABORATORY

DATE OF ISSUE 02 February 2010 SERIAL NUMBER 20653

UKAS CALIBRATION 0247

Poulten Selfe & Lee Ltd
Russell House,
Burnham Business Park,
Burnham-on-Crouch,
Essex CM0 8TE, England

Tel: +44 (0) 1621 787100
Fax: +44 (0) 1621 787175
email: info@rheotek.com
www.rheotek.com

Supplied to: Poulten Selfe and Lee Ltd.
Russell House,Burnham-on-Crouch, Essex CMO 8TE

Labelled:

ASTM reference:	**S3**
Product code:	2700-V04
Batch number:	22063
Date of calibration:	03 November 2009
Date of expiry:	01 February 2012
Bottle number:	61518

APPROVED SIGNATORY

Quality Manager S.P. Sims

A sample taken from this calibrated reference oil was measured against reference viscometers traceable to ASTM D 2162-06 held at the Laboratory and the following values were determined.

CERTIFIED VALUES

Temperature °C	Kinematic viscosity mm^2/s	Dynamic viscosity mPa.s	Density g/cm^3
20.00	4.107	3.347	0.8150
25.00	3.654	2.966	0.8117
40.00	2.693	2.158	0.8012
50.00	2.251	1.788	0.7944
80.00	1.449	1.121	0.7734
100.00	1.145	0.8691	0.7590

UNCERTAINTIES

Kinematic viscosity mm^2/s	Dynamic viscosity mPa.s	Uncertainty %
Up to 6	Up to 6	+/- 0.22
6 to 19	6 to 19	+/- 0.22
19 to 100	19 to 100	+/- 0.27
100 to 450	100 to 450	+/- 0.34
451 to 1750	450 to 1750	+/- 0.46
1750 and over	1750 and over	+/- 0.70

These uncertainties are largely random in nature.

The reported expanded uncertainty is based on a standard uncertainty multiplied by a coverage factor k=2, providing a level of confidence of approximately 95%. The uncertainty evaluation has been carried out in accordance with UKAS requirements.

ACCREDITED TO ISO 17025:2005

CERTIFICATE OF CALIBRATION

ISSUED BY THE PSL CALIBRATION LABORATORY

DATE OF ISSUE 19 February 2010 SERIAL NUMBER 21063

UKAS CALIBRATION 0247

Poulten Selfe & Lee Ltd
Russell House,
Burnham Business Park,
Burnham-on-Crouch,
Essex CM0 8TE, England

Tel: +44 (0) 1621 787100
Fax: +44 (0) 1621 787175
email: info@rheotek.com
www.rheotek.com

Supplied to: Poulten Selfe and Lee Ltd.
Russell House,Burnham-on-Crouch, Essex CMO 8TE

Labelled:

ASTM reference:	**S6**
Product code:	2700-V05
Batch number:	22192
Date of calibration:	10 February 2010
Date of expiry:	18 February 2012
Bottle number:	62304

APPROVED SIGNATORY

Quality Manager S.P. Sims

A sample taken from this calibrated reference oil was measured against reference viscometers traceable to ASTM D 2162-06 held at the Laboratory and the following values were determined.

CERTIFIED VALUES

Temperature °C	Kinematic viscosity mm^2/s	Dynamic viscosity mPa.s	Density g/cm^3
20.00	9.748	8.124	0.8334
25.00	8.344	6.925	0.8299
40.00	5.564	4.563	0.8201
50.00	4.409	3.586	0.8133
80.00	2.531	2.007	0.7931
100.00	1.898	1.479	0.7794

UNCERTAINTIES

Kinematic viscosity mm^2/s	Dynamic viscosity mPa.s	Uncertainty %
Up to 6	Up to 6	+/- 0.22
6 to 19	6 to 19	+/- 0.22
19 to 100	19 to 100	+/- 0.27
100 to 450	100 to 450	+/- 0.34
451 to 1750	450 to 1750	+/- 0.46
1750 and over	1750 and over	+/- 0.70

These uncertainties are largely random in nature.

The reported expanded uncertainty is based on a standard uncertainty multiplied by a coverage factor k=2, providing a level of confidence of approximately 95%. The uncertainty evaluation has been carried out in accordance with UKAS requirements.

1. Identification of the substance/preparation and of the company/undertaking

Product name **S3, S6, N10, S20**

Product Use Viscosity standard.

Supplier Poulten Selfe and Lee Ltd.
Russell House
Burnham Business Park
Burnham-on-Crouch
Essex CM0 8TE
United Kingdom

EMERGENCY TELEPHONE NUMBER +44 (0) 1621 787100

2. Composition/information on ingredients

Highly refined mineral oil (IP 346 DMSO extract < 3%). Proprietary performance additives.

Chemical name	CAS no.	%	EINECS / ELINCS.	Classification
Kerosine - unspecified	64742-47-8	50-100	265-149-8	Xn; R65 R66

See Section 16 for the full text of the R Phrases declared above
Occupational Exposure Limit(s), if available, are listed in Section 8

3. Hazards identification

This preparation is classified as dangerous according to Directive 1999/45/EC as amended and adapted.

Physical/chemical Hazards Not classified as dangerous.

Human health hazards Harmful: may cause lung damage if swallowed.
Repeated exposure may cause skin dryness or cracking.

Environmental hazards Unlikely to be harmful to aquatic organisms.

Effects and symptoms

Eyes No significant health hazards identified.

Skin Prolonged or repeated contact can defat the skin and lead to irritation and/or dermatitis.

Inhalation No significant health hazards identified.

Ingestion Aspiration hazard if swallowed - harmful or fatal if liquid is aspirated into lungs.

4. First-aid measures

Eye Contact In case of contact, immediately flush eyes with a copious amount of water for at least 15 minutes. Get medical attention if irritation occurs.

Skin contact Immediately wash exposed skin with soap and water. Remove contaminated clothing and shoes. Wash clothing before reuse. Clean shoes thoroughly before reuse. Get medical attention if irritation develops.

Inhalation If inhaled, remove to fresh air. Get medical attention if symptoms appear.

Ingestion If swallowed, do NOT induce vomiting. Never give anything by mouth to an unconscious person. Aspiration hazard if swallowed- can enter lungs and cause damage. Obtain medical attention.

Notes to physician Treatment should in general be symptomatic and directed to relieving any effects.

5. Fire-fighting measures

Extinguishing Media

Suitable In case of fire, use water fog, foam, dry chemical or CO2 extinguisher or spray.

Not Suitable Do not use water jet.

Hazardous decomposition products These products are carbon oxides (CO, CO2).

Unusual fire/explosion Hazards None identified.

Special fire-fighting procedures None identified.

AAKJ T001

DEUTSCHER KALIBRIERDIENST DKD

Kalibrierlaboratorium / *Calibration laboratory*

Akkreditiert durch die / *accredited by the*
Akkreditierungsstelle des Deutschen Kalibrierdienstes

Zentrum für Messen und Kalibrieren GmbH
Zentrum für Messen und Kalibrieren -ANALYTIK- GmbH

DKD-K-06901

04-1436
DKD-K-06901
09-11

Kalibrierschein
Calibration certificate

Kalibrierzeichen
Calibration mark

Gegenstand *Object*	Newtonsche Normalprobe der Viskosität *Newtonian viscosity standard specimen*
Hersteller *Manufacturer*	ZMK -ANALYTIK- GmbH
Typ *Type*	1 BW
Fabrikat/Serien-Nr. *Serial number*	21
Auftraggeber *Customer*	NPL Management Ltd National Physical Laboratory Hampton Road UK-Teddington, Middlesex TW11 0LW
Auftragsnummer *Order No.*	371072
Anzahl der Seiten des Kalibrierscheines *Number of pages of the certificate*	4
Datum der Kalibrierung *Date of calibration*	05.11.2009

Dieser Kalibrierschein dokumentiert die Rückführung auf nationale Normale zur Darstellung der Einheiten in Übereinstimmung mit dem Internationalen Einheitensystem (SI).
Der DKD ist Unterzeichner der multilateralen Übereinkommen der European co-operation for Accreditation (EA) und der International Laboratory Accreditation Cooperation (ILAC) zur gegenseitigen Anerkennung der Kalibrierscheine.
Für die Einhaltung einer angemessenen Frist zur Wiederholung der Kalibrierung ist der Benutzer verantwortlich.
This calibration certificate documents the traceability to national standards, which realize the units of measurement according to the International System of Units (SI).
The DKD is signatory to the multilateral agreements of the European co-operation for Accreditation (EA) and of the International Laboratory Accreditation Cooperation (ILAC) for the mutual recognition of calibration certificates.
The user is obliged to have the object recalibrated at appropriate intervals.

Stempel *Seal*	Datum *Date*	Leiter des Kalibrierlaboratoriums *Head of the calibration laboratory*	Bearbeiter *Person in charge*
Deutscher DKD-K-06901 Kalibrierdienst	05.11.2009	Frau Dr. Werner	Frau Faivre

Kalibrierlaboratorium für Länge, elektrische, mechanische, thermodynamische und analytische Messgrößen
Calibration laboratory for length, electrical, mechanical, thermodynamical and analytical measuring quantities

Ortsteil Wolfen, P-D ChemiePark Bitterfeld-Wolfen, Areal A, Filmstraße Nr.7, 06766 Bitterfeld-Wolfen
Telefon (03494) 69730 • FAX (03494) 697334 • email info@zmk-wolfen.de

DQS-zertifiziert nach DIN EN ISO 9001
Reg.-Nr.: 054774 QM

Die englische Fassung des Kalibrierscheines ist eine unverbindliche Übersetzung. Im Zweifelsfall gilt der deutsche Originaltext.

The English version of the calibration certificate is not a binding translation. In case of doubt the German original text shall provail.

Kalibriergegenstand
Calibration object

Newtonsche Normalprobe der Viskosität *Newtonian viscosity standard specimen*	1 BW
Proben-Nr. *Specimen no.*	21

Kalibrierverfahren
Procedure of the calibration

Die kinematische Viskosität der Normalprobe wurde mit auf das nationale Normal der Einheit der Viskosität rückgeführten Kapillarviskosimetern nach Ubbelohde bestimmt.

The kinematic viscosity of the Newtonian viscosity standard specimen was measured using a capillar viscosimeter of the Ubbelohde type, which is traceable to the national standard of the viscosity.

Umgebungsbedingungen
Environmental conditions

Raumtemperatur - *room temperature:*	(23 ± 5) °C
rel. Feuchte - *rel.humidity:*	(50 ± 20) %

Messunsicherheit
Uncertainty of measurement

Die relative Messunsicherheit der Viskosität beträgt:
U = 0,24 %
Angegeben ist die erweiterte Messunsicherheit, die sich aus der Standardmessunsicherheit durch Multiplikation mit dem Erweiterungsfaktor k = 2 ergibt. Sie wurde gemäß DKD-3 ermittelt. Der Wert der Messgröße liegt mit einer Wahrscheinlichkeit von 95 % im zugeordneten Werteintervall.

Die angegebene erweiterte Messunsicherheit der Viskositätswerte wird für 6 Monate bei Einhaltung der Handhabungs- und Aufbewahrungshinweise garantiert.

The relative uncertainty of measurement of viscosity is equal:
U = 0,24 %
Reported is the expanded uncertainty which results from the standard uncertainty by multiplication with the coverage factor k = 2. It has been calculated according to DKD-3. The value of the measurand is found within the attributed interval with a probability of approximately 95 %.

The reported expanded uncertainty of the values of viscosity is guaranteed within 6 months provided that attention is payed to the handling and storage instructions.

Messergebnisse
Measuring results

Die angegebenen Viskositätswerte sind bezogen auf die kinematische Viskosität des Wassers bei 20 °C , 1,0034 mm^2/s (ISO TR 3666 (1998)).

The mentioned values of the viscosity are related to the kinematic viscosity of water at 20°C, 1.0034 mm^2/s (ISO TR 3666 (1998)).

Viskosität der Newtonschen Normalprobe in Abhängigkeit von der Temperatur:
Viscosity of the Newtonian standard specimen as a function of the temperature

Temperatur *temperature* in °C	dynamische Viskosität *dynamic viscosity* in mPa·s	kinematische Viskosität *kinematic viscosity* in mm^2/s	Dichte *density* in g/cm^3	Temperaturkoeffizient der Viskosität *temperature coefficient* in 10^{-2} 1/K
10,00	1,138	1,440	0,7902	1,67
15,00	1,047	1,332	0,7864	1,60
20,00	0,9689	1,238	0,7826	1,53
23,00	0,9262	1,187	0,7803	1,49
25,00	0,8987	1,154	0,7788	1,46
30,00	0,8369	1,080	0,7749	1,40
40,00	0,7314	0,9534	0,7672	1,29
100,00	-	-	-	-

Die Viskositätswerte gelten für das Datum der Kalibrierung.
Die Temperaturkoeffizienten der Viskosität nach DIN 53017 sind Richtwerte.

The values of viscosity are valid for the date of calibration.
The temperature coefficients of viscosity according to DIN 53017 are standard values.

Bemerkungen
Remarks

Die Langzeitstabilität der Normalprobe wird beeinflusst durch die Art der Handhabung und Aufbewahrung. Voraussetzung für die Gültigkeit der angegebenen Viskositätswerte innerhalb eines Zeitraumes von 6 Monaten ist die Aufbewahrung der ungeöffneten Flasche im Dunkeln und bei Raumtemperatur.
Eine Mehrfachverwendung der Normalprobe ist auszuschließen.
Außerhalb des Zeitraumes von 6 Monaten muss mit Abweichungen des Viskositätswertes gerechnet werden, die größer sind als die angegebene Messunsicherheit. Erfahrungsgemäß beträgt bei Einhaltung der Aufbewahrungsbedingungen die Viskositätsänderung nicht mehr als 0,1 % pro 6 Monate.

The long-term stability of the viscosity standard specimen is influenced by handling and storage. Supposition for the validity of the reported values of viscosity within 6 months is the storage of the unopened bottle in dark and at room temperature. Repeated use of the same standard specimen has to be avoided.

AAKJ TOO2

DEUTSCHER KALIBRIERDIENST DKD

Kalibrierlaboratorium / *Calibration laboratory*

Akkreditiert durch die / *accredited by the*
Akkreditierungsstelle des Deutschen Kalibrierdienstes

Zentrum für Messen und Kalibrieren GmbH
Zentrum für Messen und Kalibrieren -ANALYTIK- GmbH

DKD-K-06901

04-1437
DKD-K-06901
09-11

Kalibrierschein
Calibration certificate

Kalibrierzeichen
Calibration mark

Gegenstand *Object*	Newtonsche Normalprobe der Viskosität *Newtonian viscosity standard specimen*
Hersteller *Manufacturer*	ZMK -ANALYTIK- GmbH
Typ *Type*	10 AW
Fabrikat/Serien-Nr. *Serial number*	39
Auftraggeber *Customer*	NPL Management Ltd National Physical Laboratory Hampton Road UK-Teddington, Middlesex TW11 0LW
Auftragsnummer *Order No.*	371072
Anzahl der Seiten des Kalibrierscheines *Number of pages of the certificate*	4
Datum der Kalibrierung *Date of calibration*	05.11.2009

Dieser Kalibrierschein dokumentiert die Rückführung auf nationale Normale zur Darstellung der Einheiten in Übereinstimmung mit dem Internationalen Einheitensystem (SI).
Der DKD ist Unterzeichner der multilateralen Übereinkommen der European co-operation for Accreditation (EA) und der International Laboratory Accreditation Cooperation (ILAC) zur gegenseitigen Anerkennung der Kalibrierscheine.
Für die Einhaltung einer angemessenen Frist zur Wiederholung der Kalibrierung ist der Benutzer verantwortlich.
This calibration certificate documents the traceability to national standards, which realize the units of measurement according to the International System of Units (SI).
The DKD is signatory to the multilateral agreements of the European co-operation for Accreditation (EA) and of the International Laboratory Accreditation Cooperation (ILAC) for the mutual recognition of calibration certificates.
The user is obliged to have the object recalibrated at appropriate intervals.

Stempel *Seal*	Datum *Date*	Leiter des Kalibrierlaboratoriums *Head of the calibration laboratory*	Bearbeiter *Person in charge*
Deutscher Kalibrierdienst DKD-K-06901	05.11.2009	Frau Dr. Werner	Frau Faivre

Kalibrierlaboratorium für Länge, elektrische, mechanische, thermodynamische und analytische Messgrößen
Calibration laboratory for length, electrical, mechanical, thermodynamical and analytical measuring quantities

DQS-zertifiziert nach DIN EN ISO 9001
Reg.-Nr.: 054774 QM

Ortsteil Wolfen, P-D ChemiePark Bitterfeld-Wolfen, Areal A, Filmstraße Nr.7, 06766 Bitterfeld-Wolfen
Telefon (03494) 69730 • FAX (03494) 697334 • email info@zmk-wolfen.de

04-1437
DKD-K-06901
09-11

Die englische Fassung des Kalibrierscheines ist eine unverbindliche Übersetzung. Im Zweifelsfall gilt der deutsche Originaltext.

The English version of the calibration certificate is not a binding translation. In case of doubt the German original text shall provail.

Kalibriergegenstand
Calibration object

Newtonsche Normalprobe der Viskosität *Newtonian viscosity standard specimen*	10 AW
Proben-Nr. *Specimen no.*	39

Kalibrierverfahren
Procedure of the calibration

Die kinematische Viskosität der Normalprobe wurde mit auf das nationale Normal der Einheit der Viskosität rückgeführten Kapillarviskosimetern nach Ubbelohde bestimmt.

The kinematic viscosity of the Newtonian viscosity standard specimen was measured using a capillar viscosimeter of the Ubbelohde type, which is traceable to the national standard of the viscosity.

Umgebungsbedingungen
Environmental conditions

Raumtemperatur - *room temperature:*	(23 ± 5) °C
rel. Feuchte - *rel.humidity:*	(50 ± 20) %

Messunsicherheit
Uncertainty of measurement

Die relative Messunsicherheit der Viskosität beträgt:
U = 0,25 %
Angegeben ist die erweiterte Messunsicherheit, die sich aus der Standardmessunsicherheit durch Multiplikation mit dem Erweiterungsfaktor k = 2 ergibt. Sie wurde gemäß DKD-3 ermittelt. Der Wert der Messgröße liegt mit einer Wahrscheinlichkeit von 95 % im zugeordneten Werteintervall.

Die angegebene erweiterte Messunsicherheit der Viskositätswerte wird für 6 Monate bei Einhaltung der Handhabungs- und Aufbewahrungshinweise garantiert.

The relative uncertainty of measurement of viscosity is equal:
U = 0,25 %
Reported is the expanded uncertainty which results from the standard uncertainty by multiplication with the coverage factor k = 2. It has been calculated according to DKD-3. The value of the measurand is found within the attributed interval with a probability of approximately 95 %.

The reported expanded uncertainty of the values of viscosity is guaranteed within 6 months provided that attention is payed to the handling and storage instructions.

Messergebnisse
Measuring results

Die angegebenen Viskositätswerte sind bezogen auf die kinematische Viskosität des Wassers bei 20 °C , 1,0034 mm^2/s (ISO TR 3666 (1998)).

The mentioned values of the viscosity are related to the kinematic viscosity of water at 20°C, 1.0034 mm^2/s (ISO TR 3666 (1998)).

Viskosität der Newtonschen Normalprobe in Abhängigkeit von der Temperatur:
Viscosity of the Newtonian standard specimen as a function of the temperature

Temperatur *temperature* in °C	dynamische Viskosität *dynamic viscosity* in mPa·s	kinematische Viskosität *kinematic viscosity* in mm^2/s	Dichte *density* in g/cm^3	Temperaturkoeffizient der Viskosität *temperature coefficient* in 10^{-2} 1/K
10,00	13,39	16,37	0,8177	3,9
15,00	11,12	13,65	0,8144	3,6
20,00	9,335	11,51	0,8110	3,4
23,00	8,454	10,45	0,8090	3,2
25,00	7,927	9,814	0,8077	3,2
30,00	6,804	8,459	0,8043	3,0
40,00	5,153	6,461	0,7976	2,6
100,00	-	-	-	-

Die Viskositätswerte gelten für das Datum der Kalibrierung.
Die Temperaturkoeffizienten der Viskosität nach DIN 53017 sind Richtwerte.

The values of viscosity are valid for the date of calibration.
The temperature coefficients of viscosity according to DIN 53017 are standard values.

Bemerkungen
Remarks

Die Langzeitstabilität der Normalprobe wird beeinflusst durch die Art der Handhabung und Aufbewahrung. Voraussetzung für die Gültigkeit der angegebenen Viskositätswerte innerhalb eines Zeitraumes von 6 Monaten ist die Aufbewahrung der ungeöffneten Flasche im Dunkeln und bei Raumtemperatur.
Eine Mehrfachverwendung der Normalprobe ist auszuschließen.
Außerhalb des Zeitraumes von 6 Monaten muss mit Abweichungen des Viskositätswertes gerechnet werden, die größer sind als die angegebene Messunsicherheit. Erfahrungsgemäß beträgt bei Einhaltung der Aufbewahrungsbedingungen die Viskositätsänderung nicht mehr als 0,1 % pro 6 Monate.

The long-term stability of the viscosity standard specimen is influenced by handling and storage. Supposition for the validity of the reported values of viscosity within 6 months is the storage of the unopened bottle in dark and at room temperature. Repeated use of the same standard specimen has to be avoided.

AAKS T003

DEUTSCHER KALIBRIERDIENST DKD

Kalibrierlaboratorium / *Calibration laboratory*

Akkreditiert durch die / *accredited by the*
Akkreditierungsstelle des Deutschen Kalibrierdienstes

Zentrum für Messen und Kalibrieren GmbH
Zentrum für Messen und Kalibrieren -ANALYTIK- GmbH

DKD-K-06901

04-1438
DKD-K-06901
09-11

Kalibrierschein
Calibration certificate

Kalibrierzeichen
Calibration mark

Gegenstand *Object*	Newtonsche Normalprobe der Viskosität *Newtonian viscosity standard specimen*
Hersteller *Manufacturer*	ZMK -ANALYTIK- GmbH
Typ *Type*	50 BW
Fabrikat/Serien-Nr. *Serial number*	69
Auftraggeber *Customer*	NPL Management Ltd National Physical Laboratory Hampton Road UK-Teddington, Middlesex TW11 0LW
Auftragsnummer *Order No.*	371072
Anzahl der Seiten des Kalibrierscheines *Number of pages of the certificate*	4
Datum der Kalibrierung *Date of calibration*	05.11.2009

Dieser Kalibrierschein dokumentiert die Rückführung auf nationale Normale zur Darstellung der Einheiten in Übereinstimmung mit dem Internationalen Einheitensystem (SI).
Der DKD ist Unterzeichner der multilateralen Übereinkommen der European co-operation for Accreditation (EA) und der International Laboratory Accreditation Cooperation (ILAC) zur gegenseitigen Anerkennung der Kalibrierscheine.
Für die Einhaltung einer angemessenen Frist zur Wiederholung der Kalibrierung ist der Benutzer verantwortlich.
This calibration certificate documents the traceability to national standards, which realize the units of measurement according to the International System of Units (SI).
The DKD is signatory to the multilateral agreements of the European co-operation for Accreditation (EA) and of the International Laboratory Accreditation Cooperation (ILAC) for the mutual recognition of calibration certificates.
The user is obliged to have the object recalibrated at appropriate intervals.

Stempel *Seal*	Datum *Date*	Leiter des Kalibrierlaboratoriums *Head of the calibration laboratory*	Bearbeiter *Person in charge*
Deutscher Kalibrierdienst DKD-K-06901	05.11.2009	Frau Dr. Werner	Frau Faivre

Kalibrierlaboratorium für Länge, elektrische, mechanische, thermodynamische und analytische Messgrößen
Calibration laboratory for length, electrical, mechanical, thermodynamical and analytical measuring quantities

DQS-zertifiziert nach DIN EN ISO 9001
Reg.-Nr.: 054774 QM

Ortsteil Wolfen, P-D ChemiePark Bitterfeld-Wolfen, Areal A, Filmstraße Nr.7, 06766 Bitterfeld-Wolfen
Telefon (03494) 69730 • FAX (03494) 697334 • email info@zmk-wolfen.de

Die englische Fassung des Kalibrierscheines ist eine unverbindliche Übersetzung. Im Zweifelsfall gilt der deutsche Originaltext.

The English version of the calibration certificate is not a binding translation. In case of doubt the German original text shall provail.

Kalibriergegenstand
Calibration object

Newtonsche Normalprobe der Viskosität *Newtonian viscosity standard specimen*	50 BW
Proben-Nr. *Specimen no.*	69

Kalibrierverfahren
Procedure of the calibration

Die kinematische Viskosität der Normalprobe wurde mit auf das nationale Normal der Einheit der Viskosität rückgeführten Kapillarviskosimetern nach Ubbelohde bestimmt.

The kinematic viscosity of the Newtonian viscosity standard specimen was measured using a capillar viscosimeter of the Ubbelohde type, which is traceable to the national standard of the viscosity.

Umgebungsbedingungen
Environmental conditions

Raumtemperatur - *room temperature:*	(23 ± 5) °C
rel. Feuchte - *rel.humidity:*	(50 ± 20) %

Messunsicherheit
Uncertainty of measurement

Die relative Messunsicherheit der Viskosität beträgt:
U = 0,32 %
Angegeben ist die erweiterte Messunsicherheit, die sich aus der Standardmessunsicherheit durch Multiplikation mit dem Erweiterungsfaktor k = 2 ergibt. Sie wurde gemäß DKD-3 ermittelt. Der Wert der Messgröße liegt mit einer Wahrscheinlichkeit von 95 % im zugeordneten Werteintervall.

Die angegebene erweiterte Messunsicherheit der Viskositätswerte wird für 6 Monate bei Einhaltung der Handhabungs- und Aufbewahrungshinweise garantiert.

The relative uncertainty of measurement of viscosity is equal:
U = 0,32 %
Reported is the expanded uncertainty which results from the standard uncertainty by multiplication with the coverage factor k = 2. It has been calculated according to DKD-3. The value of the measurand is found within the attributed interval with a probability of approximately 95 %.

The reported expanded uncertainty of the values of viscosity is guaranteed within 6 months provided that attention is payed to the handling and storage instructions.

04-1438
DKD-K-06901
09-11

Messergebnisse
Measuring results

Die angegebenen Viskositätswerte sind bezogen auf die kinematische Viskosität des Wassers bei 20 °C , 1,0034 mm^2/s (ISO TR 3666 (1998)).

The mentioned values of the viscosity are related to the kinematic viscosity of water at 20°C, 1.0034 mm^2/s (ISO TR 3666 (1998)).

Viskosität der Newtonschen Normalprobe in Abhängigkeit von der Temperatur:
Viscosity of the Newtonian standard specimen as a function of the temperature

Temperatur *temperature* in °C	dynamische Viskosität *dynamic viscosity* in mPa·s	kinematische Viskosität *kinematic viscosity* in mm^2/s	Dichte *density* in g/cm^3	Temperaturkoeffizient der Viskosität *temperature coefficient* in 10^{-2} 1/K
10,00	90,81	109,9	0,8263	5,6
15,00	69,66	84,63	0,8231	5,2
20,00	54,26	66,18	0,8199	4,9
23,00	47,08	57,55	0,8180	4,7
25,00	42,96	52,60	0,8167	4,5
30,00	34,50	42,41	0,8136	4,2
40,00	23,16	28,69	0,8073	3,7
100,00	4,515	5,868	0,7695	2,0

Die Viskositätswerte gelten für das Datum der Kalibrierung.
Die Temperaturkoeffizienten der Viskosität nach DIN 53017 sind Richtwerte.

The values of viscosity are valid for the date of calibration.
The temperature coefficients of viscosity according to DIN 53017 are standard values.

Bemerkungen
Remarks

Die Langzeitstabilität der Normalprobe wird beeinflusst durch die Art der Handhabung und Aufbewahrung. Voraussetzung für die Gültigkeit der angegebenen Viskositätswerte innerhalb eines Zeitraumes von 6 Monaten ist die Aufbewahrung der ungeöffneten Flasche im Dunkeln und bei Raumtemperatur.
Eine Mehrfachverwendung der Normalprobe ist auszuschließen.
Außerhalb des Zeitraumes von 6 Monaten muss mit Abweichungen des Viskositätswertes gerechnet werden, die größer sind als die angegebene Messunsicherheit. Erfahrungsgemäß beträgt bei Einhaltung der Aufbewahrungsbedingungen die Viskositätsänderung nicht mehr als 0,1 % pro 6 Monate.

The long-term stability of the viscosity standard specimen is influenced by handling and storage. Supposition for the validity of the reported values of viscosity within 6 months is the storage of the unopened bottle in dark and at room temperature. Repeated use of the same standard specimen has to be avoided.

Beyond the period of 6 months deviations of the viscosity values have to be expected, which are larger than the reported measuring uncertainty. From experience the changes of viscosity values within 6 months are not larger than 0.1 %.

Hinweis
Note

Der Deutsche Kalibrierdienst ist Unterzeichner der multilateralen Übereinkommen der European co-operation for Accreditation (EA) und der International Laboratory Accreditation Cooperation (ILAC) zur gegenseitigen Anerkennung der Kalibrierscheine. Die weiteren Unterzeichner innerhalb und außerhalb Europas sind den Internetseiten von EA (www.european-accreditation.org) und ILAC (www.ilac.org) zu entnehmen.
The DKD is signatory to the multilateral agreements of the European co-operation for Accreditation (EA) and of the International Laboratory Accreditation Cooperation (ILAC) for the mutual recognition of calibration certificates.
The other signatories inside and beyond Europe can be taken from the web-pages of EA (www.european-accreditation.org) and ILAC (www.ilac.org).

International Technologies
Dr. Gambert GmbH

Product Specification of:

Industrial O_2-Sensor

Type: I - 01

Part. No.: 48 00 14

Key Features: sensor contains acid electrolyte to withstand high CO_2 concentrations, shows high resistivity to acid gases and a short response time

All characteristics are based on conditions at 25°C, 50 % RH and 1013 hPa

Operating Principle: Electrical	galvanic fuel cell
Connector: Measurement	3-pin Molex
Range: Nominal Sensor Life:	0.5 - 35 Vol.% > 1,
Expected Operating Life: Output	900, 000 Vol.% h 10
Signal Delivery Condition:	years @ ambient air 10.5 - 17 mV @ dry ambient
Output Signal	air 5 - 17 mV @ dry ambient air
Range:Response	< 5 sec 0 - 2 % oxygen: ± 0.1 %
Time t_{90} : Linearity	absolute
Error:	2.1 - 35 % oxygen: ± 0.5 % relative
Drift: Operating Temperature:	< 3 % per month
Pressure Range: Influence of	0 - 50°C
Humidity: Recommended Load	750 - 1250 hPa
Resistor: Temperature	-0.03% rel. O_2 reading / % RH
Compensation: Interferences:	≥ 1 MOhm
	NTC
	< 20 ppm O_2 response to: 100 Vol.% CO 100 Vol.% CO_2 3, 000 ppm NO, balance N_2 1, 000 ppm H_2 , balance N_2 100 Vol.% C_3H_8 2, 000 ppm H_2S , balance N_2 500 ppm SO_2 , balance N_2 1, 000 ppm Benzene, balance N_2

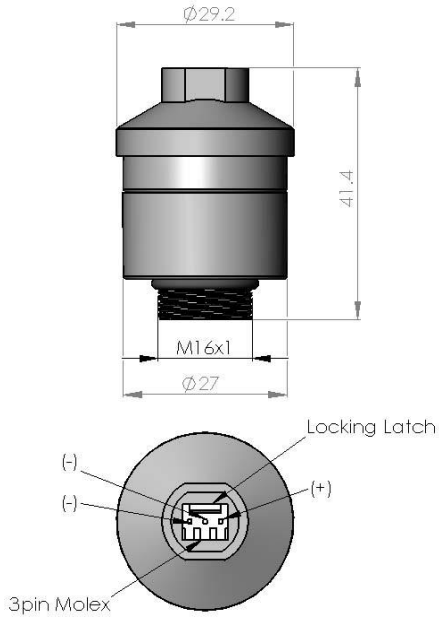

Tolerance: ± 0.15 mm

Storage Conditions

Temperature Range: maximum: - 15 - 60 °C recommended: 5 - 30 °C Ambient Pressure: 750 - 1750 hPa Humidity: up to 100 % RH Material in Contact with Media: PA12, PVC, PPS, PTFE, Stainless Steel Shelf Life: less than 6 months recommended Weight: approximately 25 g Warranty Period: 12 months Housing Colour: white

IT Dr. Gambert GmbH, Hinter dem Chor 21, 23966 Wismar, Germany
Tel.: +49 (0) 3841 22 00 50, Fax: +49 (0) 3841 22 00 522, sales@it-wismar.de, www.it-wismar.de

Standard oils employed for calibrating and verifying the Searle type equipment: G3 and D5.

Appendix III

Calculation of shear rate and shear stresses in the Searle type and Couette type viscometer.

Searle type viscometer

R_b = 24.5 mm, R_c = 25.5 mm, l_b = 32.0 mm

Shear stress

$$\sigma = \frac{M}{2\pi R_b^2 l_b} = \left[\frac{9.81 \times 10^{-5} \times M(\text{in gm. cm})}{2\pi \times (24.5 \times 10^{-3})^2 \times (32 \times 10^{-3})}\right] {}^{N}/_{m^2}$$

$$\therefore \sigma = [0.813 \times M(\text{gm. cm})] \, {}^{N}/_{m^2}$$

Shear rate

$$\dot{\gamma} = \frac{2R_c^2}{R_c^2 - R_b^2} \times \frac{2\pi}{60} \times \omega(\text{in rpm}) = \left[\frac{2 \times 25.5^2}{25.5^2 - 24.5^2} \times \frac{2\pi}{60} \times \omega(\text{in rpm})\right] s^{-1}$$

$$\therefore \dot{\gamma} = [2.724 \times \omega(\text{in rpm})] s^{-1}$$

Couette type viscometer

Shear stress

$$\sigma = \frac{M}{2\pi R_b^2 l_b}$$

Shear rate

$$\dot{\gamma} = \frac{2R_c^2}{R_c^2 - R_b^2} \times \frac{2\pi}{60} \times \omega(\text{in rpm})$$

(i) Set 1: R_c = 13 mm, R_b = 9.5 mm, l_b = 19 mm

Shear stress

$$\sigma = \left[\frac{9.81 \times 10^{-5} \times M(\text{in gm. cm})}{2\pi \times (9.5 \times 10^{-3})^2 \times (19 \times 10^{-3})}\right] {}^{N}/_{m^2}$$

$$\therefore \sigma = [9.105 \times M(\text{in gm. cm})] \, {}^{N}/_{m^2}$$

Shear rate

$$\dot{\gamma} = \left[\frac{2 \times 13^2}{13^2 - 9.5^2} \times \frac{2\pi}{60} \times \omega(\text{in rpm})\right] s^{-1}$$

$$\therefore \dot{\gamma} = [0.45 \times \omega] s^{-1}$$

(ii) Set 2: R_c = 31.86 mm, R_b = 30.65 mm, l_b = 23.57 mm

Shear stress

$$\sigma = \left[\frac{9.81 \times 10^{-5} \times M(\text{in gm. cm})}{2\pi \times (30.65 \times 10^{-3})^2 \times (23.57 \times 10^{-3})}\right] {}^{N}/_{m^2}$$

$$\therefore \sigma = [0.705 \times M(\text{in gm. cm})] \, {}^{N}/_{m^2}$$

Shear rate

$$\dot{\gamma} = \left[\frac{2 \times 31.86^2}{31.86^2 - 30.65^2} \times \frac{2\pi}{60} \times \omega(\text{in rpm})\right] s^{-1}$$

$$\therefore \dot{\gamma} = [2.81 \times \omega(\text{in rpm})] s^{-1}$$

(iii) Set 3: R_c = 31.86 mm, R_b = 30.45 mm, l_b = 23.57 mm

Shear stress

$$\sigma = \left[\frac{9.81 \times 10^{-5} \times M(\text{in gm. cm})}{2\pi \times (30.45 \times 10^{-3})^2 \times (23.57 \times 10^{-3})}\right] {}^{N}/_{m^2}$$

$$\therefore \sigma = [0.7144 \times M(\text{in gm. cm})] \, {}^{N}/_{m^2}$$

Shear rate

$$\dot{\gamma} = \left[\frac{2 \times 31.86^2}{31.86^2 - 30.45^2} \times \frac{2\pi}{60} \times \omega(\text{in rpm})\right] s^{-1}$$

$$\therefore \dot{\gamma} = [2.42 \times \omega(\text{in rpm})] s^{-1}$$

(iv) Set 4: R_c = 10 mm, R_b = 9mm, l_b = 50.5 mm

Shear stress

$$\sigma = \left[\frac{9.81 \times 10^{-5} \times M(\text{in gm. cm})}{2\pi \times (9 \times 10^{-3})^2 \times (50.5 \times 10^{-3})}\right] {}^{N}/_{m^2}$$

$$\therefore \sigma = [3.817 \times \mathrm{M(in\ gm.\,cm)}]\ {}^{\mathrm{N}}/_{\mathrm{m}^2}$$

Shear rate

$$\dot{\gamma} = \left[\frac{2 \times 10^2}{10^2 - 9^2} \times \frac{2\pi}{60} \times \omega(\text{in rpm})\right] \mathrm{s}^{-1}$$

$$\therefore \dot{\gamma} = [1.102 \times \omega(\text{in rpm})]\mathrm{s}^{-1}$$

(v) Set 5: R_c = 15 mm, R_b = 14mm, l_b = 42 mm

Shear stress

$$\sigma = \left[\frac{9.81 \times 10^{-5} \times \mathrm{M(in\ gm.\,cm)}}{2\pi \times (14 \times 10^{-3})^2 \times (42 \times 10^{-3})}\right] {}^{\mathrm{N}}/_{\mathrm{m}^2}$$

$$\therefore \sigma = [1.8966 \times \mathrm{M(in\ gm.\,cm)}]\ {}^{\mathrm{N}}/_{\mathrm{m}^2}$$

Shear rate

$$\dot{\gamma} = \left[\frac{2 \times 15^2}{15^2 - 14^2} \times \frac{2\pi}{60} \times \omega(\text{in rpm})\right] \mathrm{s}^{-1}$$

$$\therefore \dot{\gamma} = [1.625 \times \omega(\text{in rpm})]\mathrm{s}^{-1}$$

Appendix IV

Couette type viscometer

(1) Equipment is switched on.

(2) Software Ravenfield 1.17 is started and the details of the experiment: experiment Serial number, experiment name, metal tested and temperature to be tested are entered into the software.

(3) Steps (5) to (12) described in Appendix I for the Couette type viscometer are repeated.

(4) Once the inner cylinder and the bob-rod are attached to the vertical air bearing, the outer cylinder is fixed onto the steel shaft, which is connected to the motor underneath.

(5) The dial test indicator (DTI) is mounted on the iron frame which holds the vertical air bearing. This would enable the user to centre the outer cylinder with respect to the air bearing.

(6) Rotating the outer cylinder at 4 rpm, the dial test indicator is employed to centre the rotating outer cylinder along its length. Adjusting the 4 screws at the base of the steel shaft enables the centring.

(7) Once completed, the sample of metal prepared is gently introduced into the outer cylinder with the help of forceps. This needs to be carefully done to avoid the sample being stuck at an angle at the outer cylinder's mouth. Numerous repeats had to be done during the study due to the sample being stuck at the mouth.

(8) After the sample is in, the two halves of the electric furnace of the equipment are closed with a bracket and the glass door of the cabinet is firmly shut.

(9) The cabinet is evacuated at this point with the "purge on" switch which is connected to the oxygen sensor and solenoid.

(10) Once the evacuation is complete and the N_2 gas has filled the cabinet, the voltage reading in the software is about 0.37 ± 0.2. This marks the end of the purging process.

(11) Water is switched on and allowed to pass through the equipment at this stage at 2.0 litres/second.

(12) The temperature of the furnace is entered into the software after which the furnace is switched on. To allow the temperature to be uniform in the sample, the equipment is left undisturbed for 1 hour 20 minutes.

(13) After the mentioned time has elapsed, the inner cylinder is lowered into the outer cylinder. Watching the inner cylinder through the mirror attached to the equipment (Fig. 3.9), the inner cylinder is lowered to the desired height carefully.

(14) The introduction of the inner cylinder would change the temperature of the molten sample. Thus the equipment is left in this state, undisturbed, for another 30 minutes. This state enables the molten metal sample to wet the surface of the inner and outer cylinders thoroughly, therefore preventing wall-slip phenomenon during the experiments.

(15) During this time, the type of testing to be done: ramping up / fixed speed, is set in the software. The speed of rotation and time of rotation is adjusted, and the name of the experiment is entered into the software for keeping record.

(16) After the 30 minutes, the experiment is commenced.

Searle type viscometer

(1) The inner and outer cylinders of the equipment are thoroughly cleaned with 4000 grit carbide paper, washed with soap and then ethanol and later dried for 1 hour in an oven set at 120^{o}C for 1 hour to remove the moisture.

(2) The inner cylinder is mounted alongside the dial test indicator and made concentric with respect to the dial test indicator.

(3) Since the outer cylinder position is fixed, it needn't be tested. It is assumed that the outer cylinder's position has been kept in line with the torque measuring unit where the inner cylinder will be mounted.

(4) Once the inner cylinder is fixed into the torque measuring unit, the sample is introduced into the outer cylinder. The computer associated with the equipment is switched and the software is started. Details of the experiment: Serial number, name and type of metal being tested is entered into the details section of the software.

(5) The outer cylinder is then raised into position inside the muffle furnace.

(6) The inner cylinder is lowered into position into the muffle furnace and held before the inner cylinder touches the sample.

(7) N_2 gas is passed onto the inner cylinder through a steel bent tube.

(8) The temperature of the furnace is set in the software and the furnace is started.

(9) After 1 hour 20 minutes, the inner cylinder is lowered into the outer cylinder to the desired height and left undisturbed for 20 minutes during which time, the type of experiment to be conducted: ramping up or fixed speed is entered into the software. The speed of rotation and time of rotation is adjusted on the controller box.

(10) The equipment is then ready for conducting experiments.

Appendix V

Calculations of Bakhtiyarov & Overfelt and Sun *et al.*

Bakhtiyarov & Overfelt

R_b = 12.7mm, R_c = 26.75mm, l_b = 275mm (from Fig. 10 in (Bakhtiyarov and Overfelt, 1999)).

Shear rate is calculated from equation 3.2.

$$\dot{\gamma} = \frac{2 \times 26.75 \times 26.75}{(26.75^2 - 12.7^2)} \times \frac{2\pi}{60} \times \omega$$

$$\dot{\gamma} = 0.27 \times \omega$$

From Fig. 13 in the same source, apparent viscosity is plotted against shear rate.

Speed of rotation (rpm)	Shear rate (s^{-1})	Apparent viscosity (mPa.s)
4.6	1.2	2.064
50.4	13.6	2.056
99.8	26.9	2.035
149.3	40.3	2.021
199.6	53.9	2.007
250	67.5	1.99

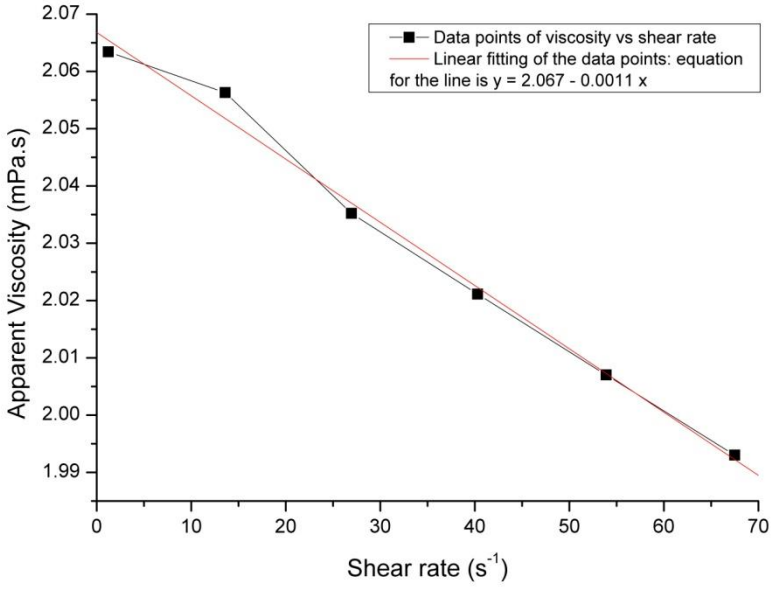

Fig. A1. Variation of apparent viscosity with shear rate for LMA-158 alloy.

Sun et al. (Sun *et al.*, 2007)

R_b = 10mm, R_c = 15mm, l_b = 40mm.

For tin at 387.5°C, from Fig. 3 in (Sun *et al.*, 2007) , the torque values are converted into shear stress and the rotational rate (rpm) is converted into shear rate.

$$\dot{\gamma} = \frac{2 \times 15 \times 15}{(15^2 - 10^2)} \times \frac{2\pi}{60} \times \omega$$

$$\dot{\gamma} = 0.377 \times \omega$$

$$\tau = \frac{M}{2\pi R_b^2 l_b} = (39.8[M]) \text{ in } {}^{N}/_{m^2}$$

Rotational rate (rpm)	Shear Rate (s^{-1})	Shear Stress (Nm^{-2})	Apparent viscosity (mPa.s)
100	37.7	310.3	8232
110	41.4	363.3	8764
120	45.2	404.8	8945
130	49.1	450.4	9181
140	52.8	479.9	9091
150	56.6	490.6	8673

Appendix VI

Uncertainty analysis in Set 5 geometry of the Couette type viscometer

$$\eta = \frac{M/_{2\pi R_b^2 l_b}}{\left(\frac{2R_c^2}{R_c^2 - R_b^2} \times \frac{2\pi}{60} \times \omega\right)} = \frac{M}{8\pi^2 l_b \left(\frac{\omega}{60}\right)}\left[\frac{1}{R_b^2} - \frac{1}{R_c^2}\right]$$

$$\therefore u(\eta) = \left[\left\{\frac{\partial \eta}{\partial M} \times u(M)\right\}^2 + \left\{\frac{\partial \eta}{\partial l_b} \times u(l_b)\right\}^2 + \left\{\frac{\partial \eta}{\partial \omega} \times u(\omega)\right\}^2 + \left\{\frac{\partial \eta}{\partial R_b} \times u(R_b)\right\}^2 + \left\{\frac{\partial \eta}{\partial R_c} \times u(R_c)\right\}^2\right]^{1/2} \quad (1)$$

The partial derivatives of η are then calculated.

$$\frac{\partial \eta}{\partial M} = \frac{1}{8\pi^2 l_b \left(\frac{\omega}{60}\right)}\left[\frac{1}{R_b^2} - \frac{1}{R_c^2}\right]$$

$$\frac{\partial \eta}{\partial l_b} = \frac{M}{8\pi^2 \left(\frac{\omega}{60}\right)}\left[\frac{1}{R_b^2} - \frac{1}{R_c^2}\right]\left(\frac{-1}{l_b^2}\right)$$

$$\frac{\partial \eta}{\partial \omega} = \frac{M}{8\pi^2 l_b \left(\frac{1}{60}\right)}\left[\frac{1}{R_b^2} - \frac{1}{R_c^2}\right]\left(\frac{-1}{\omega^2}\right)$$

$$\frac{\partial \eta}{\partial R_b} = \frac{M}{8\pi^2 l_b \left(\frac{\omega}{60}\right)}\left(\frac{-2}{R_b^3}\right)$$

$$\frac{\partial \eta}{\partial R_c} = \frac{M}{8\pi^2 l_b \left(\frac{\omega}{60}\right)}\left(\frac{2}{R_c^3}\right)$$

If the original length of the geometry at room temperature of 20°C is defined as: R_c^o = 15mm, R_b^o = 14mm and l_b^o = 42mm; the coefficient of linear expansion of steel, α = 16E-06 K^{-1}.

The length of the geometry is defined as R_c, R_b and l_b for a change in temperature of ΔT.

$R_c = R_c^o \times (1 + \alpha\,\Delta T)$; $R_b = R_b^o \times (1 + \alpha\,\Delta T)$; $l_b = l_b^o \times (1 + \alpha\,\Delta T)$.

$$u(R_c) = \left[\left\{\frac{\partial R_c}{\partial \Delta T} \times u(\Delta T)\right\}^2 + \left\{\frac{\partial R_c}{\partial R_c^o} \times u(R_c^o)\right\}^2\right]^{1/2} \quad (2)$$

$$u(R_b) = \left[\left\{\frac{\partial R_b}{\partial \Delta T} \times u(\Delta T)\right\}^2 + \left\{\frac{\partial R_b}{\partial R_b^o} \times u(R_b^o)\right\}^2\right]^{1/2} \quad (3)$$

$$u(l_b) = \left[\left\{\frac{\partial l_b}{\partial \Delta T} \times u(\Delta T)\right\}^2 + \left\{\frac{\partial l_b}{\partial l_b^o} \times u(l_b^o)\right\}^2\right]^{1/2} \quad (4)$$

$$\frac{\partial R_c}{\partial \Delta T} = R_c^o \times \alpha;\ \frac{\partial R_b}{\partial \Delta T} = R_b^o \times \alpha;\ \frac{\partial l_b}{\partial \Delta T} = l_b^o \times \alpha$$

$$\frac{\partial R_c}{\partial R_c^o} = 1 + \alpha \times \Delta T;\ \frac{\partial R_b}{\partial R_b^o} = 1 + \alpha \times \Delta T;\ \frac{\partial l_b}{\partial l_b^o} = 1 + \alpha \times \Delta T$$

The values of the uncertainties for $u(R_c^o)$,$u(R_b^o)$ and $u(l_b^o)$ is mentioned in Table 6.3.

Once the partial derivatives of the parameters are obtained, the standard uncertainties of the parameters can be calculated by using them in the equations 2, 3 and 4. The combined derivatives are employed in then calculating the total uncertainty in the apparent viscosity from equation 1. The torque values (M) and speed of rotation (ω) are different for different liquids (Table 6.3); R_b, R_c and l_b remaining same for all.

References

Alchagirov, B. and Chochaeva, A. (2000) "Temperature dependence of the density of liquid tin", *High Temperature,* vol. 38, no. 1, pp. 44-48.

Andereck, C.D., Dickman, R. and Swinney, H.L. (1983) "New flows in a circular Couette system with co-rotating cylinders", *Physics of Fluids,* vol. 26, no. 6, pp. 1395-1401.

Andereck, C.D., Liu, S.S. and Swinney, H.L. (1986) "Flow regimes in a circular Couette system with independently rotating cylinders", *Journal of Fluid Mechanics,* vol. 164, pp. 155.

Andrade, E.N.d.C. (1952) "Viscosity of Liquids", *Proceedings of the Royal Society of London.Series A, Mathematical and Physical Sciences,* vol. 215, no. 1120, pp. pp. 36-43.

Andrade, E.N.d.C. and Chiong, Y.S. (1936) "On the determination of viscosity by the oscillation of a vessel enclosing a fluid: Part 1", *Proceedings of the Physical Society,* vol. 48, no. 2, pp. 247.

Arkharov, V.I., Yershov, G.S. and Novokhatskiy, I.A. (1971) "Influence of Non-Metallic inclusions on the viscosity of Molten Steel", *Fizika Metallov i Metallovedenie,* vol. 31, no. 3, pp. 652-654.

Assael, M.J., Kalyva, A.E., Antoniadis, K.D., Banish, R.M., Egry, I., Wu, J., Kaschnitz, E. and Wakeham, W.A. (2010) "Reference Data for the Density and Viscosity of Liquid Copper and Liquid Tin", *Journal of Physical and Chemical Reference Data,* vol. 39, no. 3, pp. 033105.

Atkinson, H.V. (2008) *Modelling of semi-solid processing,* Shaker.

Bakhtiyarov, S.I. and Overfelt, R.A. (1999) "Measurement of liquid metal viscosity by rotational technique", *Acta Materialia,* vol. 47, no. 17, pp. 4311-4319.

Ball, P. (2001) *The self-made tapestry: pattern formation in nature,* Oxford University Press.

Barber, E.M., Muenger, J.R. and Villforth, F.J. (1955) "High Rate of Shear Rotational Viscometer", *Analytical Chemistry,* vol. 27, no. 3, pp. 425-429.

Battezzati, L. and Greer, A.L. (1989) "The viscosity of liquid metals and alloys", *Acta Metallurgica,* vol. 37, no. 7, pp. 1791-1802.

Beckwith, D.A. and Newell, G.F. (1957) "Theory of oscillation type viscometers: The oscillating cup", *Zeitschrift fÃ¼r Angewandte Mathematik und Physik (ZAMP),* vol. 8, no. 6, pp. 450-465.

Bell, S. (2001) *A Beginner's Guide to Uncertainty of Measurement,* National Physical Laboratory.

Bojarevics, V. and Pericleous, K. (2009) "Levitated droplet oscillations: Effect of internal flow", *Magnetohydrodynamics,* vol. 45, no. 3, pp. 267-276.

Booth, F. (1950) "The Electroviscous Effect for Suspensions of Solid Spherical Particles", *Proceedings of the Royal Society of London.Series A, Mathematical and Physical Sciences,* vol. 203, no. 1075, pp. pp. 533-551.

Brooks, R.F., Dinsdale, A.T. and Quested, P.N. (2005) "The measurement of viscosity of alloys—a review of methods, data and models", *Measurement Science and Technology,* vol. 16, no. 2, pp. 354-362.

Chambers (2011) *The Chambers Science and Technology Dictionary,* 12th edn, Chambers, 2011.

Chandrasekhar, S. (1958) "The Stability of Viscous Flow between Rotating Cylinders", *Proceedings of the Royal Society of London.Series A.Mathematical and Physical Sciences,* vol. 246, no. 1246, pp. 301-311.

Collyer, A.A. (1974) "Time dependent fluids", *Physics Education,* vol. 9, no. 1, pp. 38-44.

Collyer, A.A. (1973) "Time independent fluids", *Physics Education,* vol. 8, no. 5, pp. 333-338.

Collyer, A.A. and Clegg, D.W. (1998) *Rheological measurement,* Chapman \& Hall.

Couette, M. (1890) "Etudes sur le frottement des liquides", *Annales de Chimie et de Physique serie VI,* vol. 21, pp. 433-510.

Culpin, M.F. (1957) "The Viscosity of Liquid Indium and Liquid Tin", *Proceedings of the Physical Society.Section B,* vol. 70, no. 11, pp. 1069.

Davey, A. (1962) "The growth of Taylor vortices in flow between rotating cylinders", *Journal of Fluid Mechanics,* vol. 14, no. 03, pp. 336.

Dinsdale, A. and Quested, P. (2004) "The viscosity of aluminium and its alloys--A review of data and models", *Journal of Materials Science,* vol. 39, no. 24, pp. 7221-7228.

Donnelly, R.J. (1991) "Taylor-Couette Flow: The Early Days", *Physics Today,* vol. 44, no. 11, pp. 32-39.

Drazin, P.G. and Reid, W.H. (2004) *Hydrodynamic Stability,* Cambridge University Press.

Einstein, A. (1906) "Eine neue Bestimmung der Moleküldimensionen", *Annalen der Physik,* vol. 324, no. 2, pp. 289-306.

Etay, J., Pericleous, K., Egry, I. and Wunderlich, R.K. (2012) "Status of Viscosity Measurements by the Oscillating Drop Method in an EML under Reduced Gravity Conditions", *TMS Spring Meeting*.

Ferguson, J. and Kemblowski, Z. (1991) *Applied fluid rheology,* Elsevier Applied Science.

Ferriss, D.H. and Quested, P. (2000) *Some Comparisons of the Roscoe and Beckwith-Newell Analyses for the Determination of Viscosity of Liquid Metals using the Oscillating Cup Viscometer,* National Physical Laboratory, London.

Gale, W.F., Totemeier, T.C. and Smithells, C.J. (2004) *Smithells Metals Reference Book,* Elsevier Butterworth-Heinemann.

Genshaw, M.A., Solomons, C., Rapp, R.A., Shores, D.A., Wittenberg, L., Ofte, D., Lucas, L.D., Hondros, E.D., Robertson, W.M., Lundy, T.S., Gjostein, N.A., Walls, H.A., Wood, G.C., Kruger, J. and Frankenthal, R.P. (1970) "Physicochemical Measurements in Metals Research" in *Techniques of Metals Research,* ed. R.A. Rapp, Interscience Publishers, United States of America.

Gourlay, C.M. and Dahle, A.K. (2007) "Dilatant shear bands in solidifying metals", *Nature,* vol. 445, no. 7123, pp. 70-73.

Highgate, D.J. and Whorlow, R.W. (1969) "End effects and particle migration effects in concentric cylinder rheometry", *Rheologica Acta,* vol. 8, no. 2, pp. 142-151.

Howie, F.H. and Hondros, E.D. (1982) "The surface tension of tin-lead alloys in contact with fluxes", *Journal of Materials Science,* vol. 17, no. 5, pp. 1434-1440.

Iida, T., Morita, Z. and Takeuchi, S. (1975) "Viscosity Measurements of Pure Liquid Metals by the Capillary Method ", *Journal of the Japan Institute of Metals,* vol. 39, no. 11, pp. 1169-1175.

Iida, T., and Guthrie, R.I.L., (1988) *The physical properties of liquid metals,* Clarendon Press, Oxford.

Inglis, D.R. (1939) "Viscous Force Between Almost-Coaxial Cylinders", *Physical Review,* vol. 56, no. 10, pp. 1041-1044.

Ishikawa, T., Paradis, P., Okada, J.T. and Watanabe, Y. (2012) "Viscosity measurements of molten refractory metals using an electrostatic levitator", *Measurement Science and Technology,* vol. 23, no. 2, pp. 025305.

Jeyakumar, M., Hamed, M. and Shankar, S. (2011) "Rheology of liquid metals and alloys", *Journal of Non-Newtonian Fluid Mechanics,* vol. 166, no. 14–15, pp. 831-838.

Jones, W.R.D. and Bartlett, W.L. (1952) "The viscosity of Aluminium and Binary Aluminium Alloys", *Journal Institute of Metals,* vol. 81, pp. 145-152.

Kehr, M., Hoyer, W. and Egry, I. (2007) "A New High-Temperature Oscillating Cup Viscometer", *International Journal of Thermophysics,* vol. 28, no. 3, pp. 1017-1025.

Knappworst, A. (1952) "A new method of high temperature viscometry by the method of oscillating hollow bodies", *Zeitschrift für Physikalische Chemie,* vol. 200.

Lewis, A.J. (1936) "The absolute measurement of the viscosity of liquid tin", *Proceedings of the Physical Society,* vol. 48, no. 1, pp. 102.

Macosko, C.W. (1994) *Rheology: principles, measurements, and applications,* VCH.

Malik, M.M., Jeyakumar, M., Hamed, M.S., Walker, M.J. and Shankar, S. (2010) "Rotational rheometry of liquid metal systems: Measurement geometry selection and flow curve analysis", *Journal of Non-Newtonian Fluid Mechanics,* vol. 165, no. 13–14, pp. 733-742.

Mallock, A. (1896) "Experiments on Fluid Viscosity", *Philosophical Transactions of the Royal Society of London.Series A, Containing Papers of a Mathematical or Physical Character,* vol. 187, pp. 41-56.

Mallock, A. (1895) "Experiments on Fluid Viscosity.", *Proceedings of the Royal Society of London,* vol. 59, no. 353-358, pp. 38-39.

Mallock, A. (1888) "Determination of the Viscosity of Water", *Proceedings of the Royal Society of London,* vol. 45, pp. pp. 126-132.

Manrique, L.A. and Porter, R.S. (1975) "An improved Couette high shear viscometer", *Rheologica Acta,* vol. 14, no. 10, pp. 926-930.

McLelland, A.R.A., Henderson, N.G., Atkinson, H.V. and Kirkwood, D.H. (1997) "Anomalous rheological behaviour of semi-solid alloy slurries at low shear rates", *Materials Science and Engineering: A,* vol. 232, no. 1–2, pp. 110-118.

Mezger, T.G. (2006) *The rheology handbook: for users of rotational and oscillatory rheometers,* Vincentz Network.

Mooney, M. (1936) "The Rheology of Raw Rubber", *Physics,* vol. 7, no. 11, pp. 413-420.

Mooney, M. and Ewart, R.H. (1934) "The Conicylindrical Viscometer", *Physics,* vol. 5, no. 11, pp. 350-354.

Naidich, Y.V. and Perevertailo, V.M. (1971) "Surface and contact properties in the system composed of germanium and a tin-germanium melt", *Powder Metallurgy and Metal Ceramics,* vol. 10, no. 2, pp. 142-147.

Pai, S.I. (1943) "Turbulent flow between rotating cylinders", *Technical Notes National Advisory Committee for Aeronautics,* , no. No. 892.

Palma, G., Pezzin, G. and Busulini, L. (1967) "Viscous heating in coaxial cylinder viscometers", *Rheologica Acta,* vol. 6, no. 3, pp. 259-264.

Papathanasiou, T.D. (1998) "Explicit Corrections for the Effect of Viscous Heating in Circular Couette Viscometers", *International Journal of Thermophysics,* vol. 19, no. 1, pp. 71-88.

Passerone, A., Ricci, E. and Sangiorgi, R. (1990) "Influence of oxygen contamination on the surface tension of liquid tin", *Journal of Materials Science,* vol. 25, no. 10, pp. 4266-4272.

Piau, J.M., Bremond, M., Couette, J.M. and Piau, M. (1994) "Maurice Couette, one of the founders of rheology", *Rheologica Acta,* vol. 33, no. 5, pp. 357-368.

Piau, U.J. and Piau, M. (2005) "Letter to the Editor: Comment on ``Origin of concentric cylinder viscometry" [J. Rheol. [bold 49], 807--818 (2005)]. The relevance of the early days of viscosity, slip at the wall, and stability in concentric cylinder viscometry", *Journal of Rheology,* vol. 49, no. 6, pp. 1539-1550.

Pinkus, O. and Sternlicht, B. (1961) *Theory of hydrodynamic lubrication,* McGraw-Hill.

Protsenko, P., Terlain, A., Traskine, V. and Eustathopoulos, N. (2001) "The role of intermetallics in wetting in metallic systems", *Scripta Materialia,* vol. 45, no. 12, pp. 1439-1445.

Przyborowski, M., Hibiya, T., Eguchi, M. and Egry, I. (1995) "Surface tension measurement of molten silicon by the oscillating drop method using electromagnetic levitation", *Journal of Crystal Growth,* vol. 151, no. 1â€“2, pp. 60.

Rayleigh, L. (1917) "On the Dynamics of Revolving Fluids", *Proceedings of the Royal Society of London.Series A,* vol. 93, no. 648, pp. 148-154.

Reiner, M. (1964) "The Deborah Number", *Physics Today,* vol. 17, no. 1, pp. 62-62.

Rhim, W., Ohsaka, K., Paradis, P. and Spjut, R.E. (1999) "Noncontact technique for measuring surface tension and viscosity of molten materials using high temperature electrostatic levitation", *Review of Scientific Instruments,* vol. 70, no. 6, pp. 2796-2801.

Roach, S. and Henein, H. (2005) "A new method to dynamically measure the surface tension, viscosity, and density of melts", *Metallurgical and Materials Transactions B,* vol. 36, no. 5, pp. 667-676.

Roscoe, R. (1958) "Viscosity Determination by the Oscillating Vessel Method I: Theoretical Considerations", *Proceedings of the Physical Society,* vol. 72, no. 4, pp. 576.

Rothwell, E. (1961) "A Precise Determination of the Viscosity of Liquid Tin, Lead, Bismuth, and Aluminium by an Absolute Method", *Journal of the Institute of Metals,* vol. 90, pp. 389-394.

Saatdjian, E. and Midoux, N. (1992) "Flow of a Newtonian Fluid between eccentric rotating cylinders", *International Journal of Numerical Methods for Heat & Fluid Flow,* vol. 2, no. 3, pp. 261-270.

Shvidkovskiy, Y.G. (1962) "Certain Problems related to the Viscosity of fused metals", *NASA Technical Translation,* vol. F-88.

Sobolev, V. (2007) "Thermophysical properties of lead and lead–bismuth eutectic", *Journal of Nuclear Materials,* vol. 362, no. 2–3, pp. 235-247.

Stokes, G.G. (1880) "Math. and Phys", *Considerations relative to the greatest height of oscillatory irrotational waves which can be propagated without change of form*, vol. I, pp. 225-228.

Stott, V.H. (1933) "The measurement of the viscosity of a molten metal by means of an oscillating disc", *Proceedings of the Physical Society*, vol. 45, no. 4, pp. 530-544.

Sun, C., Geng, H., Ji, L., Wang, Y. and Wang, G. (2007) "Rheological properties of Pb, Sb, Bi, and Sn melts", *Journal of Applied Physics*, vol. 102, no. 3, pp. 034901.

Taylor, G.I. (1936) "Fluid Friction between Rotating Cylinders. I. Torque Measurements", *Proceedings of the Royal Society of London.Series A - Mathematical and Physical Sciences*, vol. 157, no. 892, pp. 546-564.

Taylor, G.I. (1923a) "Experiments on the Motion of Solid Bodies in Rotating Fluids", *Proceedings of the Royal Society of London.Series A*, vol. 104, no. 725, pp. 213-218.

Taylor, G.I. (1923b) "Stability of a Viscous Liquid Contained between Two Rotating Cylinders", *Proceedings of the Royal Society of London.Series A, Containing Papers of a Mathematical and Physical Character*, vol. 102, no. 718, pp. pp. 541-542.

Taylor, G.I. (1923c) "Stability of a Viscous Liquid Contained between Two Rotating Cylinders", *Philosophical Transactions of the Royal Society of London.Series A, Containing Papers of a Mathematical or Physical Character*, vol. 223, no. 605-615, pp. 289-343.

Terasaki, H., Kato, T., Urakawa, S., Funakoshi, K., Suzuki, A., Okada, T., Maeda, M., Sato, J., Kubo, T. and Kasai, S. (2001) "The effect of temperature, pressure, and sulfur content on viscosity of the Fe–FeS melt", *Earth and Planetary Science Letters*, vol. 190, no. 1–2, pp. 93-101.

Thresh, H. and Crawley, A. (1970) "The viscosities of lead, tin, and Pb-Sn alloys", *Metallurgical and Materials Transactions B*, vol. 1, no. 6, pp. 1531-1535.

Tsai, M.H., Hwang, W.S. and Chou, H.H. (2009) "The micro-droplet behavior of a molten lead-free solder in an inkjet printing process", *Journal of Micromechanics and Microengineering*, vol. 19, no. 12, pp. 125021.

Van Wazer, J.R. (1963) *Viscosity and flow measurement: a laboratory handbook of rheology*, Interscience Publishers.

Varsani, V. (2006) *Rheological Behaviour of Metallic Liquids*, Brunel University,2006.

Varsani, V. and Fan, Z. (2007) "Non-Newtonian Behaviour of Liquid Metals", *TMS 2007 Annual Meeting & Exhibition*, pp. 67.

Vignau, J.M., Azou, P. and Bastien, P. (1967) "Viscosity of Aluminium and Aluminium-Silicon alloys - Influence of the film of alumina", *Comptes rendus de l'Académie des Sciences: Serie C*, vol. 264, pp. 177.

Wan Cho, S., Han, K., Yi, Y., Kang, S., Yoo, K., Jeong, K. and Whang, C.-. (2006) "Thermal Oxidation Study on Lead-free Solders of Sn-Ag-Cu and Sn-Ag-Cu-Ge", *Advanced Engineering Materials,* vol. 8, no. 1-2, pp. 111-114.

Watanabe, T., Toya, Y. and Nakamura, I. (2005) "Development of free surface flow between concentric cylinders with vertical axes", *Journal of Physics: Conference Series,* vol. 14, pp. 09-19.

Webster, J.G. (1999) *The Measurement, Instrumentation, and Sensors Handbook,* CRC Press.

Whorlow, R.W. (1980) *Rheological techniques,* E. Horwood.

Wilhelm, R.H. and Wroughton, D.M. (1939) "Concentric-Cyclinder Motor-Driven Viscometer", *Industrial & Engineering Chemistry,* vol. 31, no. 4, pp. 482-486.

Wittenberg, L.J., Ofte, D. and Curtiss, C.F. (1968) "Fluid Flow of Liquid Plutonium Alloys in an Oscillating-Cup Viscosimeter", *The Journal of chemical physics,* vol. 48, no. 7, pp. 3253-3260.

-x-